



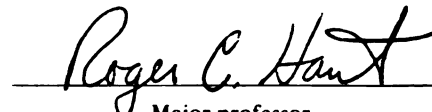
This is to certify that the  
thesis entitled  
**An Analysis of Some of the Effects of  
Surgical and Mechanical Trauma on the  
Mechanical Stiffness of Rabbit Articular Cartilage**

presented by

**Dennis Elburn Shelp**

has been accepted towards fulfillment  
of the requirements for

Masters degree in Mechanics

  
Major professor

Date April 6, 1994



**LIBRARY**  
**Michigan State**  
**University**

**PLACE IN RETURN BOX to remove this checkout from your record.**  
**TO AVOID FINES return on or before date due.**

DATE DUE	DATE DUE	DATE DUE
JUL 13 2002 061802		

MSU is An Affirmative Action/Equal Opportunity Institution  
c:\circ\dtduea.pm3-p.1

**AN ANALYSIS OF SOME OF THE EFFECTS  
OF SURGICAL AND MECHANICAL TRAUMA  
ON THE MECHANICAL STIFFNESS OF RABBIT ARTICULAR CARTILAGE**

**By**

**Dennis Elburn Shelp**

**A THESIS**

**Submitted to  
Michigan State University  
in partial fulfillment of the requirements  
for the degree of**

**MASTER OF SCIENCE**

**Department of Materials Science and Mechanics**

**1994**

## **ABSTRACT**

### **AN ANALYSIS OF SOME OF THE EFFECTS OF SURGICAL AND MECHANICAL TRAUMA ON THE MECHANICAL STIFFNESS OF RABBIT ARTICULAR CARTILAGE**

**By**

**Dennis Elburn Shelp**

Osteoarthritis is a degenerative joint disease causing painful instability and loss of motion. Traumatic injury, such as a single blunt impact, has been speculated as a possible pathogenesis leading to this disease. The results of previous impact studies performed on a rabbit model, have suggested that traumatic fissures and surgical synovitis may reduce patellar articular cartilage stiffness possibly leading to degeneration. In an acute study we found that impact induced fissures caused a reduction in the instantaneous stiffness of cartilage, while exposure to a surgical synovitis created a decrease in its equilibrium stiffness. The simultaneous combination of these two factors not only decreased cartilage stiffness but also its flow viscosity. However, although the overall load carry capacity of the cartilage was reduced, the existence of an interaction between the fissures and synovitis could not be proven. A second study was performed to investigate the possibility of creating a synovitis under closed joint conditions through blunt impact to the synovial tissue. Six days after synovial trauma, unfissured patellar cartilage specimens demonstrated an overall increase in stiffness and flow viscosity, while the fissured specimens demonstrated overall decreases. Again, however, a statistical interaction between the fissures and synovitis could not be proven. Interestingly, hyperflexion of the limb during the induction of synovial trauma was found to prevent changes in cartilage stiffness in both intact and fissured specimens.

## **ACKNOWLEDGEMENTS**

I would like to begin by thanking my advisor, Dr. Roger Haut, for his guidance, friendship, and occasional words of motivation.

I would also like to thank the following people: Dr. Charles DeCamp for his surgical expertise, Jean Atkinson for her work on the rabbits, Jane Walsh for her histological preparations, and Tammy Haut for her help in tabulating data and preparing figures.

Finally, I would like to thank Brenda Robinson for her long hours of typing and good sense of humor.

These studies were entirely supported by a grant from the Centers for Disease Control.

## **TABLE OF CONTENTS**

	<b><u>Page</u></b>
<b>LIST OF TABLES</b>	<b>ix</b>
<b>LIST OF FIGURES</b>	<b>xiii</b>
<b>LIST OF SYMBOLS</b>	<b>xv</b>
<b>INTRODUCTION</b>	<b>1</b>
<b>Articular Cartilage</b>	<b>1</b>
<b>Collagen</b>	<b>2</b>
<b>Proteoglycans</b>	<b>5</b>
<b>Water</b>	<b>7</b>
<b>Osteoarthritis Research</b>	<b>8</b>
<b>Load Trauma Models</b>	<b>10</b>
<b>Gross Observable Damage</b>	<b>13</b>
<b>Arthritis and the Synovium</b>	<b>17</b>
<b>Synovial Morphology</b>	<b>18</b>
<b>Synovial Fluid</b>	<b>19</b>
<b>Mechanisms of Synovitis</b>	<b>19</b>
<b>Background Studies</b>	<b>22</b>
<b>THE OPEN JOINT STUDY</b>	<b>23</b>

<b>OPEN JOINT MATERIALS AND METHODS</b>	<b>23</b>
Impacting Device	23
Pressure Sensitive Film	25
Preliminary Studies	26
The <i>In Vivo</i> Study	27
Surgical Impact Trauma	27
Test Procedure	28
<b>OPEN JOINT RESULTS</b>	<b>29</b>
Blunt Impact	29
Mechanical Results	30
Sham Data	36
Biochemistry	36
<b>THE CLOSED JOINT STUDY</b>	<b>37</b>
<b>CLOSED JOINT MATERIALS AND METHODS</b>	<b>37</b>
The <i>In Vivo</i> (Closed Joint) Study	37
Blunt Impact	38
Data Collection	39
Grip Assembly	39
Test Procedure	41
<b>CLOSED JOINT RESULTS</b>	<b>45</b>
Impact Trauma	45

Mechanical Testing	45
Six Days	45
Three Months	46
Six Months	47
One Year	47
Shams	48
Comparison of Background Studies	48
Supplemental Animals	53
DISCUSSION OF BACKGROUND STUDIES	55
OBJECTIVES OF THE STUDY	59
THE ACUTE STUDY	60
ACUTE STUDY MATERIAL AND METHODS	61
The Acute <i>In Vivo</i> Study	61
Surgery/Blunt Impact	62
Testing Procedure	
(Rigid indenter)	63
(Porous indenter)	63
Biomechanical Properties	65
Elastic/Viscoelastic Analysis	66
Biphasic Theory	73
Biphasic Analysis	78
Statistical Analysis	82
Histology	83
ACUTE STUDY RESULTS	84
Blunt Impact	84
Gross Observations	84

Mechanical Test: (Solid Indenter)	
Time Zero, High Impact	87
One Day, Shams (No Impact)	87
One Day, High Impact	88
Between Group Comparisons and Interactions	88
Mechanical Test: (Porous Indenter)	
Biphasic Results	89
Elastic/Viscoelastic Results	91
Histology	92
SYNOVITIS STUDY	94
The Synovitis <i>In Vivo</i> Study	95
Soft Tissue Trauma/Blunt Impact	96
Testing Procedure	97
Biomechanical Properties	98
SYNOVITIS STUDY RESULTS	99
Blunt Impact	99
PART I: (Synovitis created without the use of the restraining chair)	99
Part I: Gross Observations	
Sham Group	99
Impact Group	100
Part I: Mechanical Tests (Solid Indenter)	
Sham Group	100
Impact Group	101
Part I: Mechanical Tests (Porous Indenter)	101
Part I: Elastic/Viscoelastic Results	102
Part I: Histology (Articular Cartilage)	103
Part I: Histology (Synovial Lining)	
Sham Group	104
Impact Group	105

<b>PART II: (Synovitis created while restrained in the chair)</b>	<b>105</b>
<b>Part II: Gross Observations</b>	
Sham Group	105
Impact Group	106
<b>Part II: Mechanical Tests (Rigid Indenter)</b>	
Sham Group	106
Impact Group	106
<b>Part II: Mechanical Tests (Porous Indenter)</b>	107
<b>Part II: Elastic/Viscoelastic Results</b>	108
<b>Part II: Histology (Articular Cartilage)</b>	109
<b>Part II: Histology (Synovial Lining)</b>	
Sham Group	110
Impact Group	111
<b>Chair and Impact Interactions</b>	111
<b>DISCUSSION</b>	<b>113</b>
Acute Study	114
Synovitis Study	118
<b>SUMMARY</b>	<b>126</b>
<b>RECOMMENDATIONS</b>	<b>129</b>
<b>APPENDIX</b>	<b>130</b>
<b>REFERENCES</b>	<b>166</b>

## **LIST OF TABLES**

<b>Table 1:</b>	<b>Impact Intensities</b>
<b>Table 2:</b>	<b>Average Peak Impact Loads and Contact Pressure Ranges for the Open Joint Study</b>
<b>Table 3:</b>	<b>Six Day Low Impact Force Parameters from the Blunt Impact Procedure</b>
<b>Table 4:</b>	<b>Six Day High Impact Force Parameters from the Blunt Impact Procedure</b>
<b>Table 5:</b>	<b>Three Month Low Impact Force Parameters from the Blunt Impact Procedure</b>
<b>Table 6:</b>	<b>Three Month High Impact Force Parameters from the Blunt Impact Procedure</b>
<b>Table 7:</b>	<b>Six Month, Low Impact Closed Joint Force Parameters from the Blunt Impact Procedure</b>
<b>Table 8:</b>	<b>Six Month, High Impact, Closed Joint, Force Parameters from the Blunt Impact Procedure</b>
<b>Table 9:</b>	<b>One Year, Low Impact, Closed Joint Force Parameters from the Blunt Impact Procedure</b>
<b>Table 10:</b>	<b>One Year, High Impact, Closed Joint, Force Parameters from the Blunt Impact Procedure</b>
<b>Table 11:</b>	<b>Results of Mechanical Tests on the 6 Day, Low Level Impact Closed Joint Group</b>
<b>Table 12:</b>	<b>Results of the Mechanical Tests on the 6 Day, High Level Impact, Closed Joint Group</b>
<b>Table 13:</b>	<b>Results of the Mechanical Tests on the 3 Month, Low Level Impact, Closed Joint Group</b>

<b>Table 14:</b>	<b>Results of the Mechanical Tests on the 3 Month, High Level Impact, Closed Joint Group</b>
<b>Table 15:</b>	<b>Results of the Mechanical Tests on the 6 Month, Low Level Impact, Closed Joint Group</b>
<b>Table 16:</b>	<b>Results of the Mechanical Tests on the 6 Month, High Level Impact, Closed Joint Group</b>
<b>Table 17:</b>	<b>Results of the Mechanical Tests on the 1 Year, Low Level Impact, Closed Joint Group</b>
<b>Table 18:</b>	<b>Results of the Mechanical Tests on the 1 Year, High Level Impact, Closed Joint Group</b>
<b>Table 19:</b>	<b>Results of Mechanical Tests on the 6 Day Sham, Closed Joint Group</b>
<b>Table 20:</b>	<b>Three Month, Low Impact, Open Joint, Force Parameters from the Blunt Impact Procedure</b>
<b>Table 21:</b>	<b>Three Month, High Impact, Open Joint, Force Parameters from the Blunt Impact Procedure</b>
<b>Table 22:</b>	<b>Results of the Mechanical Tests on the 3 Month, Low Impact, Supplemental Group</b>
<b>Table 23:</b>	<b>Results of the Mechanical Tests on the 3 Month, High Level Impact, Supplemental Group</b>
<b>Table 24:</b>	<b>Results of the High Level, Blunt Impacts for the Acute Study Impact</b>
<b>Table 25:</b>	<b>Results of the Solid Indenter Mechanical Tests on the Time Zero, High Impact, Acute Rabbit Group</b>
<b>Table 26:</b>	<b>Results of the Solid Indenter Mechanical Tests on the One Day, Sham Operated (No Impact), Acute Rabbit Group</b>
<b>Table 27:</b>	<b>Results of the Solid Indenter Mechanical Tests on the One Day, High Impact, Acute Rabbit Group</b>
<b>Table 28:</b>	<b>Biphasic Material Properties for the Acute Study Porous Tests, Rate = 1.0 sec.</b>
<b>Table 29:</b>	<b>Biphasic Material Properties for the Acute Study Porous Tests, Rate = 2.0 sec.</b>

<b>Table 30:</b>	<b>Elastic and Viscoelastic Parameters for the Acute Study, Porous Tests, Rate = 1.0 sec.</b>
<b>Table 31:</b>	<b>Elastic and Viscoelastic Parameters for the Acute Study, Porous Tests, Rate = 2.0 sec.</b>
<b>Table 32:</b>	<b>Results of the High Level, Blunt Impacts for the Synovitis Study Impact Groups</b>
<b>Table 33:</b>	<b>Results of the Solid Indenter Mechanical Tests on the 6 Day Synovitis Study, Sham Group. (Synovitis created without the use of the restraining chair).</b>
<b>Table 34:</b>	<b>Results of the Solid Indenter Mechanical Tests on the 6 Day Synovitis, Impact Group. (Synovitis created without the use of the restraining chair).</b>
<b>Table 35:</b>	<b>Biphasic Material Properties for the Synovitis Study Porous Tests, Rate = 1.0 sec. (Synovitis induced without the use of restraining chair).</b>
<b>Table 36:</b>	<b>Biphasic Material Properties for the Synovitis Study Porous Tests, Rate = 2.0 sec. (Synovitis induced without the use of restraining chair).</b>
<b>Table 37:</b>	<b>Elastic and Viscoelastic Parameters for the Synovitis Study, Porous tests, Rate = 1.0 sec. (Synovitis created without the use of the restraining chair).</b>
<b>Table 38:</b>	<b>Elastic and Viscoelastic Parameters for the Synovitis Study, Porous tests, Rate = 2.0 sec. (Synovitis created without the use of the restraining chair).</b>
<b>Table 39:</b>	<b>Results of the Solid Indenter Mechanical Tests on the 6 Day Synovitis, Sham Group. (Synovitis created while restrained in chair).</b>
<b>Table 40:</b>	<b>Results of Solid Indenter Mechanical Tests on the 6 Day Synovitis, Impact Group. (Synovitis created while restrained in chair).</b>
<b>Table 41:</b>	<b>Biphasic Material Properties for the Synovitis Study Porous Tests, Rate = 1.0 sec. (Synovitis induced while restrained in chair).</b>
<b>Table 42:</b>	<b>Biphasic Material Properties for the Synovitis Study Porous Tests, Rate = 2.0 sec. (Synovitis induced while restrained in chair).</b>
<b>Table 43:</b>	<b>Elastic and Viscoelastic Parameters for the Synovitis Study, Porous tests, Rate = 1.0 sec. (Synovitis created while restrained in chair).</b>

**Table 44:** Elastic and Viscoelastic Parameters for the Synovitis Study, Porous tests,  
Rate = 2.0 sec. (Synovitis created while restrained in chair).

## **LIST OF FIGURES**

- Figure 1:** Cartilage layers.
- Figure 2:** Cartilage under shear loading.
- Figure 3:** Proteoglycan aggregate.
- Figure 4:** Micro-damage to collagen increasing cartilage water carrying capacity.
- Figure 5:** Sagittal (a) and frontal (b) views of the anatomy of the human knee joint with the synovial lining shown in red.
- Figure 6:** The gravity impactor.
- Figure 7:** A typical impact fissure.
- Figure 8:** Histogram of  $G_u$  from the open joint, low level impact groups.
- Figure 9:** Histogram of  $G_u$  from the open joint, high level impact groups.
- Figure 10:** Histogram of  $G_r$  values from the open joint, low level impact groups.
- Figure 11:** Histogram of  $G_r$  value from the open joint, high level impact groups.
- Figure 12:** Histogram of  $\eta$  values from the open joint, low level impact groups.
- Figure 13:** Histogram of  $\eta$  values from the open joint, high level impact groups.
- Figure 14:** Vice-like grip used to hold patellae.
- Figure 15:** Bath-grip mount assembly.
- Figure 16:** Patella held in grip.
- Figure 17:** The six day, closed joint test sites.
- Figure 18:** The closed joint test sites following six day time point.

- Figure 19: Open joint study, high vs low level impact,  $G_u$  trends.
- Figure 20: Closed joint study, high vs low level impact,  $G_u$  trends.
- Figure 21: Open joint, high vs low level impact,  $G_r$  trends.
- Figure 22: Closed joint, high vs low level impact,  $G_r$  trends.
- Figure 23: Open joint, high vs low level impact,  $\eta$  trends.
- Figure 24: Closed joint, high vs low level impact,  $\eta$  trends.
- Figure 25: Porous indenter.
- Figure 26: Porous indentation test sites.
- Figure 27: Indentation test.
- Figure 28: A stress-relaxation load-time response curve.
- Figure 29: A load-time plot of a thickness test.
- Figure 30: A generalized Maxwell model.
- Figure 31: The theoretical response of a generalized Maxwell model.
- Figure 32: The application of Tobolsky's analysis (1960) on experimental stress relaxation data.
- Figure 33: The confined compression test.
- Figure 34: The unconfined compression test.
- Figure 35: Creep relaxation as a function of  $t_r$ .
- Figure 36: Shifting of the theoretical biphasic response curves by  $S = \log_{10}(a^2/kH_A)$ .
- Figure 37: A typical pressure profile from the acute study.
- Figure 38: Typical impact fissures created during the acute study. The sites of the indentation testing are seen as small circular defects to the right (lateral) of the fissures.
- Figure 39: A histological cross section of two impact fissures.
- Figure 40: Histological cross section showing the loss of PGs and tidemark observed in some of the patellae in the acute study groups.

## LIST OF SYMBOLS

$a$	- radius of the indenter
$d$	- fluid flow length
$e$	- strain tensor
$E_i$	- exponential integral function
$E_0$	- relaxation time spectrum constant
$g^*$	- Fredholm integral solution
$G$	- shear modulus
$G_r$	- relaxed shear modulus
$G_u$	- unrelaxed shear modulus
$h$	- thickness of elastic layer (cartilage)
$H_A$	- aggregate modulus
$H(\tau)$	- relaxation time spectrum
$H(\tau)$	- slope of log time relaxation plot
$I$	- identity matrix
$k$	- permeability
$p$	- fluid pressure
$P$	- resistive load of elastic layer (cartilage)
$R$	- thickness test ramp rate

$R_o$  - rate of compression parameter  
 $s$  - LaPlace transform variable  
 $S$  - biphasic curve shift value  
 $t$  - time  
 $t_i$  - time corresponding to the onset of cartilage loading  
 $t_f$  - time corresponding to contact with subchondral bone  
 $t_g$  - characteristic gel diffusion time  
 $t'$  - dimensionless time ( $t/t_g$ )  
 $u$  - cartilage creep displacement  
 $v^s$  - velocity of solid phase  
 $v^f$  - velocity of fluid phase  
 $V_o$  - indentation rate of loading  
 $w$  - Simpson's weights

$\alpha$  - ratio of solid volume to fluid volume  
 $K$  - finite thickness correction factor  
 $\mu_s$  - Lamé constant of solid matrix  
 $\eta$  - flow viscosity  
 $\eta_s$  -  $(1-\nu_s)/(1-\nu_s)$   
 $\nu$  - Poisson's ratio  
 $\nu_s$  - Poisson's ratio of the solid matrix  
 $\tau$  - elemental time constant

- $\tau_{\min}$  - minimum relaxation time
- $\tau_{\max}$  - maximum relaxation time
- $\sigma^f$  - stress tensor of fluid phase
- $\sigma^s$  - stress tensor of solid matrix
- $\pi^f$  - diffusive force of fluid phase
- $\pi^s$  - diffusive force of solid matrix
- $\omega_0$  - depth of indentation

## **INTRODUCTION**

Osteoarthritis (OA) is a degenerative disease primarily affecting the articular cartilage (AC) of load bearing joints (Howell, 1976). OA is the most prevalent of all joint diseases, responsible for thirty times as many sick leave days as rheumatoid arthritis (RA) (Kramer, et al., 1983). Diagnosis of this disease is primarily based upon radiographic assessment and clinical examination of features (Altman, et al., 1986; Altman, et al., 1987). Although the stages of this disease have been described in detail (Mankin, 1974), many questions still exist about its pathogenesis and the sequence of events leading to its formation. Traumatic joint injury has been speculated as a possible triggering mechanism for the onset of OA (Radin, et al., 1970; States, 1970). It has been hypothesized that articular cartilage damage sustained during impact may lead to altered joint loading and progressive degeneration (Repo and Finlay, 1977). It has further been suggested that the development of OA is not solely due to mechanical causes, but may involve biochemical interaction with the synovium as well (Shinmei, et al., 1989; Walker, et al., 1991).

### **Articular Cartilage:**

Articular cartilage is a smooth, dense, connective tissue covering the ends of bones in articulating joints. This tissue provides a low friction, load bearing surface which is important for the large degree of movement required in diarthral joints

(Armstrong and Mow, 1984). Human articular cartilage ranges between 2-4 mm in thickness (Howell, 1976). This thin layer of tissue must repeatedly withstand loads between four and five times body weight during normal gait, and loads as high as ten times body weight during deep knee bends (Solokoff, 1969; Howell et al., 1976). The resilience of this relatively thin tissue is a product of its composite structure of which collagen, proteoglycans, and water are the major components.

### Collagen

Collagen makes up 40-50% of the dry weight of normal AC (Parson and Black, 1987). Type II collagen is the principal structural component comprising the collagen framework. Types V, VI, IX and XI are also present, but compared with Type II each makes up only 3% of the total collagen content (Broom, 1988). The collagen network is divided into layers described by their depth from the articulating surface and fiber orientation (Figure 1). The collagen rich surface layer is composed of random fibers which lie tangent to the articulating surface. In the range of physiological loading fluid flow across this layer is the primary mechanism of viscous deformation (Parsons and Black, 1987). A healthy surface layer is required to maintain fluid pressure within the AC during compressive loading (Setton, et al., 1993). Directly below the thin surface layer lie the middle and deep layers. These layers comprise the majority of the cartilage thickness. The collagen fibers in these layers are randomly oriented and homogeneously dispersed (Askew and Mow, 1978; Armstrong and Mow, 1984).

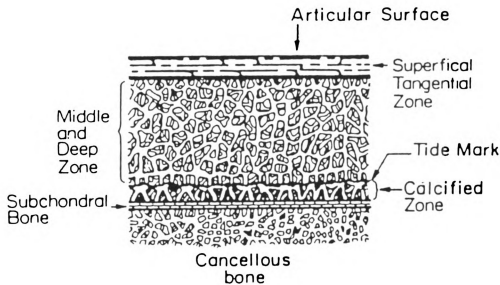


Figure 1: Cartilage layers.

The calcified cartilage zone lies at the cartilage-bone interface. Here the random collagen fibers come together to form radial bundles which pass through the calcified cartilage and bind with the underlying subchondral bone (Howell, 1976; Armstrong and Mow, 1984).

The shear rigidity of AC under compression is produced by tensile forces generated in these random fibers (Figure 2). The tensile response of the collagen network is believed to play the major role in controlling the instantaneous deformation of cartilage (Mizrahi et al., 1986). Enzymes have been used by investigators to disrupt the collagen network and/or the extracellular matrix in order to isolate their function within AC. Creep tests performed on cartilage, which has had all or part of its matrix

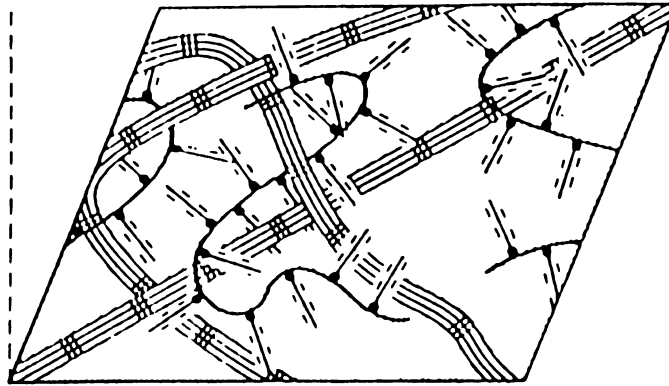


Figure 2: Cartilage under shear loading.

removed, show no significant change in its instantaneous stiffness (Parsons and Black, 1987; Jurvelin, et al., 1988). After running slow rate tensile tests on control samples of AC, Schmidt, et al., (1990) enzymatically removed the extrafibrillar matrix and carried out tensile test on the remaining collagen framework. They found no change in the stiffness or strength characteristics of the matrix devoid cartilage. Enzyme damaged collagen was found to have a reduced transient elastic response during damping coefficient measurements (Bader, et al., 1992). The results of these studies support the definitive role of collagen as the initial load bearing element within AC. In the description of the remaining cartilage elements it will become apparent, however, that the overall response of AC is dependent on interaction between all of its components.

### Proteoglycans

Between the collagen fibrils lies a gel-like matrix. The chief components of this matrix are proteoglycans (PGs). Proteoglycans make up approximately 20-30% of the dry weight of AC (Mow et al., 1984). Proteoglycan monomers consist of a single protein core to which 50-100 glycosaminoglycans (GAG) chains are covalently bonded. These GAG chains are composed of chondroitin and keratin sulfate groups which are spaced approximately 10-15Å apart along the protein core (Buckwalter, et al., 1985; Bader, 1992; Gu, 1993). In turn, the protein core of these monomers are linked to hyaluronic acid (HA) to form a proteoglycan aggregate (Figure 3). The sulfate groups are negatively charged. Due to their "like" charge, PGs spread out to maximize spacing and inhibit diffusion through the matrix (Howell, 1976). This large fixed charge density (FCD) attracts counter ions creating a Donnan osmotic pressure making PGs highly hydrophilic (Mow, et al., 1984).

The osmotic pressure created by the PGs has a secondary affect on AC deformation. The collagen network resists the tendency of PGs to swell creating tensile forces in the collagen fibers and hydrostatic pressure in the interstitial water (Mizrahi, et al., 1986; Maroudas, et al., 1979). By enzymatically removing PGs, Bader, et al. 1992, reduced the swelling pressure of the cartilage and found that larger deformations were required to achieve the same loads acquired prior to PG removal. Following confined compression tests on AC samples with various PG contents, Schmidt, et al., 1989, concluded that the most important function of PGs may be to control the rate at which the collagen network stretches thereby preventing damage. The viscoelastic (i.e. rate dependent) behavior of PGs has also been reported by other investigators. The

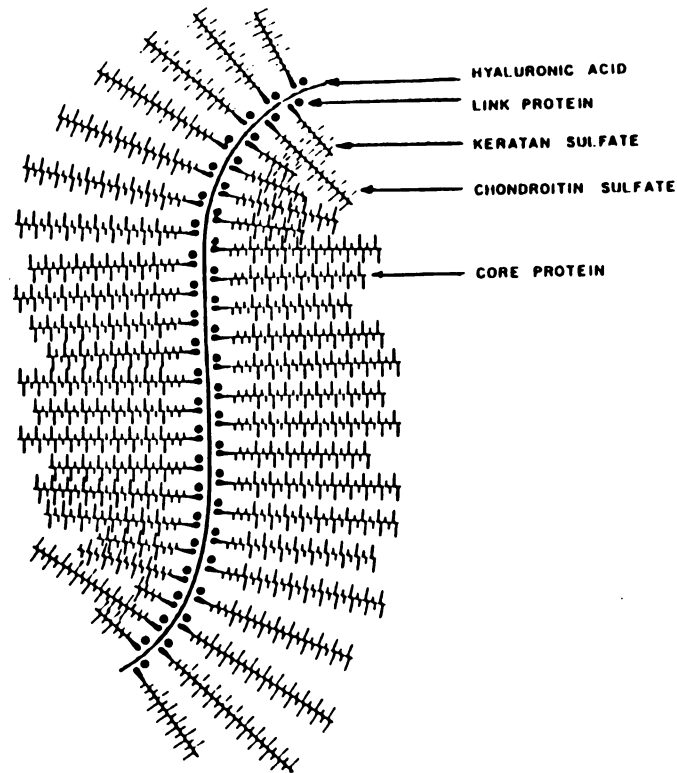


Figure 3: Proteoglycan aggregate.

concentration of PGs has been shown to inversely affect the rate of creep and directly influence the "flow independent" equilibrium stiffness of AC (Parson and Black, 1987; Jurvelin, 1988). An inverse relationship between cartilage permeability and PG content has also been documented (Mow, et al., 1984). The ability of PGs to affect cartilage deformation stems from the relation between their FCD and the corresponding osmotic

pressure it induces (Mizrahi, et al., 1986).

### Water

Water makes up 70-80% of the wet weight of normal mammalian AC (Simon and Wohl, 1982). This water is divided into three types: structural, bound, and free. Structural water, associated with the crystal, can be described by a specific stoichiometry much as the hydrates of inorganic salts. The term bound water is frequently used to describe protein-water interactions. For collagen the amount of bound water is generally on the order of 0.35 g/g (Nomura, 1977). Torzilli has estimated that approximately 30% cartilage water is associated with the collagen (Torzilli, 1982). Maroudas has described interfibrillar water as a function of osmotic pressure difference between extrafibrillar and interfibrillar space or the equivalent mechanical pressure (Maroudas, et al., 1991). However, the majority of water inside AC is free to move through the tissue (Mow, et al., 1984; Maroudas, et al., 1991). As previously noted, fluid flow and the corresponding mechanical behavior of cartilage are affected by such things as osmotic pressure and tissue permeability. A proper balance between the interarticular water and the extra fibrillar matrix is essential for the proper function of AC. Water content has been shown to be directly related to the permeability and inversely related to the equilibrium stiffness of AC (Armstrong and Mow, 1982). The affinity of PGs for water has previously been described. Direct correlations have been made between the presence of PGs and water in AC (Parsons and Black, 1987; Burton-Wurster and Lust, 1986). The integrity of the collagen network may also affect the water carrying capabilities of AC. Donahue, et al., 1983, measured an increase in the water content of canine patellar

cartilage two weeks after impact. They suggested that micro-damage to the collagen fibrils may have allowed proteoglycans to spread out increasing their water carrying capacity, Figure 4.

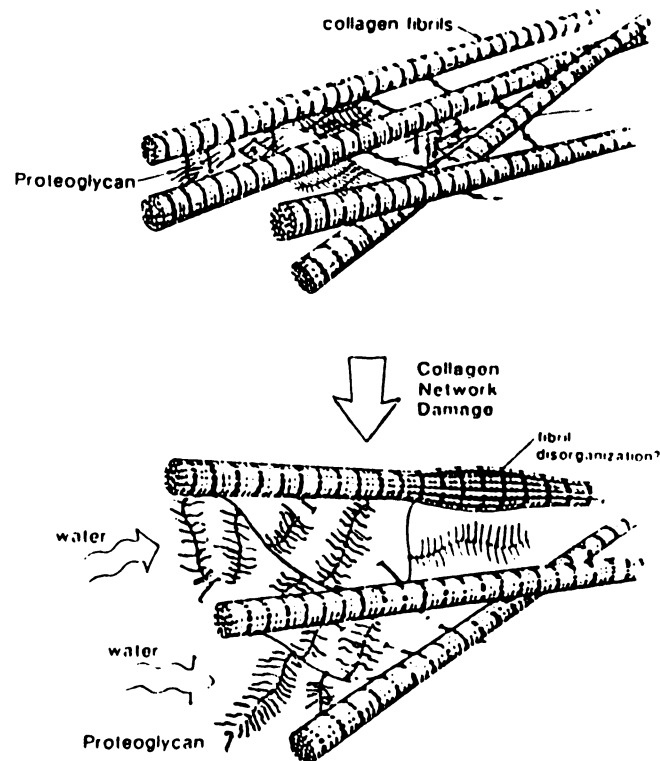


Figure 4: Micro-damage to collagen increasing cartilage water carrying capacity.

#### Osteoarthritis Research:

The majority of OA research has been carried out with the help of animal models. Although a gamut of animals have been used, the models themselves typically fall into

one of two categories, joint instability or load trauma. Joint instability models usually involves surgical disruption of the supportive connective tissue in or around the joint. In 1970, Hulth introduced the first instability model. His intent was to produce a slow progressive degeneration of the AC. Production of this model involved the removal of the medial meniscus, and transection of the anterior cruciate, posterior cruciate, and medial collateral ligaments. Since its conception this model has been used by other OA investigators (Svalastoga and Reiman, 1985; Lucoschek, et al., 1986). Less disruptive models such as medial meniscectomy (Hoch, et al., 1983) and anterior cruciate ligament transection (Altman, et al., 1984; Myers, et al., 1986; Brandt, et al., 1991 (a) and (b)) have also been used. Altman, et al., 1984, measured an increase in the stiffness of canine femoral cartilage out to 12 weeks post-transection of the ACL. Similarly, Myers, et al., 1986, also measured an increase in cartilage stiffness out to 12 weeks following ACL transection in tibial plateau cartilage under the menisci. During these post-transection test periods neither Altman, et al. or Myers, et al. reported any signs of cartilage fibrillation. Interestingly, at 23 weeks Myers, et al., 1986, measured a drop in cartilage stiffness and noted signs of fibrillation. Shelp, et al., 1993, at 24 weeks post-transection of the ACL, also reported a significant drop in the stiffness of fibrillated canine femoral cartilage. The most extensive instability studies were carried out by Brandt, et al., 1991 (b), where alterations in canine knee cartilage have been tracked out to 4 1/2 years post-transection of the anterior cruciate ligament. Hypertrophic repair mechanisms, including increases in cartilage thickness and PG synthesis, were measured in the unstable joint out to 36 months following transection. These repair trends ceased by 45 months and a marked loss of cartilage thickness was observed. At 54 months

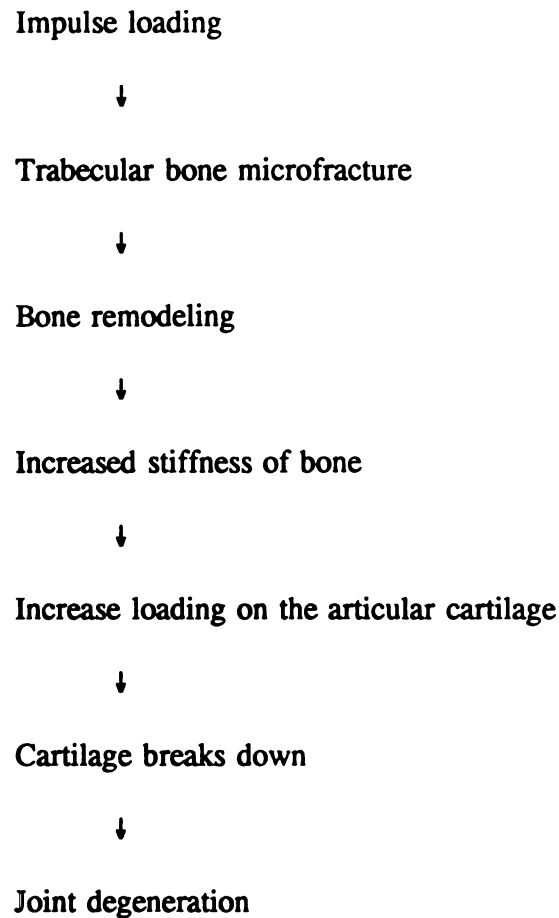
areas of complete cartilage loss and increased subchondral bone thickness, similar to that observed in human OA, were present. Long term observations such as these seem to validate the effectiveness of the instability methods as a bonafide model for the study of OA. The major draw back to instability models are that they require the artificial alteration of joint loading to create the desired degenerative effects.

Unlike the joint instability models the damaging affects of load trauma models are aimed directly at the cartilage and bone. These models typically involve either a single blunt impact or repetitive impulse loading. Due to their direct relevance to the study at hand, these models and their results are discussed in detail in the following text.

#### Load Trauma Models

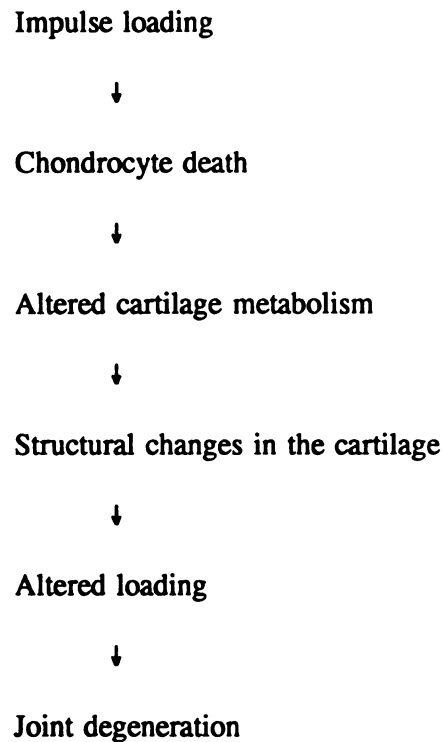
Automobile accidents, sports injuries and falls are three common causes of trauma, with the knee being the joint most often affected (States, 1970). Many times joint damage does not show up in radiographs immediately following the traumatic event (Pritsch, 1984). However, it has been hypothesized that a single blunt impact may cause micro-damage leading to osteoarthritis (Radin, 1970; Insall, 1976).

In 1970, Radin and Paul found that removal of cartilage from bovine stifle joints did not significantly reduce the force attenuating properties of the joint (Radin and Paul, 1970). Similar observations were made during cyclic loading of human knees (Chu and Yazdani-Ardakani, 1986). Based on this result it has been hypothesized that bone (in particular the subchondral bone because of its porosity) is responsible for the majority of shock absorption across the knee joint. From this conclusion the following chain of events were proposed as a possible pathogenesis leading to traumatic OA:



(Radin, 1972). Using a rabbit model and cyclic impulse loading, Radin was able to measure an increase in the subchondral bone stiffness as well as progressive decreases in the proteoglycan content of cartilage in the traumatized knee (Radin, et al., 1973; Radin, et al., 1978). In a more recent study, increased bone volume and formation were reported to have a parallel correlation to the severity of OA degeneration observed in human AC (Shimizu, et al., 1993). The results of studies such as these have prompted many investigators to believe the OA formation is mediated by initial changes in the subchondral bone. However, in 1977, Repo and Finlay conducted blunt impact studies on unconfined cartilage-bone plugs. They reported obtaining cartilaginous fissures which did not involve the underlying bone and determined that an average stress of 25 MPa

could result in chondrocyte death. They proposed the following pathogenesis based upon their findings:



(Repo and Finlay, 1977). This study suggests that traumatic osteoarthritis may be initiated without damage to the underlying bone. Currently the definitions of lower extremity injury are predominantly based upon the occurrence of bone fracture (Nyquist and King, 1985). However, it has been shown that stresses greater than 25 MPa can be generated in human patello-femoral joints during impact at force levels below those required to create bone fracture (Haut, 1986). Results such as these continue to raise questions about the type and degree of trauma required to produce a degenerative process.

### Gross Observable Damage

The form of joint damage created during load trauma experiment is usually described by its depth or extent from the articulating surface. Fibrillations are the most superficial form of structural damage. Their presence is often noted by a dull appearance of the cartilage or by the increased absorption of india ink (Donohue, et al., 1983). Fibrillations have been reported in canine and rabbit patellar cartilage subjected to both blunt trauma and repetitive impulse loading (Radin, et al., 1973; Donahue, 1983; Yang, et al., 1989). The appearance of these rough surfaces are often associated with specimens observed days, weeks and years following impact. Ghadially, in 1974, studied AC surface defects using a scanning electron microscope (SEM). He suggested that small defects in the articulating surface may lead to increased friction between contacting joint surfaces. Increased contact loads have been implicated as a cause of cartilage wear and loss of stiffness (Shelp, et al., 1993).

Acute fissures are the most frequently reported form of impact damage to AC. These fissures most often begin at the surface and extend downward into the middle/deep zones of the cartilage (Repo & Finlay, 1977; Broom, 1986; Haut, 1986; Thompson, 1990; Silyn-Roberts and Broom, 1990; Ide, et al., 1991; Thompson, et al., 1991; Tomatsu, et al., 1992; Thompson, et al., 1993). In some cases, impact fissures are induced which extend all the way from the surface to the zone of calcified cartilage and into the underlying subchondral bone (Thompson, 1990; Thompson, et al., 1991; Tomatsu, et al., 1992; Thompson, et al., 1993). Surface fissures, like the ones mentioned above, have been observed in cases of human OA (Mankin, 1974). The average depth of these fissures increase with the advancing state of the disease.

The damage induced by impact trauma does not always include the articulating surface. Step off, or cleft, fractures in the subchondral bone are often seen in conjunction with fissures that extended up into the cartilage but do not reach the articular surface (Thompson, et al., 1991; Vener, et al., 1992; Thompson, et al., 1993). Separation of the cartilage from the underlying bone in the zone of calcified cartilage has also been reported in response to blunt impact (Armstrong, et al., 1982). These defects are many times undetectable by surface observation and could possibly be over looked during a clinical examination leading to future degeneration (Thompson, et al., 1991).

The frequent occurrence of surface fissures has raised questions about the physical conditions within the joint leading to this form of damage. Staining ruptured cartilage with india ink has revealed that fissures tend to propagate parallel to the orientation of the collagen fibrils, i.e. the Hultkrantz lines (Repo and Finlay, 1977; Silyn-Roberts and Broom, 1990). This corresponds to a path perpendicular to the direction of minimal strength as determined by tensile tests performed on bovine cartilage (Schmidt, et al., 1990). Cross sections of impacted AC have also revealed that most fissures begin at a 45 degree orientation to the articulating surface. This observation has lead to the hypothesis that fissures are the result of shear stress generated during impact (Silyn-Roberts and Broom, 1990). Elastic math models subjected to impact load profiles have shown that tensile strains, rather than stresses, may be a more reliable predictor of where fissures are likely to form (Askew, et al., 1978; Ide, 1992). These models have also predicted large shear stresses at the cartilage/bone interface which may account for separations seen experimentally (Askew, et al., 1978; Chin, et al., 1986). Surface integrity and sufficient stiffness have also been associated with the ability to induce

impact fissures (Silyn-Roberts and Broom, 1990). The geometry of the traumatized joint may also control the degree of damage imparted by impact (Vener, et al., 1992). The fissures reported in uniformly loaded, flat, cartilage/bone plugs are located in the center of the contact region (Repo and Finlay, 1977; Silyn-Roberts and Broom, 1990). Bimodal load patterns in the knee joint of rabbits create patellar fissures which occurred at the edge of contact zones where the pressure gradients are high (Ide, 1992). Due to the viscoelastic nature of AC not only the amount of impact energy but the rate at which it is employed is crucial to the type of cartilage damage elicited (Yang, et al., 1989). The condition of matrix itself has been shown to affect the cartilage response to impact. Human tibial cartilage depleted of PGs by the enzyme papain showed an average decrease in impact energy absorption of 17.2%. The increase in strain created by such decreased attenuating properties could result in damage to the collagen network (Finlay, et al., 1986). It can easily be seen from these various studies that the formation of traumatic cartilage fissures involves multiple factors. Defining the exact conditions under which fissures will form continues to challenge researchers using load trauma models.

In recent years, several impact models have been used to study the in vivo processes leading to the development of OA. These models typically involve a single, concentrated blow to the test joint in order to inflict trauma. The patello-femoral joint is frequently used because of its clinical significance and the ability to directly traumatize the articular surfaces via a transarticular impact. The trauma induced by transarticular impact can be divided into two categories based on the extent of the damage. These categories include (1) fracture models which result in subchondral bone fractures (often including damage to the overlying AC) and (2) sub-fracture models which cause damage

to the articular cartilage without disruption of the underlying bone or calcified cartilage.

Bone fracture models have been extensively used at the University of Minnesota (Thompson, et al., 1991; Thompson, et al., 1993; Pickvance, et al., 1993). In these studies, non-invasive, transarticular impacts (of approximately 2000 N.) were delivered to canine patello-femoral joints. These impacts typically result in step-off fractures of the patellar subchondral bone. The fractures are often accompanied by fissures in the overlying articular cartilage. In the earliest of these studies osteoarthritic-like changes were histologically noted out to six months post-impact (Thompson, et al., 1991). These changes included a loss of PG content and thickening of the subchondral bone. In more recent studies, scanning electron microscopy, magnetic resonance-imaging (Thompson, et al., 1993) and biochemical (Pickvance, et al., 1993) analysis methods have been added to the study of this model. Early OA-like changes were again detected, however, by one year post-impact damaged regions of the patellae showed signs of repair. Bone fractures, and cartilage fissures which extended into the zone of calcified cartilage, were healed and the PG content of the cartilage had returned to normal. Only superficial cartilage fissures remained showing no signs of healing.

OA-like changes have also been reported in sub-fracture models (Donohue, et al., 1983; Ide, 1992). Donohue, et al., 1983, reported increases in cartilage water content two weeks after transarticular impact. This edema had subsided by 4 weeks post-impact, but injury responses such as chondrocytes cloning and increased vascularity were still evident. In 1992, Ide used mechanical methods to study changes in the stiffness of rabbit patellar cartilage out to one year following transarticular impact. Although it was not significant, a softening trend was observed in fissured cartilage specimens at one year

post-impact. Except for presence of the fissures, histologically the cartilage appeared relatively normal. The surface fissures, which did not extend down beyond the middle zone, showed no signs of healing.

Its unclear from the results of these impact investigations exactly what type of jury or post-impact duration is required to initiate cartilage degeneration. The longest in vivo impact studies to date have only been carried out to one year following trauma induction. The long term fate of these animal models is yet unknown. Of particular interest are the long term affects of the unhealing surface fissures on the load bearing capabilities of the cartilage. As previously noted the integrity of the cartilage surface has been linked to the normal function of cartilage (Setton, et al., 1993). It is possible that a period of several years, similar to that reported for ACL transection (Brandt, et al., 1991), may be required for this fissured cartilage to deteriorate and form full thickness lesions.

#### Arthritis and the Synovium:

The primary role of the synovial lining (SL) in the development of rheumatoid arthritis (RA) has long been accepted. RA begins with an acute inflammation of the SL, i.e. a synovitis. As this synovitis continues a pannus growth develops on the SL and eventually spreads over the surface of the AC. Concurrently centripetal erosion and thinning of the cartilage takes place (Beesley, 1992). Unlike RA, OA degeneration is not proceeded by an acute inflammation of the SL. However, synovial inflammations of varying degree have been found in human OA joints (Howell, 1976; Peyron, 1981; Goldberg, 1982). These OA synovitis incorporate all the classic signs of inflammation;

hyperplasia, vascular changes and infiltration of leukocytes.

### Synovial Morphology

The synovial membrane covers the inside of the tissue surrounding the knee joint forming a closed sac called the synovial cavity, Figure 5. It is composed of both loose and fibrous connective tissue. The capsule is thrown into folds or projections which are composed of connective tissue, adipose tissue, and blood vessels (Goss, 1963). The inner most layer of this membrane is the synovial lining (SL). In the rabbit the SL is approximately 1-3 cells thick. This lining consists primarily of two kinds of cells, A and B.

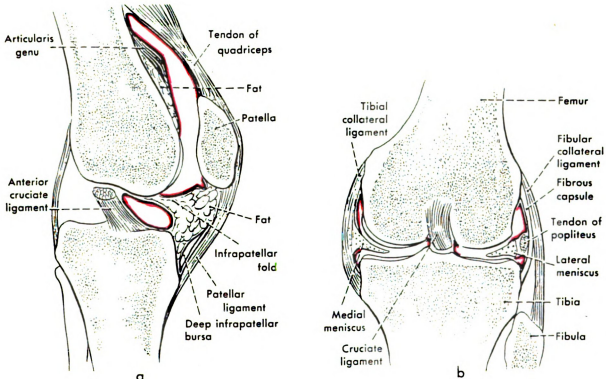


Figure 5: Sagittal (a) and frontal (b) views of the anatomy of the human knee joint with the synovial lining shown in red.

Type A cells are distinguished by their prominent golgi system while B cells are denoted by their rough endoplasmic reticulum (Ghadially and Ray, 1966). The major role of the SL is the production and maintenance of the synovial fluid.

### Synovial Fluid

The synovial fluid (SF) is a clear, viscous fluid, with a consistency similar to that of an egg white (Goss, 1963). This fluid provides nutrition for the avascular AC and lubrication for the articulating surfaces. The main components of this fluid are dialysate of blood plasma, hyaluronic acid (HA) and protein macromolecule complexes (Hlavacek, 1993). Typically the amount of SF within the joint is just enough to cover the surfaces of the cavity but human SF levels can range from 0.50 ml to 100 ml depending on the state of pathology (Lohmander, 1989).

### Mechanisms of Synovitis

The pathways to OA inflammation are poorly understood (Peyron, 1981). However, the role of cytokines and enzymes seems to be promising. Enzymes such as collagenase, cathepsin (D, G, B and L) and stromelysin all have degrading effects on AC matrix and have been found at elevated levels in OA joints (Roughley, 1991; Okada, 1992; Pelletier, et al., 1983; Pickvance, et al., 1993; Howell, 1976). In healthy joints most of these enzymes are kept in check by inhibitors. An imbalance between these enzymes and their inhibitors may lead to OA (Glynn, 1977). Of the enzymes mentioned, stromelysin appears to be the most likely candidate because its active at neutral pH (Okada, et al., 1992). Stromelysin, also known as metalloproteinase (MMP-3), can be synthesized by both synovial cells and AC chondrocytes. The cytokines IL-1 $\beta$

(interlukin) and TNF- $\alpha$  (tumor necrosis factor) are believed to play a key role in the initiating stromelysin production (Roughley, 1991; Beesley, 1992; Pickvance, et al., 1993; Ridge, et al., 1980). Like stromelysin, these cytokines can also be produced by both the synovial cells and the AC chondrocytes. A direct correlation has been measured between the level of these diffusive cytokines and the degree of synovial inflammation. However, a similar correlation has not been established between the state of synovitis and the actual catabolic enzymes. This suggests that cytokines are the predominant mediators of the synovial response (Pelletier, et al., 1985). Typically proteoglycans inhibit the diffusion of IL-1 $\beta$  and TNF- $\alpha$  into the AC. However, in fissured areas devoid of PGs, increase permeability to these cytokines may exist (Okada, et al., 1992). Stromelysin, IL-1 $\beta$ , and TNF- $\alpha$  have all been measured in increased amounts in the middle/deep zones along the edge of fissures up to two weeks following transarticular impact of canine knee joints (Pickvance, 1993).

The exact trigger mechanism leading to the release of these cytokines and enzymes is yet unknown. To study the effects of synovitis foreign materials have been introduced into joints to induce inflammation. Some of the material used include; talcum powder, teflon, carbon fibers, and even ordinary synovial fluid (Frost and Ghosh, 1984; Messner, et al., 1993; Gershuni and Kuei, 1984). Natural substances, like blood (hemarthrosis) can also elicit a synovial response thereby affecting the AC (Ghadially, 1983). It has been suggested that in a natural trauma scenario, substances released by the AC into the SF may induce a degenerating synovial response (Howell, 1976; Schumaker, et al., 1981; Pelletier, 1985). As previously mentioned, increased levels of PG aggregates have been measured in the SF for extended periods following damage to

AC (Lohmander, et al., 1989). Keratin sulfate, from GAG chains, have also been found in higher than normal concentrations in patients with OA (Thonar, et al., 1985). It has been proposed that elevated levels of such substances measured in body fluids (SF, blood serum and urine) may some day provide a means of detecting cartilage damage following joint injury (Lohmander, et al., 1992). Interestingly cases of reactive arthritis are sometimes reported following infections of other parts of the body, although no microorganisms are detected within the joint (Saxne and Hienegard, 1992).

The exact role of the synovium in the sequence of events leading to a state of pathology is unknown. It is well documented that direct damage to the synovium during surgery has a transitory degrading effect on AC (Thompson, 1975; Frost and Ghosh, 1984; Svalastoga and Reiman, 1985; Pelletier, et al., 1985; Walker, 1991; Messner, et al., 1993). In 1985, Svalastoga and Reiman used the Hulth joint instability model to study the effects cartilage degeneration with respect of changes in the SL. The Hulth method was performed on the right leg of each test rabbit. Consecutively, the left leg underwent arthrotomy and served as a surgical control. In the first two weeks following surgery the test and control joints both showed signs of cell proliferation in their SL as well as a surface loss of cartilage PGs. By four weeks post-surgery the control joint had returned to normal, however, on the test side hypertrophy of the SL continued. Between 4 and 6 weeks the first signs of cartilage fibrillation appeared in the test joint. These results suggested that the inflammatory response of the SL may have contributed to the initial breakdown of the AC. In turn, the breakdown of the cartilage may have stimulated further response by the SL. In 1986, Lucoschek, et al., did a comparison study between the Hulth instability model and the non-invasive, repeated impulse loading

(RIL) model used by Radin (1973). The results of the Hulth model were similar to those seen by Svalastoga and Reiman (1985). However, in the RIL model early signs of inflammation did not appear in the SL. Unlike the Hulth model, progressive inflammatory changes in the SL were not observed until after superficial damage to the AC appeared. This suggested that damage to the cartilage itself could initiate an interactive synovial inflammation. The results of these two studies suggest that interactions between the cartilage and synovium may occur during times of joint injury. However, both of these studies involved extraneous joint loading scenarios applied over a period of months. Neither addresses the possibility of an interaction between acute surface damage to the AC accompanied by a traumatic synovitis.

#### **Background Studies:**

A review of two previous studies will be presented before the current topics of research are covered. These background studies are key to the development of the questions which motivated the current investigations. The first study, the open joint study, will lay out the ground work involved in developing the animal model which was used. The results of this study will develop important questions about the affects of mechanical trauma on AC. The second study, the closed joint study, will detail the continuation of the work begun in the open study, and in addition it will also raise questions about the effects of arthrotomy on AC. Following this review the reasons for carrying out the current studies will be clearer.

## **THE OPEN JOINT STUDY**

The purpose of this study was to develop an animal model in order to study the effects of blunt trauma on AC. The hypothesis being that the altered mechanics of damaged cartilage would lead to the degenerative stages associated with OA. Biomechanical tests were used in concurrence with histology and biochemistry in order to relate changes in the mechanical load response of the cartilage with alterations in its physical structure. The following sections describe the methods, materials and results of this study. Only those parts of the study which pertain to the current investigations are covered. For complete details see reference Ide, 1992.

## **OPEN JOINT MATERIALS AND METHODS**

The rabbit was chosen as the animal model on which to study the effects of blunt trauma to AC. This impact induced trauma was delivered under the acceleration of gravity. One patella per rabbit was traumatized. Pressure sensitive film placed within the patello-femoral space recorded contact pressures. The details of these procedures and the processes leading up to them will be described in the following text.

### **Impacting Device:**

Gravity provided a simple and consistent means of delivering a repeatable impact. A free falling mass has a constant gravitational acceleration of  $9.81 \text{ m/s}^2$  (at sea level).

The energy imparted (E) during impact can easily be calculated by multiplying the mass of the object (m) by the acceleration of gravity (g) and the relative height from which it is released above the impact surface (h), i.e.  $E = mgh$ .

Due to the surgical nature of the open joint study, the impactor was designed to operate within a sterile field. The base plate and supportive scaffolding were constructed of aluminum. The impacting rod was made of steel and was guided by two low friction bearings. At the lower end of this rod a flat, aluminum impact head (1" in diameter) was attached by way of a load cell (500 lb. range). At the upper end of the rod a mass could be added to obtain desired impact energies from any given drop height. Figure 6, depicts the gravity impactor described.

The load cell output was recorded by an IBM compatible PC. A solenoid held the impact rod supporting the raised mass. The PC was programmed to disengage the solenoid following input from the operator. Upon impact the PC began collecting the load-time data at the rate of 10,000 Hz. When the load readings returned to zero the solenoid was re-engaged catching the impact mass and preventing it from striking a second time.

A fixture was needed to properly position the rabbit's hind limb to be impacted below the impact mass. It was desired that the patella itself receive the entire force of the impact. Therefore, a seating structure was constructed out of 3/4" plexiglass. The animal was placed in the chair supine with the right leg hyperflexed. The right leg (arbitrarily chosen) was held in place by a spring loaded aluminum bar clamp. A vinyl strap was used to secure the contralateral limb preventing rotation during impact. This seat configuration aligned the patella and underlying femur vertically with the impact

mass (radiographically confirmed).

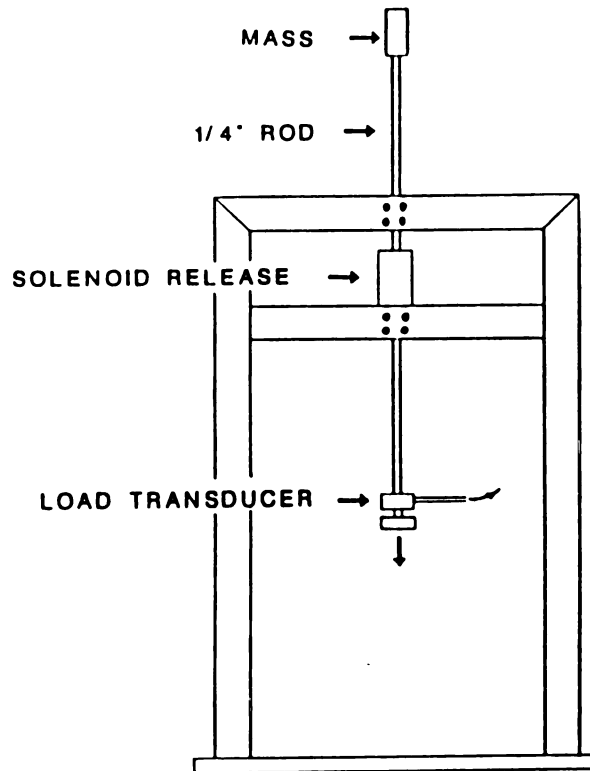


Figure 6: The gravity impacter.

**Pressure Sensitive Film:**

This film consists of a thin sheet of plastic covered with microscopic beads of red dye. When compressed between two contacting surfaces the beads burst marking the area of contact. The larger the force over a given area, the greater the number of beads which break. The intensity of the stain reveals the magnitude of the force. The medium

sensitivity, prescale film used (Fuji Co.) provided a linear stain intensity for statically applied pressures between 10 and 50 MPa. This film, covered by a thin, sterile, plastic sheath, was placed between the patella and the femur via medial and lateral incision. The film provided a record of contact pressures over the cartilage surface during impact. A computer analysis package was used to convert the relative stain intensities to pressures according to a predetermined calibration curve.

#### Preliminary Studies:

The rabbit was chosen because of its low cost and ease in handling. Originally the New Zealand White breed of rabbit was chosen but examination of their patellar cartilage revealed a commonly occurring, and quite extensive, baseline pathology. The Dutch Belted species of rabbit also displayed baseline AC pathology. The fawn colored Flemish Giant breed was found to have the healthiest cartilage. Due to their large size, these animals had the added advantage of large AC surfaces for testing.

Six Flemish Giants were used to determine the appropriate seat design and impact energy levels. The levels of impact energy were chosen as follows, the "low" energy impact level was set based on the largest impact energy that did not result in fissuring of the AC. The "high" impact level was set as the smallest impact energy resulting in AC fissures, but not bone fracture. These levels are shown in Table 1.

Table 1. Impact Intensities.

Impact Intensity	Energy (J)	Drop Height (m)	Mass (kg)
Low	0.90	0.20	0.43
High	6.30	0.46	1.33

The medium sensitivity pressure film was found to provide adequate stain intensity at both levels.

#### The *In Vivo* Study:

Once the impacting procedure was established the next step was to devise an in vivo study. At each impact level, three rabbits were traumatized at each of the following time points: 1, 3, 6, and 14 days, and 3, 6, and 12 months. When the animals reached their predetermined test date they were euthanized and their patellas extracted for biomechanical, biochemical and histologic analysis.

Fifteen animals were also subjected to the same surgery, film insertion and hyperflexion of the limb, but were not impacted. Three animals received surgery, but no film or hyperflexion. Another three rabbits received only surgery, but no film or hyperflexion. These groups served as controls for the procedures itself. All of the rabbits used were mature (six months or older) and were bought from a single supplier.

#### Surgical Impact Trauma:

The rabbits' right leg was prepared for surgery by a veterinary technician. The rabbits were anesthetized with ketamine (11 mg/kg) and xyaline (1.1 mg/kg) and maintained on isoflurine (2-2.5%) per (2L) of oxygen. The rabbit was placed in the restraining seat with its right leg unflexed. As previously stated bilateral incisions were made on the medial and lateral sides of the patellar tendon and patella. The pressure sensitive film was placed in a sterile plastic sleeve and was slid through the incisions placing it between the patella and femur. The surgical limb was then hyperflexed and secured by the bar clamp. Impact was then carried out with the gravity impactor

previously described. Following surgery the film and sleeve were removed and the knee was sutured. Resorbable sutures were placed in the bilateral incisions along the tendon and patella. Non-resorbable sutures were used to close the outer skin incision. All surgeries were carried out by Charles DeCamp, D.V.M. The animals were returned to cage activity immediately following surgery.

#### Test Procedure:

On the day of testing the animals were euthanized and both patellas were removed for immediate testing. The patellas were potted in an epoxy resin, bone side down, leaving the untouched cartilage surface exposed. The AC was kept bathed in physiologic phosphate buffered saline while the epoxy cured and during testing.

The mounted patella was placed directly beneath a plane ended, rigid, cylindrical indenter, 0.50 mm in radius. This probe was connected to the actuator of a servo-hydraulic testing machine by way of a load cell (25 lb. range). Actuator displacement was monitored by an accompanying LVDT. Both load and displacement data were recorded using a Nicolet storage oscilloscope. The indenter probe was brought into contact with the surface of the articular cartilage and was preloaded to 0.02 N. The probe was then indented 0.10 mm into cartilage using a ramp function. The ramp duration was slightly greater than 50 msec. The indentation was maintained for 100 sec. while resistive cartilage forces were measured. The hold time of 100 sec. was set by the limited storage capabilities of the Nicolet. Two indentations were performed per patella; one at the lateral rim and the other just lateral of the centerline which lies between the medial and lateral facets.

Cartilage thickness data was required for the computation of its shear moduli. A small needle-like probe replaced the larger indenter used during the stress-relaxation test. The needle probe was brought down into contact with cartilage surface at the same site as the preceding indentation test. The needle probe was then rammed into the cartilage at the rate of 1 mm/sec. The needle probe was allowed to penetrate the cartilage until a sharp increase in load signaled that contact with the underlying bone had been made. The distance the needle probe traveled between the first signs of loading and contact with the bone (recorded by the LVDT) gave the thickness of the uncalcified cartilage. This method of thickness measurement, unlike sectioning, left the patella in tack for further histological and biochemical analysis.

From each stress-relaxation test three mechanical parameters were calculated. Using the measurements of peak load, equilibrium load and cartilage thickness an unrelaxed ( $G_u$ ) and relaxed shear moduli ( $G_r$ ) were calculated from Hayes solution of an elastic layer bonded to a rigid half space. From the time dependent relaxation portion of the cartilage response a flow viscosity ( $\eta$ ) term was calculated based on Tobolsky's analysis of a generalized Maxwell material (see Biomechanical Analysis).

## **OPEN JOINT RESULTS**

### **Blunt Impact**

Table 2 shows the maximum loads and contact pressures generated in the patello-femoral joint during impact. The peak impact loads were determined by the PC data collection program. The contact pressures were obtained from the Fuji pressure film. The peak contact pressures on the lateral facet were found to be statistically greater than

those on the medial facet by a 8 MPa offset. The average peak pressures generated on lateral facet during high level impacts were significantly larger than those at low impact levels.

**Table 2. Average Peak Impact Loads and Contact Pressure Ranges for the Open Joint Study**

<b>Impact Level</b>	<b>Impact Load (N)</b>	<b>Contact Pressure Range (MPa)</b>	
		<b><u>(Medial)</u></b>	<b><u>(Lateral)</u></b>
Low	200 $\pm$ 21	7.5 $\pm$ 4.4	15.6 $\pm$ 2.9
High	516 $\pm$ 73	19.2 $\pm$ 3.8	26.0 $\pm$ 3.7

Figure 7 shows an impact induced fissure. Typically, these fissures were located at the proximal end, just lateral of the centerline and ran parallel to the long axis of the patella. This location corresponded with large shear stress and tensile strains as indicated by the pressure film. Histological sections revealed that the fissures ran parallel to the major collagen bundles. Surface fissuring was documented in 6 of 24 low level impacts and 18 of 24 high level impacts.

### **Mechanical Results**

The unrelaxed shear modulus ( $G_u$ ) and relaxed shear modulus ( $G_r$ ) were computed by Hayes solution (eq. 1), see Biomechanical Analysis. The unrelaxed modulus was calculated from the peak load and the relaxed modulus was computed after 100 s of stress-relaxation. A two way ANOVA showed no statistical differences between the test and control moduli ( $G_u$  and  $G_r$ ) with respect to post-impact time. Histograms of the data did, however, reveal some interesting trends with respect to post-impact time.



Figure 7: A typical impact fissure.

Figure 8, is a histogram of the post-impact time average response values for Gu, based on the centerline data from the low level study. A tendency can be seen in Figure 8 for Gu values to decrease below controls after day 1, reaching a minimum at 14 days and then rising back to control levels by 6 months. The response trend seen in Gu at high impact levels was different, Figure 9. From 1 to 6 days average test side Gu values were less than controls. From 14 days to 6 months, Gu values approached control

## UNRELAXED MODULUS

Open Joint Study

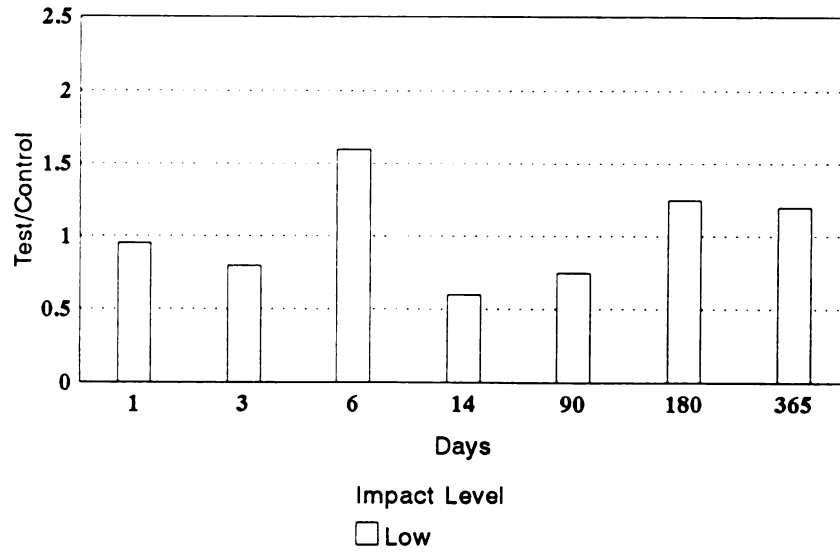


Figure 8: Histogram of  $G_u$  from the open joint, low level impact groups.

## UNRELAXED MODULUS

Open Joint Study

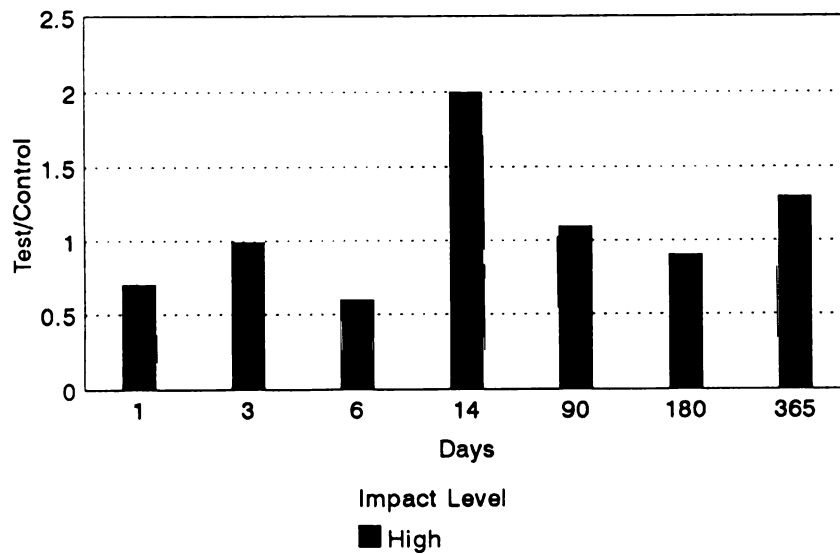


Figure 9: Histogram of  $G_u$  from the open joint, high level impact groups.

levels.

Figure 10, shows the time response trends for the relaxed modulus, centerline values from the low level impact groups. A gradual decrease can be seen in the Gr test values starting at 1 day, reaching a low at 14 days, and then returning back to control levels by 1 year.

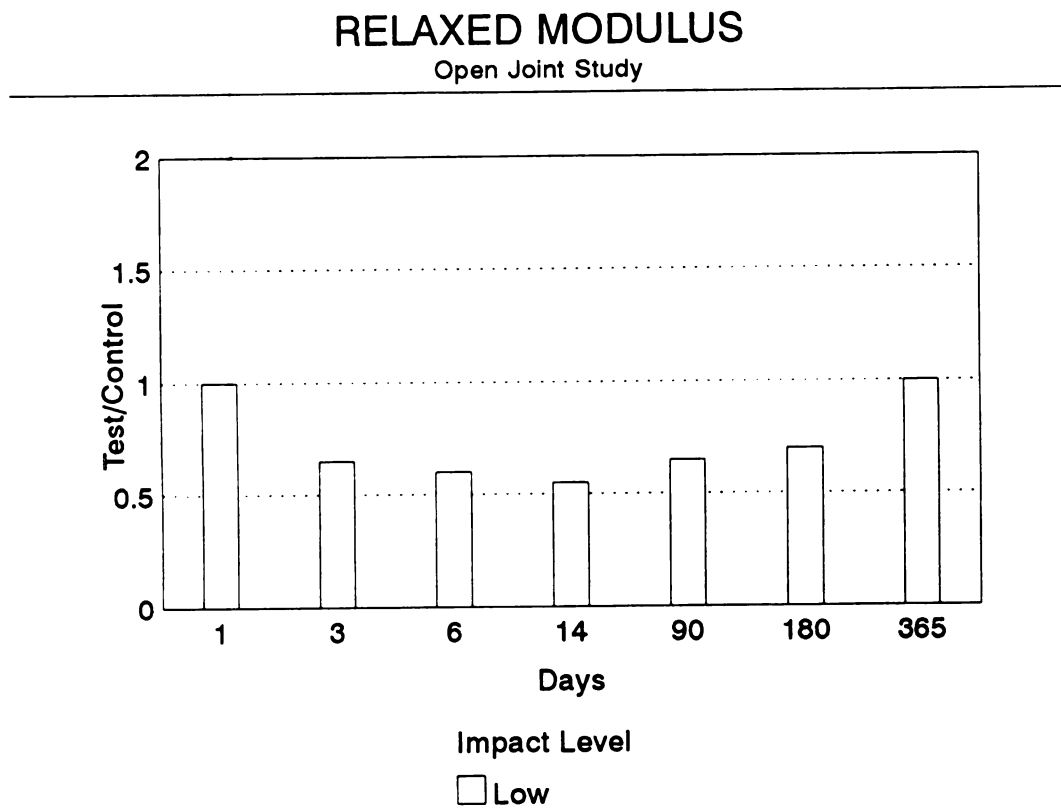


Figure 10: Histogram of Gr values from the open joint, low level impact groups.

At high impact levels the time response of Gr values did not resemble that seen at low impact, Figure 11. Test Gr values were considerably lower than controls beginning at 1 day and continuing out to 6 days post-impact. After 6 days they returned to control levels where they remained.

## RELAXED MODULUS

Open Joint Study

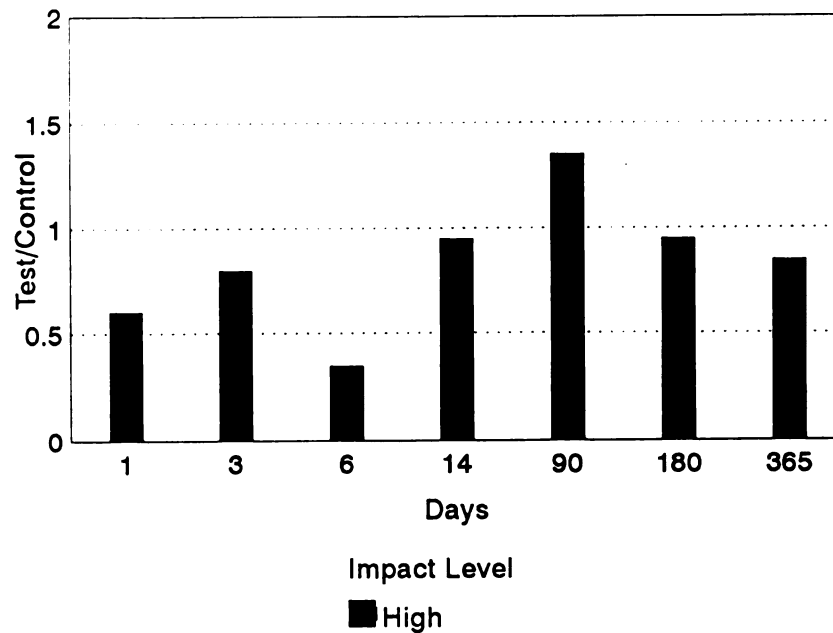
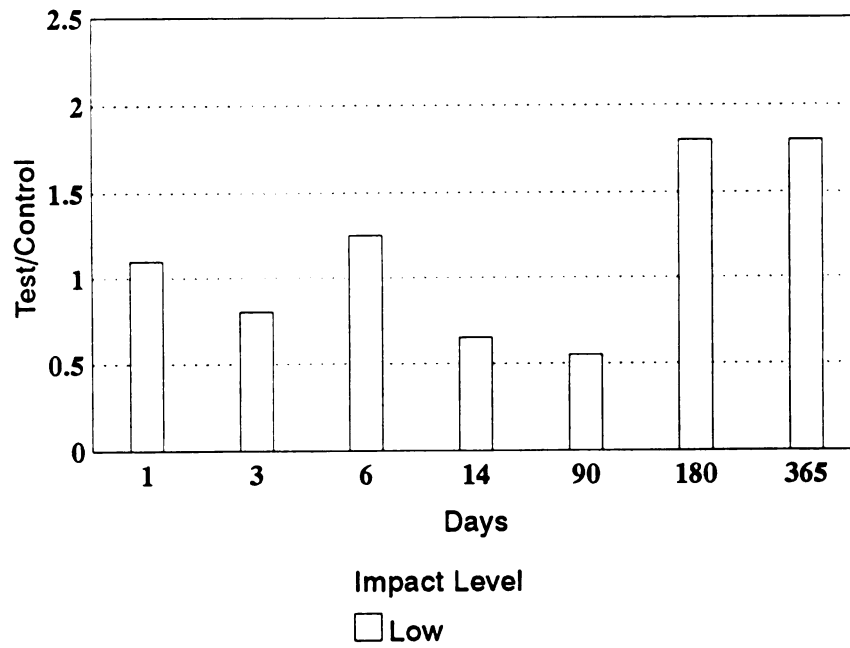


Figure 11: Histogram of Gr value from the open joint, high level impact groups.

Flow viscosity ( $\eta$ ) values were calculated from Tobolsky's analyses of a generalized Maxwell material, see Biomechanical Analysis. This parameter was calculated as a means of characterizing the time dependent relaxation portion of the cartilage response curve. Figure 12 shows the post-impact time viscosity trends for the low level impact groups. Test side values were basically the same as controls out to 6 days. At 14 days and 3 months the test values dropped below controls and then demonstrated an increasing trend back toward normal out to 1 year. At high impact levels an overall decrease was seen in test side viscosity values except at 14 days, Figure 13.

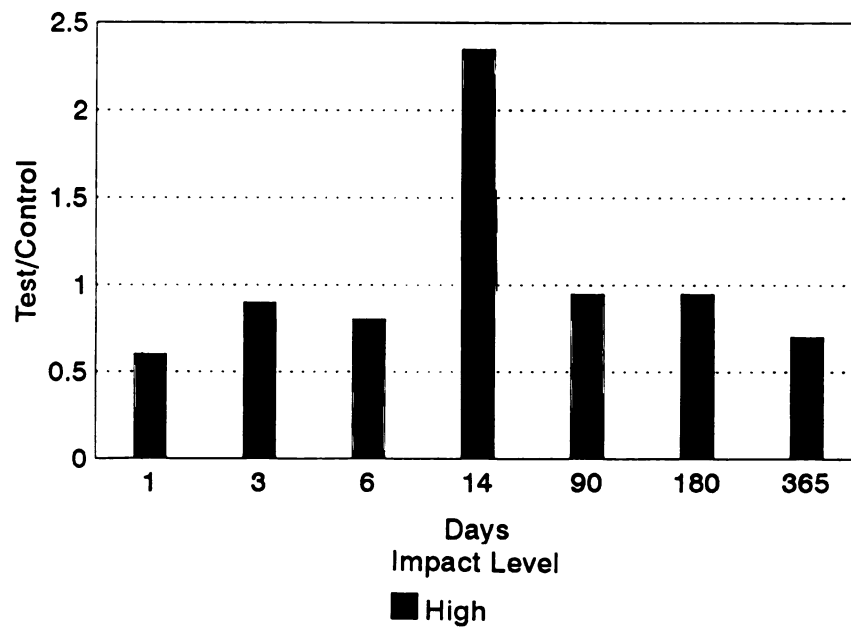
## FLOW VISCOSITY

Open Joint Study

Figure 12: Histogram of the  $\eta$  value from the open joint, low level impact groups.

## FLOW VISCOSITY

Open Joint Study

Figure 13: Histogram of  $\eta$  values from the open joint, high level impact groups.

### Sham Data

In the sham group subjected to surgery, film insertion and hyperflexion, decreases of 25 and 5 percent were seen in test side Gr and Gu values out to 6 days post-impact. These changes were not significant but they did warrant further investigation. This prompted the investigation of the other sham groups. The sham group which included surgery, hyperflexion but no film insertion demonstrated decreases similar to those of the first sham group. The last sham group which underwent arthrotomy, but was not placed in the restraining chair with its leg hyperflexed, did not show any signs of change test versus control.

### Biochemistry

Eighteen cases were randomly chosen from the four short term study groups (1, 3, 6, and 14 days). Cartilage samples were cored from the lateral facet of each patellar pair (test and control). The water content of each sample was determined. The average water percent of the impacted cartilage was  $73.1 \pm 7.9$  compared to  $72.4 \pm 11.0$  in controls. This difference was not statistical. However, in 7 of 10 cases where the test side water content was greater than controls there were no surface fissures. On the contrary, of the 8 test specimens which had a water content greater than their respective controls only 2 of them possessed surface fissures.

## THE CLOSED JOINT STUDY

The use of arthrotomy in the first study was necessary for the evaluation of pressure profiles existing within the joint during impact. With these conditions thoroughly documented, closed joint trauma was the next step in the development of the animal model. The closed joint model served a dual purpose. First, the closed joint scenario more closely represents the joint environment present during an actual *in vivo* knee injury. Secondly, it prevented the cartilage from being exposed to possible transient surgical affects which were believed to have altered the mechanical response of the open joint test specimens. Most of the procedures followed in this study, other than surgery, were unchanged from those in the open joint study. However, some alterations in the methods and materials were made to increase the quantity of information available from each animal.

## CLOSED JOINT MATERIALS AND METHODS

### The *In Vivo* Study:

In the open joint study the low number of rabbits at each time point ( $n=6$ , 3 high and 3 low) made the statistical differences hard to establish. To increase statistical power in the closed joint study, additional rabbits were added. Sixteen Flemish Giant rabbits were placed in each of the following post-impact time periods; six days, three months, six months, and one year. These time points correspond with postoperative dates used

in the open joint study. Of the sixteen rabbits at each time point, half were subjected to high level impacts, the other half low level. These impact energy levels were the same as those used previously (i.e. low level = 0.9 J, and high level = 6.3 J).

In the interim following impact the animals were individually housed and allowed cage activity (36" x 24" x 15.6"). On the predetermined test date each rabbit was anesthetized, using ketamine and xyaline, and then euthanized using Ecklimide (2 ml). Both the right (test) and left (control) patellas were immediately removed for biomechanical testing.

Due to the effects of arthrotomy seen in the open joint sham group out to 14 days post-surgery, a 6 day, closed joint, sham group was added to the study. The six rabbits in this sham group were placed in the restraining seat with their right leg hyperflexed and held in place by the bar clamp. The animals remained in the hyperflexed position for five minutes. They were then returned to their cages. Six days later the rabbits were euthanized and their patellae tested.

#### Blunt Impact:

Patellar impact and data collection were carried out using the same gravity impactor, load cell, and accompanying computer system previously described (see Open Joint Materials and Methods). The restraining seat was again used to hold the hyperflexed right leg, thereby preventing full body movement during impact. Prior to impact the rabbits were anesthetized with ketamine (15 mg/kg) and xyaline (2 mg/kg) and were held under during impact with isoflurine (2%-2.5%) per 2L of oxygen as previously described. The right knee was shaved, then swabbed with alcohol and betadine prior to

placing it in the restraining seat. Immediately following the impact, the rabbits were given an injection of butorphenol (0.10 cc) to help reduce pain. The animals were then returned to their cages.

#### Data Collection:

As in the previous study, indentation relaxation tests were carried out on the patellar AC. The indentation procedures were carried out using a servohydraulic testing machine (MTS models 1330 and 8500). Cartilage response loads were measured by a load cell (25 lb. range). The load cell outputs were amplified using a Validyne amplifier prior to data collection. Data collection was carried out with a Commodore Amiga computer. Data collection software was created for the Amiga (Jim Husch, programmer) which provided real time display of both the load response and actuator displacement. Load-time data was collected at a rate of 20 Hz. The raw ascii data was transferred to a Sun sparc station 10 computer for analysis, see Biomechanical Analysis.

#### Grip Assembly:

For the closed joint study a new system of holding the patella during mechanical testing was developed. A single screw, stainless steel, vice-like grip was built. Unlike the potting method used in the "open joint" study, the grip allowed testing access to both the medial and lateral facet of the patella. This grip was attached to a 1 1/4 inch, stainless steel post, 1/2 inch in diameter, with a 1/2 inch threaded section at the opposing end (Figure 14). A clear acrylic bath with an inner diameter of four inches was designed to slide up and down on the grip post by way of a hole in the bottom of the bath. A rubber 'o' ring lining the hole prevented loss of bath saline. This allowed the bath to be

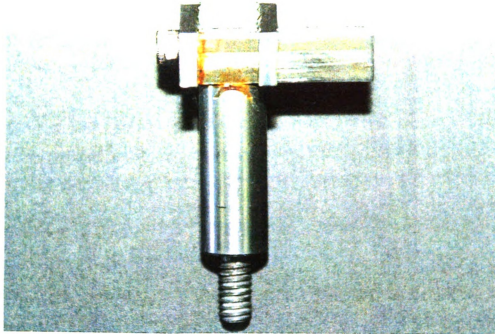


Figure 14: Vice-like grip used to hold patellae.

lowered exposing the grip in order to change specimens or align the surface of the patella. This grip-bath assembly was attached to the head of a camera mount by the threaded portion at the base of the grip post. The ball and socket joint of the mount head allowed the bath-grip assembly to be rotated  $360^\circ$  while simultaneously being tilted as far as  $90^\circ$  from its vertical position. The top of the bath was cut at a  $45^\circ$  angle to allow a full bath to be tilted without spilling. A trigger release mechanism allowed entire assembly to be adjusted to the desired position and locked into place. This entire bath-grip mount assembly allowed the surface of the patellar AC to be visually aligned perpendicular to the indenter while maintaining the bath environment, Figure 15. Furthermore, the bath-grip mount was fixed to a double axis slide platform which

allowed horizontal movement of the entire assembly. This allowed a specific position on the AC to be directly aligned beneath the fixed position of the indenter.

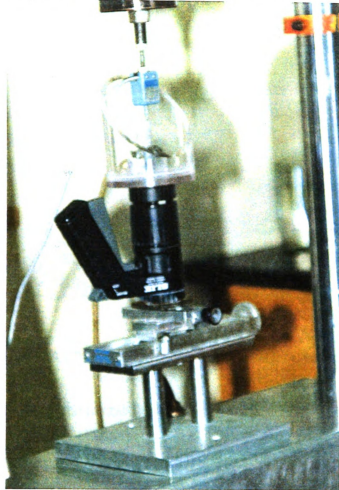


Figure 15: Bath-grip mount assembly.

#### Test Procedure:

The patella was placed in the grip end to end with medial and lateral facets exposed, Figure 16. The bath, filled with 0.10 M phosphate buffered saline at room temperature, was then raised immersing the patella. The patella remained immersed except for brief periods when the indentation site was changed and the articular surface was aligned.

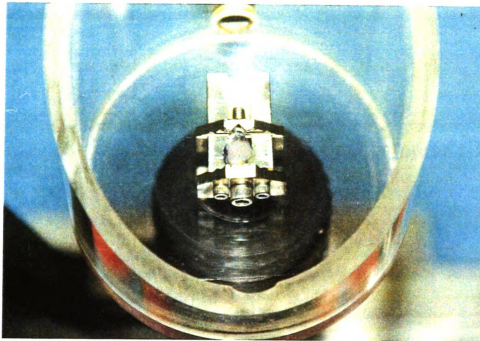


Figure 16: Patella held in grip.

Testing was carried out on the lateral facet. As in the open joint study, stress relaxation tests were again carried out using a solid, rigid, cylindrical, flat ended indenter 0.50 mm in radius. Indentations were performed with a ramp rate of 1.20 mm/s to a depth of 0.10 mm where the indenter was held for 150 seconds while resistive cartilage loads were monitored. The new data collecting system allowed the acquisition time to be increased from 100 sec in order to assure that the cartilage reached equilibrium. A needle probe was again used to determine the thickness of the cartilage at the site of the indentation immediately following the stress-relaxation test. At the six day time point, two stress-relaxation tests were performed in the center of the lateral facet. One on the proximal half and the other on the distal half, Figure 17. At the later test times, a third

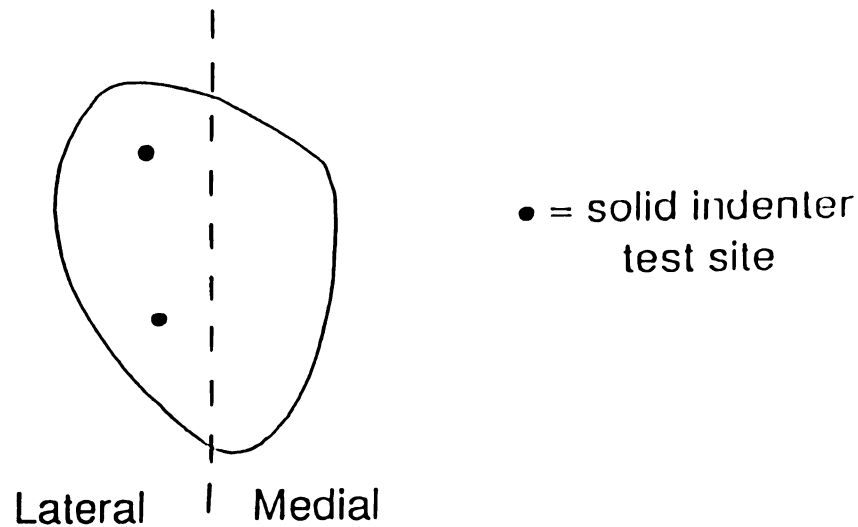
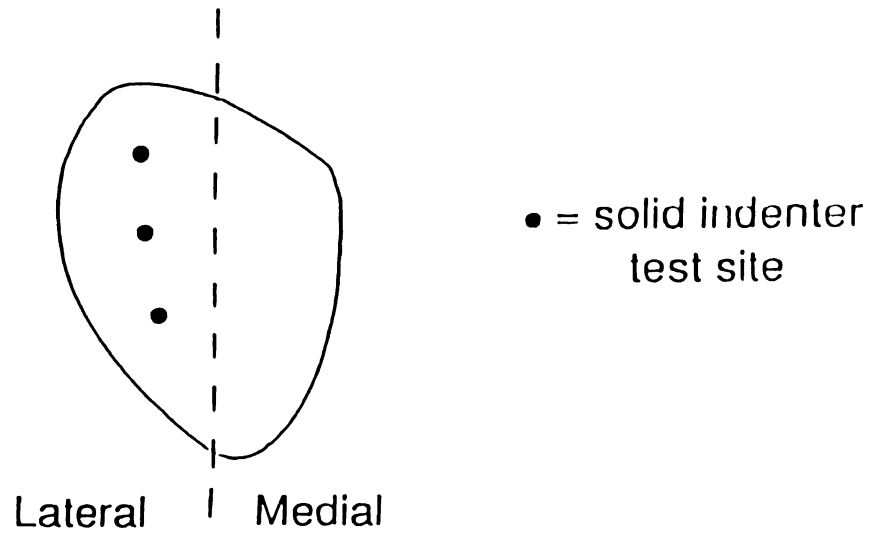


Figure 17: The six day, closed joint test sites.

test was added, Figure 18. At six days and three months tests were also performed on the medial facet of each patella. A visual comparison of the medial test values ( $G_u$ ,  $G_r$  and  $\eta$ ) revealed spatial differences between the mechanical response of the two facets. For comparison reasons only the lateral facet results will be presented.

A total of 64 rabbits entered into the closed joint study. Two, one year, low level, animals died and one, high level, one year, animal was dropped in into the 3 month time period. Two more rabbits, one high level and one low, were removed from the 3 month time point for an alternate study after it became apparent that their inclusion in the results would not alter the overall outcome.



**Figure 18:** The closed joint test sites following six day time point.

## **CLOSED JOINT RESULTS**

### **Impact Trauma:**

The peak impact loads were determined by the plotting program. The average impact load for the low and high level impacts group were  $158 \pm 20$  and  $562 \pm 53$ , respectively. At low levels only 2 of the 28 animals impacted were fissured. At high impact levels 24 out of 30 animals were fissured. These impact results are comparable to those seen in the open joint study. A complete record of the closed joint impact parameters are presented in Tables 3 through 10 in the Appendix.

### **Mechanical Testing:**

#### **Six Days**

The following results are based only upon the mechanical tests carried out on the lateral facet of the patellae. For the low level group the average instantaneous shear modulus ( $G_u$ ) was increased 6.3% on the test side compared to the contralateral control side. The relaxed modulus ( $G_r$ ) was up 2.5% on the test side and the viscosity ( $\eta$ ) was 15.5% larger on the test side relative to controls. None of these differences, test vs. control, were found to be significant. The calculated material parameters for the six day, low level, impact animals are compiled in Table 11, see Appendix.

At high impact levels the average  $G_u$  values were increased 17.7% on the test

side. Both the average test and control values for Gr were 0.200 MPa. The viscosity values were up slightly an average 14.2% on the test side. Neither of the differences in Gu and  $\eta$  values were found to be significant. The six day, high impact, results are tabulated in Table 12 in the Appendix.

Overall, the ANOVA detected no significant difference between the results of the low and high impact levels for any of the mechanical parameters (Gu, Gr and  $\eta$ ) within the test and control groups (e.g. low test Gu vs. high test Gu).

### Three Months

Similar to the six day results, little change was found between the test and control values of the low or high level impact groups. At low levels test values of Gu and Gr were only slightly higher than those of controls by 4.1% and 3.6%, respectively. Low impact  $\eta$  values were a mere 1.9% greater on the test side compared with controls. None of these small differences were found to be significant, see Appendix Table 13.

In contrast to the slight increases in stiffness measured in the low level group, the high level group showed a slight decrease in test side stiffness. Gu values were down by an average of 2.4% on the test side and Gr values by 2.6%. However, like the low level group, a slight increase in  $\eta$  was again seen on the test side, 6.3%. None of these differences were found to be significant, see Appendix Table 14.

In a comparison between low and high level parameters a significant difference was detected between the test side values of Gr, and between Gr values on the control side ( $P = 0.00$  and  $P = 0.00$ ). No significant difference was detected for either Gu or  $\eta$  values with respect to impact level.

### Six Months

At six months the results continued to show little or no change between test and control values for either low or high impact levels. The low level average  $G_u$  values showed the largest difference with an increase of 27.3% on the test side. The low level  $G_r$  values were essentially unchanged between test and controls (0.05%). The  $\eta$  values seemed to follow the same trend as  $G_u$ , increasing 20% on the test side. None of these differences were found to be significant.

At high impact levels only small variations were measured.  $G_u$  values were slightly down an average of 8.0% on the test side, while  $G_r$  were slightly up 4.5%. The average value for  $\eta$  was down 4.8% on the test side. As has previously been the case, none of these differences were significant. The mechanical parameters for the high and low impact groups are presented in Tables 15 and 16 in the Appendix.

The overall ANOVA did reveal a significant difference between high and low level impacts within parameter  $G_r$  at the six month time point. Interestingly, this difference was seen not only between test side values, but also between control values  $P = 0.001$ . Multiple researchers were involved in collecting the mechanical test data at this time point. Small variations in the testing procedure between investigators may have contributed to some of these differences.

### One Year

At one year post-impact an overall decrease in test values was measured in the low level group. The unrelaxed and relaxed shear modulus were down 33% and 14%, respectively. After removing an extraneous viscosity measurement (rabbit BN3, control,

site 2), the test side was found to be decreased by 19%. None of these decreases were found to be statistically significant.

At high impact levels, similar decreases were measured in the test side values. Gu and Gr were down 22% and 12%, respectively.  $\eta$  was reduced by 25%. Both Gu and  $\eta$  were found to be significantly less than control values ( $P = 0.04$ ,  $P = 0.03$ , respectively). The mechanical results for the low and high impact groups are presented in Tables 17 and 18, respectively.

### Shams

Unlike the open joint study, Gu and Gr test values were virtually unchanged compared to controls. The test side Gu and Gr values were 5% and 2% higher than their respective controls. This suggests that early differences in the open joint study were predominantly an affect of arthrotomy (see Appendix Table 19).

### Comparison of Background Studies

Upon completion of the background studies, comparisons were made not only between the affect of impact level, but also the affects of using either the open or closed joint model. Histograms of ratios (test/control) were used to visually depict the time varying trends of the measured mechanical parameters. The ratios in these histograms were determined from parameter averages and not the average values of the individual test ratios (i.e. the last 3 columns of Tables 11 through 19, see Appendix). Ratios are not normally distributed, therefore the mean of these ratios does not accurately represent the relationship between the average test and control values. Figure 19 represents a comparison between high and low level impact, Gu ratios of the Open Joint Study.

### UNRELAXED MODULUS (Gu) Open Joint Comparison

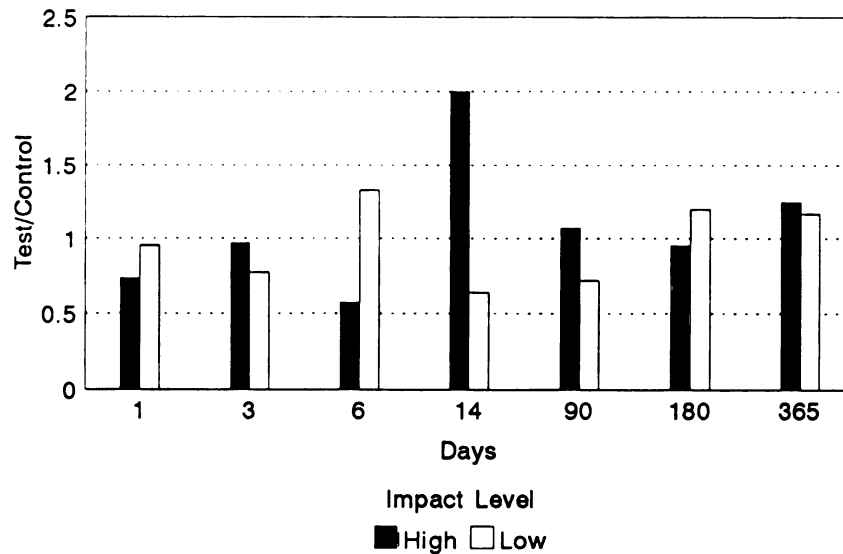


Figure 19: Open joint, high vs low level impact, Gu trends.

Except for an increase at 6 days, the low level impact groups showed a gradual decreasing trend after day one which reached a minimum at 14 days. By six months the test values had returned to control levels where they remained out to one year post-impact. At high impact levels an immediate drop in stiffness was measured at one day post-impact. The test values remained at or below control values out to 14 days when a large increase in the unrelaxed modulus was measured. After 14 days the test values returned to control levels where they remained. This same comparison was carried out for the closed joint study, Figure 20. A general decreasing trend was noted in the high impact groups over the one year test period. In the low impact groups the test values remained at or above control levels until 1 year post-impact. By 1 year test values at

## UNRELAXED MODULUS (Gu)

Closed Joint Comparison

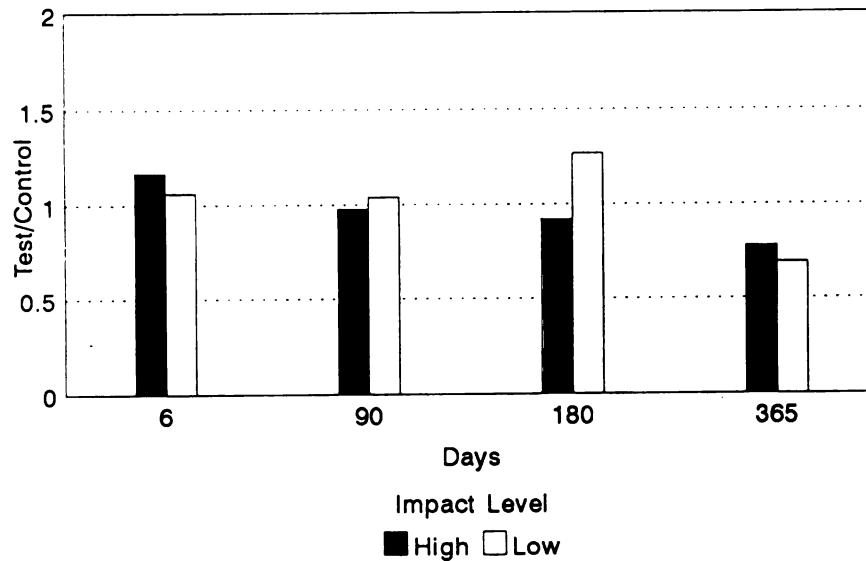


Figure 20: Closed joint, high vs low level impact, Gu trends.high impact levels

both impact levels showed a decrease below controls. At this decrease was significant ( $P = 0.04$ ).

The time trends measured in Gr in the open joint study were similar to those described for Gu, Figure 21. A gradual decrease in stiffness was noted out to 14 days post-impact at low impact levels. After 14 days, a gradual increase was noted. By 1 year the modulus values had returned to control levels. On the contrary, at high impact levels, Gr dropped substantially at 1 day and remained low out to 3 months. At 3 months a sharp increase was noted in the test values. This was followed by a decrease at 6 and 12 months back towards control levels.

### RELAXED MODULUS (Gr) Open Joint Comparison

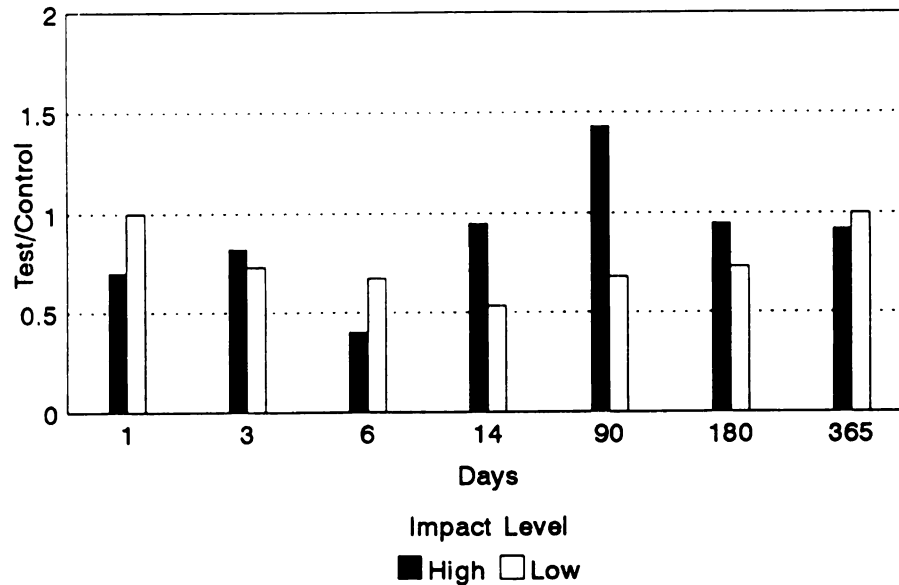


Figure 21: Open joint, high vs low level impact, Gr trends.

In the closed joint model large differences were not noted in Gr between impact levels, Figure 22. The Gr values were consistently close to control levels until 1 year post-impact where both low and high impact groups displayed a slight decrease.

Specific time trends were not apparent in flow viscosity in the open joint study, Figure 23. Except at 1 and 6 days, low level test viscosity values remained below controls. The high impact test values were also consistently low, except at 14 days where a large increase in viscosity was measured.

In the closed joint study, the flow viscosity trends resembled those of Gu, Figure 24. At high impact levels an overall decrease in the test values was noted over the one year test period. At low levels, the average test side viscosities values were at or above

### RELAXED MODULUS (Gr)

Closed Joint Comparison

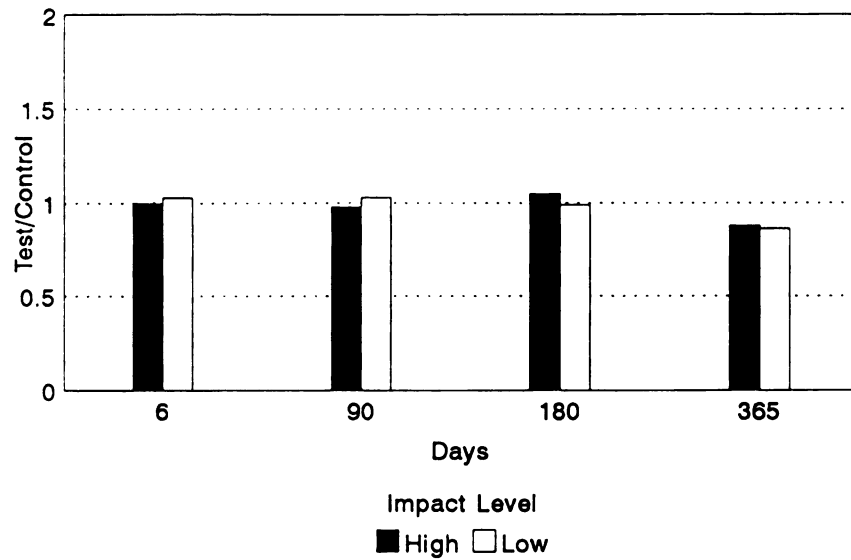


Figure 22: Closed joint, high vs low level impact, Gr trends.

### FLOW VISCOSITY

Open Joint Comparison

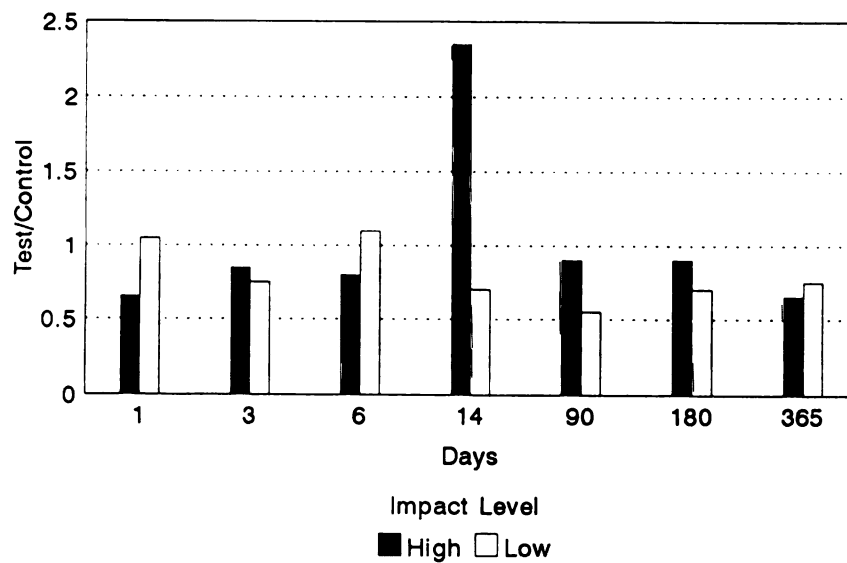


Figure 23: Open joint, high vs low level impact,  $\eta$  trends.

## FLOW VISCOSITY

### Closed Joint Comparison

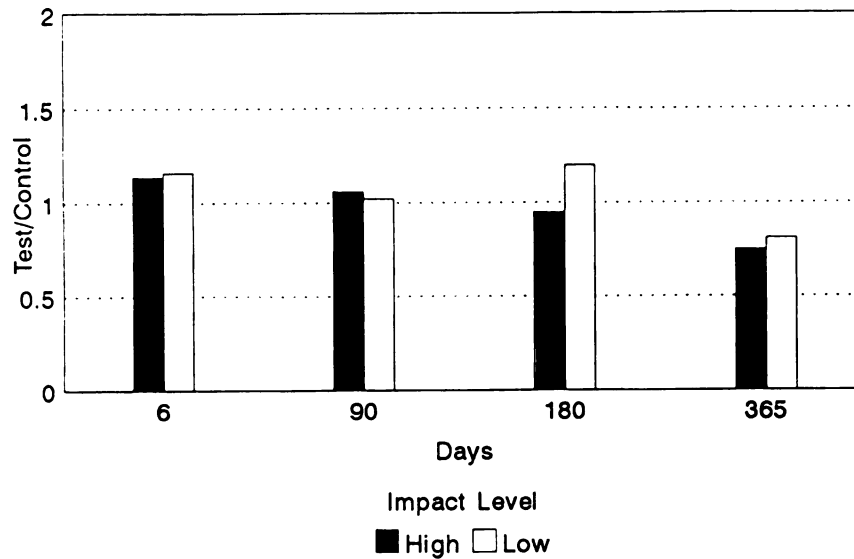


Figure 24: Closed joint, high vs low level impact,  $\eta$  trends.

control levels out to 1 year post-impact. At 1 year the test side viscosities at both impact levels were below their respective controls. At high impact levels this decrease was significant ( $P = 0.03$ ).

### Supplemental Animals

The results of the open joint study were based upon three observations per group at each time point. The differences between the closed and open joint results prompted the addition of further testing. A total of 16 rabbits underwent open joint impact (eight at each impact level) and were placed into a three month test group. The 3 month test period was chosen because of large discrepancies between the Gr and  $\eta$  results of the open and closed joint studies at this time point. The mechanical testing procedure carried

out on these supplemental groups was the same as that used in the closed joint study.

The results of the supplemental groups closely matched the results of the 3 month closed joint groups. At both low and high impact levels the test side values were close to control levels. The large increases measured in Gr and  $\eta$  at high impact levels in the open joint study were not detected in the supplemental groups (see Appendix Tables 20-23 for results of the 3 month, supplemental groups).

As a personal point of interest, two rabbits were subjected to high level open joint impacts which included the insertion of pressure film. These rabbits were euthanized at six days post-impact and their patellae removed for testing. The unrelaxed and relaxed moduli were decreased an average of 17.6% and 54.3%, respectively. These results provided additional confirmation of the 6 day, open joint, high impact results.

## **DISCUSSION OF BACKGROUND STUDIES**

The primary goal of the open joint study was to investigate the degenerative effects of blunt trauma on AC. An additional goal was to document the load conditions within the joint during impact. This documentation process required the use of arthrotomy. In the study that followed, blunt impact was delivered under non-invasive closed joint conditions. This impact scenario eliminated possible cartilage softening due to a transient surgical synovitis. In both studies indentation stress-relaxation tests were performed at predetermined post-impact times. The mechanical parameters,  $G_u$ ,  $G_r$  and  $\eta$ , were calculated for both studies using identical analysis methods. A comparison of results revealed differences in the time dependent responses of these mechanical parameters. These differences were not only found to be a function of impact level, but also of the model type (i.e. open vs. closed joint).

Within the open joint study, differences were noted in the stiffness results (i.e.  $G_u$  and  $G_r$ ) between the low and high level impact groups with respect to the post-impact test time. These differences were most obvious in  $G_r$ . At low impact levels,  $G_r$  values gradually decreased out to 14 days post-impact. However, at high impact levels an acute drop in  $G_r$  was noted immediately 1 day after impact and these values remained low out to 14 days. As previously noted the softening effects of arthrotomy have been documented ((Thompson, 1975; Frost and Ghosh, 1984; Svalastoga and Reiman, 1985;

Pelletier, et al., 1985; Walker, 1991; Messner, et al., 1993). This softening may explain the overall decrease in stiffness measured in both low and high impact levels at early time points in the open joint study. However, it does not explain the acute decrease measured at high impact levels. This difference was attributed to the extensive trauma (i.e. fissures) imparted by the high energy impacts (Ide, 1992). This structural damage was believed to have compromised the load carrying ability of the cartilage thereby initiating an irreversible degeneration process. The sharp rise in stiffness measured at 3 months was thought to be the result of cartilage breakdown and compaction. The gradual decreases measured at 6 months and one year were the result of continued breakdown.

At the low impact levels, in the open joint study, only 25% of the test side patellae showed signs of impact fissuring. Therefore, in the majority of the low impact specimens the structural integrity of the cartilage was unharmed. The gradual softening observed in the first two weeks following impact was probably solely an effect of surgical synovitis. Without structural damage this cartilage was able to recover.

Based on the hypothesis that impact fissures have a degenerative effect on cartilage stiffness, an acute reduction in stiffness was anticipated at high impact levels in the closed joint study. However, although 75% of the test patellae were fissured, a marked decrease in stiffness was not measured at the six day time point. In fact, unlike the open joint study, no large differences were noted between high and low impact levels in the closed joint study. By one year post-impact all three mechanical parameters at both impact levels were decreased on the test side. At high impact levels,  $G_u$  and  $\eta$  were significantly decreased. These results suggest a long term degeneration process, like that

reported following ACL transection (Brandt, et al, 1991), may be required for the development of OA using this closed joint model.

Two possible explanations have been considered to explain differences between the open and closed joint studies. The first possibility is that the differences between impact levels observed in the open joint study, may have been caused by animal to animal variation and the small sample size used at each time point ( $n=3$ , per impact level). The second possibility is that an interaction may have taken place between the fissured cartilage and damage synovium in the high impact groups. This interaction may have enhanced the cartilage degeneration resulting in the stiffness differences between the high and low impact levels of the open joint study. In an attempt to address the small sample size, the supplemental groups were added. The results of the 3 month, open joint supplemental tests closely matched the results from 3 month, closed joint study at both low and high impact levels. Based on these results it would appear that the small sample sizes was the cause of the differences between impact levels in the open joint study. However, the results of the two additional high impact, open joint supplemental rabbits tested at 6 days post-impact overwhelmingly supported the decreases in stiffness measured at 6 days in the original open joint study. At the conclusion of the supplemental tests, questions still remained about the differences between the results of the low and high impact groups of the open joint study, and the differences between the open and closed joint studies.

The first question dealt with the effects of impact fissures. It was still unclear whether the presence of fissuring alone, without a synovial inflammation, could produce a measurable decrease in cartilage stiffness. Secondly, questions remained as to whether

or not an interaction may have occurred between the fissured cartilage and the damaged synovium which contributed to the large decrease in stiffness measured at high impact levels in the open joint study. If such an interaction exists, it would also help explain the differences between the results of the high impact groups in the open and closed joint studies. Finally, assuming that transient synovial inflammation can enhance the degeneration of fissured cartilage, can a synovitis be created by mechanical means under closed joint conditions.

## **OBJECTIVES OF THE STUDY**

The investigation developed in the following pages will be presented in two segments. The first segment, the Acute Study, will address questions about the effects of severe trauma and surgical synovitis. The initial goal of this study will be to define the effects of severe trauma, in particular surface fissures, on the mechanical response of AC. After documenting these effects, the study will attempt to measure any enhanced degradation effects which may occur when fissures are present simultaneously with a surgical synovitis. The second segment, the Synovitis Study, will investigate the possibility of inducing a synovial inflammation using non-invasive blunt trauma to the synovial tissue surrounding the joint. Biomechanical and histological analysis will be used to determine the effects of this trauma on the AC and synovium. These investigations will further introduce biphasic theory into the ongoing OA research carried out in our laboratories. Unlike the elastic and viscoelastic analysis used in the background studies, biphasic theory is based upon the microstructure of the cartilage. It does not incorporate a phenomenologic material model to quantify the mechanical characteristics of cartilage. By incorporating biphasic analysis in the present studies we hope to directly correlate changes in the material properties of the cartilage, specifically permeability, to the presence of trauma (i.e. fissures).

## **THE ACUTE STUDY**

As previously mentioned this study will address two main objectives. The first objective will be to measure the affects of impact induced fissures on the mechanical response of AC. This objective requires the induction of surface fissures which are unexposed to a possible interaction with the surrounding synovial membrane. The second goal will be to measure possible changes in the mechanical response of fissured AC which may occur when exposed to a surgically induced synovitis. In order to detect an interaction between the fissures and surgical synovitis, the effects of the synovitis on healthy cartilage will first be determined. Then by combining these two factors (i.e. fissuring and synovitis) their coupled effect on the mechanical response of AC will be determined. By defining these effects we hope to discern possible reasons for the short term response differences noted between the two background studies. For instance, differences between cartilage which has been subjected only to surgical synovitis, and that which has been exposed to both synovitis and fissuring, may help explain differences between the low (unfissured) and high (fissured) level impact groups in the open joint study. Further comparison between the response of fissured cartilage and fissured cartilage exposed to a synovitis may provide a possible explanation for differences between the results of the open and closed joint, high impact groups.

## **ACUTE STUDY MATERIAL AND METHODS**

### **The Acute *In Vivo* Study:**

Three separate treatment groups were used in this study. The first group was the fissure isolation group. The right patella of this group was impacted to induce cartilage fissures while the left leg served as a non-surgical control. Both patellae were immediately removed from the animal following the blunt trauma procedure for mechanical testing. The immediate removal of the test patella prevented the cartilage from being exposed to a transient softening affect associated with post-surgical synovitis. Differences between the test and control responses in this group were directly associated with the presence of the fissures. This group was referred to as the Time Zero, High Impact group.

The second group acted as a surgical isolation group. Arthrotomy was performed on the right leg of these animals. The rabbits were then returned to cage activity for 24 hours. One day after surgery these rabbits were euthanized and their patellae extracted for testing. Differences between the test and control responses in this group were attributed to the 24 hour exposure to the surgical disrupted joint. This group was described as the One Day, Sham group.

The last group combined the affects of impact fissures and surgical synovitis. Immediately following arthrotomy the test leg was subjected to blunt impact. The rabbits

were then returned to their cages until the following day when they were euthanized and their patellae excised for testing. This exposed the mechanically fissured cartilage to a surgically disrupted joint environment. Differences between the results of this test group and those of the time zero and sham group would suggest a possible interaction between the cartilage fissures and surgically damaged joint. This third group was called the One Day, High Impact group.

#### Surgery/Blunt Impact

An open joint surgery was performed on the right hind limb of all 18 rabbits in the acute study (6 rabbits per group). The left leg served as a non-surgical control. The time zero, high impact animals were euthanized just prior to surgery. An unsterile arthrotomy was performed on these animals by the principle investigator. The surgeries performed on the one day animal groups were done under sterile conditions by Dr. Charles E. DeCamp. All surgeries included the insertion of pressure sensitive film between the patella and femur, regardless of the impact status. Both the time zero and one day, high impact groups received blunt trauma to the right knee during the surgical procedure. These impacts were carried out using the gravity impactor and data acquisition system described previously (see Open Joint Materials and Methods). All impacts were delivered at the high energy level (6.3J). As previously stated in the description *in vivo* study, the patellae from the time zero, high impact rabbits were immediately removed following impact for mechanical testing. The one day animals were sutured after surgery and/or impact and returned to cage activity for 24 hours.

## Testing Procedure

### (Rigid indenter)

Three stress-relaxation tests were performed on the test and control patellae of each rabbit using a rigid, solid, cylindrical indenter 1.0 mm in diameter. All three tests were aligned proximal to distal along the center of the lateral facet, refer to Figure 17 in the Closed Joint study. A ramp rate of 1.2 mm/s was used to indent the cartilage to a depth of 0.10 mm. This indentation was maintained for 150 sec. while resistive cartilage forces were measured. The patella was held in place during testing by a grip assembly (described in the Closed Joint Materials and Methods). Immediately following each test a thickness measurement was made at the site of indentation using a needle-like probe to penetrate through the cartilage to the underlying bone.

### (Porous indenter)

Two additional stress-relaxation tests were carried out on each patella using a rigid, porous, cylindrical indenter 1.0 mm diameter. Figure 25, shows a photograph of this indenter. Both porous indentation tests were indented into the surface of the cartilage to a depth of 0.05 mm and were held at this depth for 1000 sec. while resistive forces were recorded. These porous tests were performed at two separate loading rates. The first was brought to the maximum indentation depth in 1.0 seconds, while the other was done over a 2.0 second interval. Figure 26, depicts the position of the porous tests on the surface of the patellar cartilage with respect to the positions of the three rigid indentation tests. The porous stress-relaxation data from two rabbits in each of the three test groups was analyzed using biphasic theory.

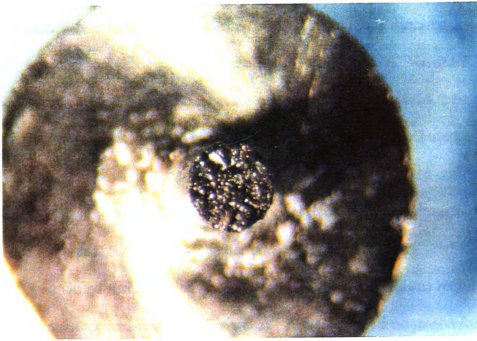


Figure 25: Porous indenter.

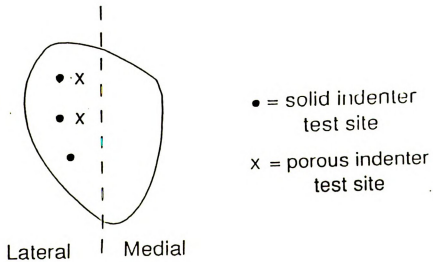


Figure 26: Porous indentation test sites.

There were two main reasons for the addition of the porous indenter tests. The first reason was directly related to the boundary conditions required by the biphasic model for the solution of an indentation stress-relaxation test. In order to achieve a closed form solution, the articular surface of the cartilage is assumed to be permeable to water flow during the loading phase (Mak, et al., 1987). The pitted surface of the porous indenter allows water to escape through the articular surface during the loading phase. The rigid indenter, does not allow the exudation of water through the surface in the area of contact between the indenter and cartilage. Without a permeable boundary condition, a closed form solution does not exist and biphasic analysis requires the use of a finite element approximation (Spilker, et al., 1991). The second reason for the addition of the porous tests is related to the goals of the acute study. It was anticipated that the fissures created during impact would cause a decrease in the structural stiffness of the AC. We further hypothesize that this mechanical disruption of the collagen network would also result in increased cartilage permeability, specifically at the surface where fissures are present. As previously noted, the integrity of the cartilage surface layer plays a key role in restricting fluid exudation during loading (Setton, et al., 1993). The presence of surface fissures should increase the ability of water to escape through the cartilage surface. With the permeable boundary conditions incorporated in the porous indenter, we hope to detect increases in permeability which may have been masked by the impermeable rigid indenter.

### Biomechanical Properties

The indentation testing method was chosen in the original open joint study because

it allows the *in situ* determination of cartilage material characteristics. The servohydraulic test machine used for mechanical testing was incapable of applying a constant load of small enough magnitude to perform a creep test ( $P < 0.7N$ , Parsons and Black, 1977). The testing machine was, however, capable of generating small constant displacements ( $<0.10mm$ ) making it compatible with stress-relaxation testing. Both the elastic solution of Hayes, et al., 1972, and the viscoelastic analysis of Tobolsky (1960) were used to compute the shear moduli ( $G_u$  and  $G_r$ ) and the flow viscosity ( $\eta$ ), respectively, from the test data. For comparison reasons, these same analysis techniques were also applied in the current studies. In addition, biphasic analysis was also incorporated to obtain material properties for the cartilage, the permeability in particular, based upon its microstructural composition. Due to its relative newness to our OA investigations, a historic development of the biphasic theory has been included prior to description of the analysis process.

#### Elastic/Viscoelastic Analysis

In 1972, Hayes, et al., determined a solution for the indentation of a linear elastic layer bonded to a rigid half-space. Assuming small strains, the shear modulus ( $G$ ) for the case of a rigid, cylindrical, plane-ended indenter is expressed as

$$G = \frac{P(1-\nu)}{4a\omega_o K(a/h, \nu)} \quad (1)$$

where; ( $P$ ) is the resistive load of the elastic layer, ( $a$ ) is the radius of the indenter, ( $\nu$ ) is Poisson's Ratio, ( $h$ ) is the layer thickness, and ( $\omega_o$ ) is the indentation depth (Figure

27). The variable ( $K$ ) is a correction factor, which adjusts for the finite thickness of the elastic layer based on the aspect ratio ( $a/h$ ) and a predetermined value for  $\nu$ .

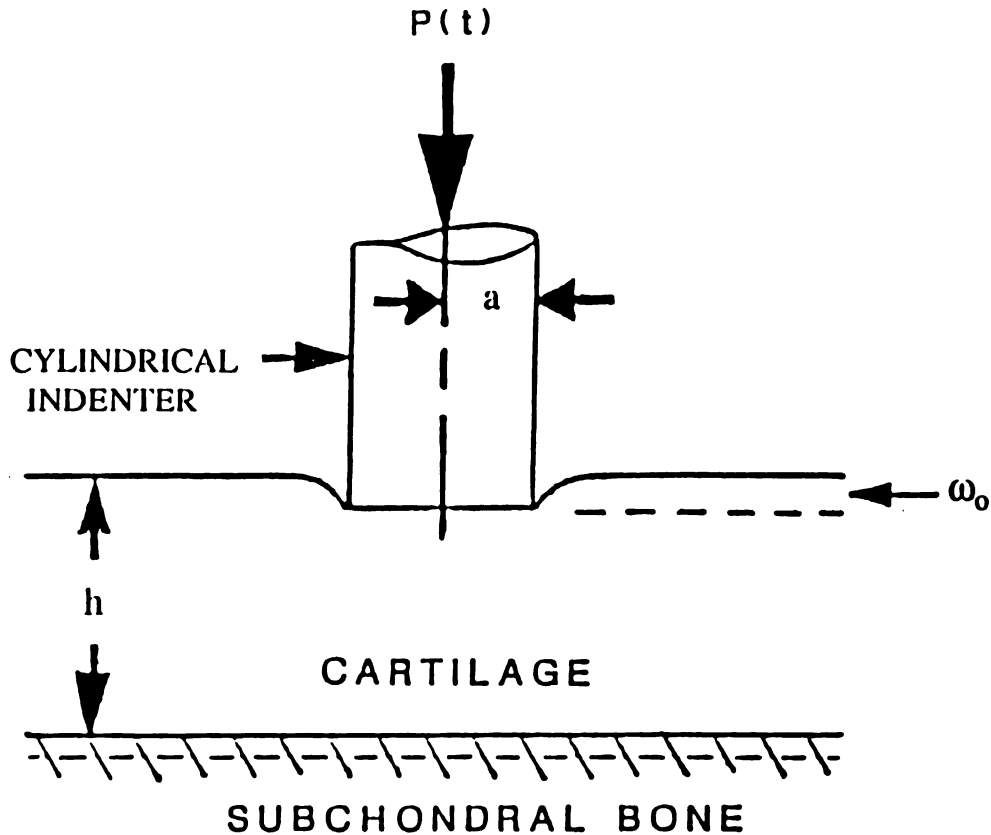


Figure 27: Indentation test.

Due to the high rate of loading used in our rigid indentation tests, the cartilage is considered to be instantaneously incompressible (Mak, et al., 1987) and a Poisson's ratio of 0.50 is used for the computation of  $G_u$  from peak response load. The computation of the relaxed shear modulus ( $G_r$ ) was based on the equilibrium load. An average Poisson's ratio of 0.4 was used for this calculation. The equilibrium Poisson's ratio was based upon prior experimentally determined values for  $\nu$  (Parsons and Black,

1977). Figure 28, shows a load-time curve for a typical stress-relaxation indentation test and depicts the response regions used for the computation of  $G_u$  and  $G_r$ . The actual calculation of  $G_u$  and  $G_r$  was carried out via a computer program.

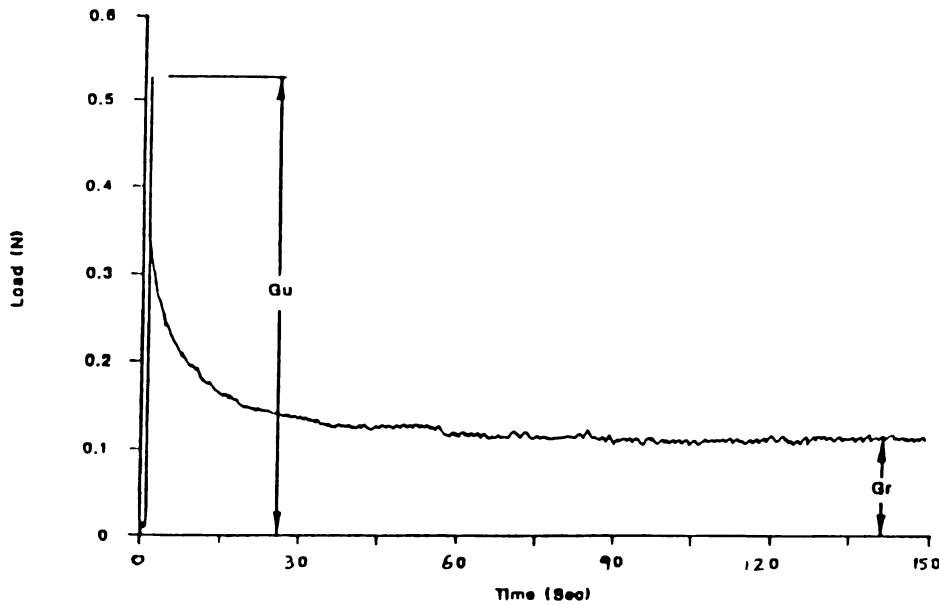


Figure 28: A stress-relaxation load-time response curve.

The thickness of the cartilage at the site of the indentation test is required for the computation of the correction factor ( $K$ ). This measurement was made using a needle-like probe described previously. A typical load-time plot from a thickness test is shown in Figure 29. The thickness of the cartilage ( $h$ ) is calculated graphically as follows

$$h = (t_r - t_i) \times (R) \quad (2)$$

where,  $t_i$  is the time corresponding to the onset of loading,  $t_r$  is the time corresponding

to the sharp rise in load indicating contact with the subchondral bone, and R is the ramp rate of the needle-like probe.

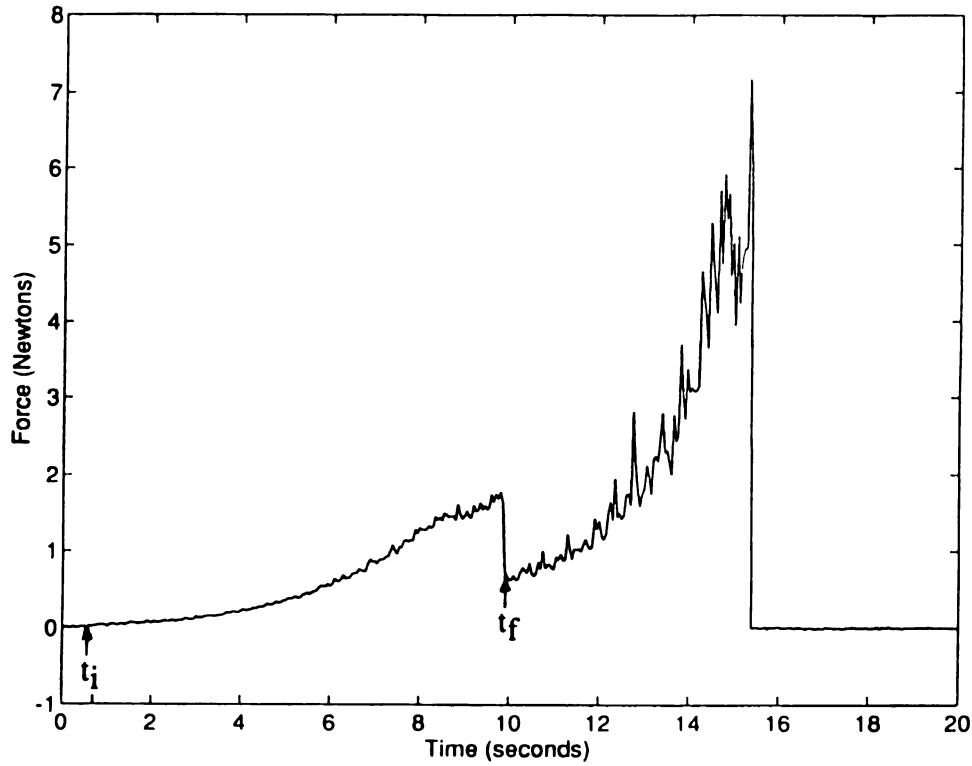


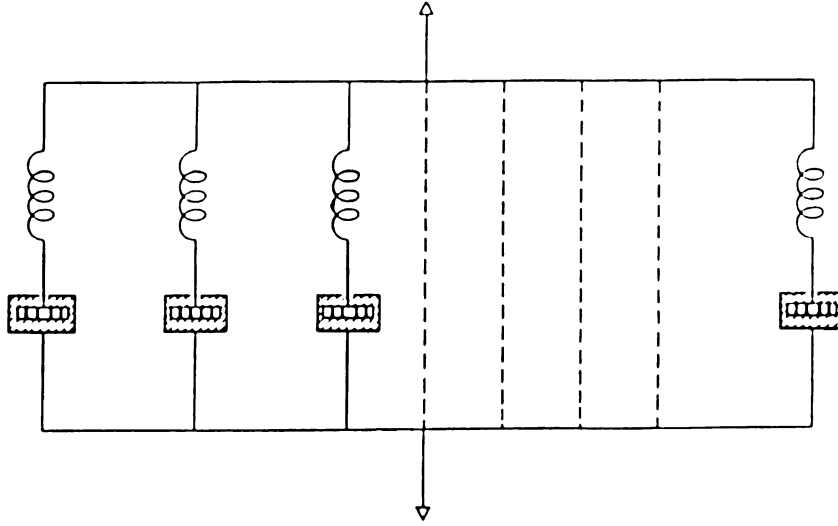
Figure 29: A load-time plot of a thickness test.

The calculation of the flow viscosity is based upon Tobolsky's analysis of the rheological behavior of a generalized Maxwell model (GMM), Figure 30. Based on this analysis the time dependent shear modulus ( $G(t)$ ) of the GMM is given in terms of the time constant ( $\tau$ ) as

$$G(t) = \int_{-\infty}^{\infty} H(\tau) \exp(-t/\tau) d(\ln\tau) \quad (3)$$

Where,  $H(\tau)$  is the relaxation time spectrum. In turn the flow viscosity ( $\eta$ ) can be expressed as

$$\eta = \int_{-\infty}^{\infty} G(\tau) d\tau \quad (4)$$



Generalized Maxwell Model

Figure 30: A generalized Maxwell model.

By assuming the viscous elements of the GMM have relaxation times with a box distribution,  $H(\tau)$  can be expressed as a constant ( $E_o$ ) within the response region bonded by  $\tau_{\min} \leq t \leq \tau_{\max}$ . Therefore, the shear modulus is given by

$$G(t) = E_o [E_1(t/\tau_{\max}) - E_1(t/\tau_{\min})] \quad (5)$$

where  $E_1$  is the resulting exponential integral function. Outside of this range  $H(\tau)=0$ . If the values of  $\log(\tau_{\min})$  and  $\log(\tau_{\max})$  differ by more than one, which has been shown to be true for cartilage (Woo, et al., 1980), then the central portion of the  $G(t)$  vs.  $\log(t)$  plot can be considered linear. The slope of this linear portion ( $H(\tau)$ ) is equal to

$$H(\tau) = 2.303E_o = 2.303H(\tau) \quad (6)$$

see Figure 31. By substitution, the flow viscosity (equation 5) can be reduced to

$$\eta = H(\tau) [\tau_{\max} - \tau_{\min}] \quad (7)$$

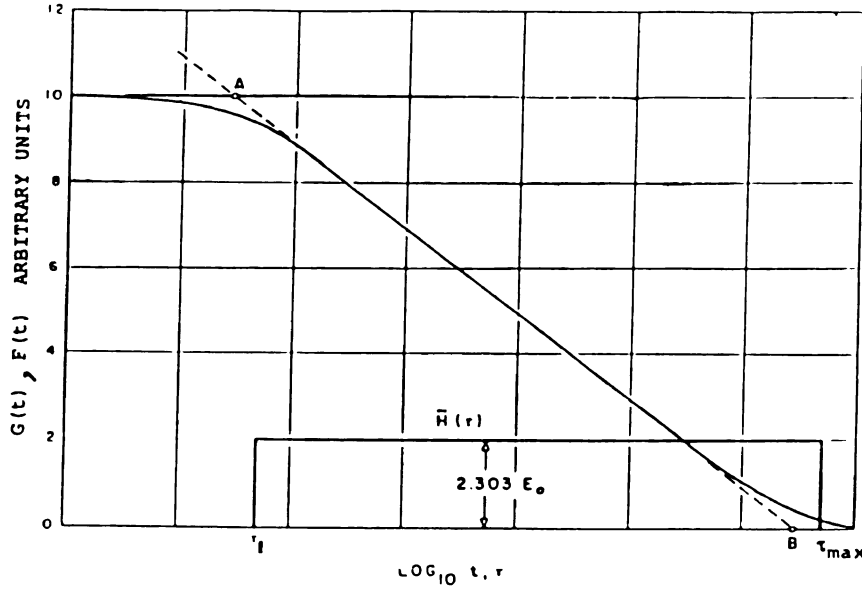


Figure 31: The theoretical response of a generalized Maxwell model.

The exact value of  $\tau_{\max}$  is not experimentally easy, or practical to determine, considering cartilage under indentation conditions requires approximately 10,000 seconds to reach complete relaxation (Mak, et al., 1987). However, as a property of the exponential function  $\tau_{\max}$  is related to the intersection time ( $T_B$ ) by the following relation

$$\tau_{\max} = 1.781(T_B) \quad (8)$$

Figure 32, shows the application of Tobolsky's analysis on an actual stress-relaxation load-logtime plot. By assuming that the cartilage is loaded instantaneously, and that relaxation begins immediately following maximum indentation,  $\tau_{\min}$  can be assumed to

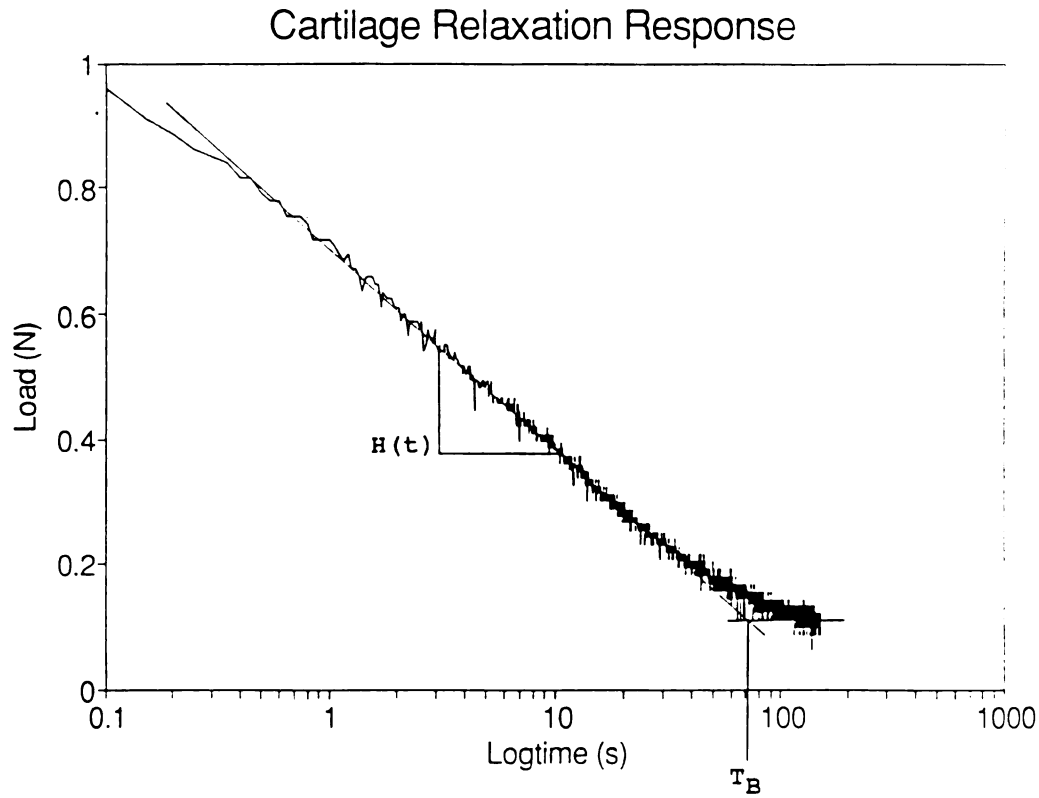


Figure 32: The application of Tobolsky's analysis (1960) on experimental stress relaxation data.

be approximately zero. Thereby, reducing equation (7) to

$$\eta = H(\tau) \tau_{\max} \quad (9)$$

By fitting a line through the average equilibrium load an intersection time ( $T_B$ ) was determined for the experimental data. The calculations of the flow viscosity were carried out via computer analysis.

The elastic calculations of  $G_u$ ,  $G_r$ , and the viscoelastic calculation of  $\eta$ , were carried out for all the rigid indentation tests performed in the acute study. As a point of

interest these analysis techniques were also applied to the porous tests of the two rabbits from each group which were analyzed by the biphasic model. Theoretically, the slower rates of loading used for the porous tests (1 - 2 seconds) should allow the afflux of fluid out of the cartilage. This should result in  $G_u$  values smaller than those calculated for the fast, solid indenter tests. Under stress-relaxation indentation conditions, fluid flow through the cartilage has ceased by equilibrium and the loads are supported by the solid matrix (Mow and Hayes, 1991). Therefore, the  $G_r$  values calculated from the porous tests should be approximately the same as those calculated for the solid indenter. The flow viscosity represents the average viscosity of the GMM damping elements. Therefore, increases in  $\eta$  represent an increase in the resistance of cartilage to relaxation. The permeability, measured by the biphasic analysis (see following text), is a measure of the ease with which fluid moves through the cartilage. Increases in permeability are directly related to increases in relaxation. Therefore, an inverse relationship between the flow viscosity and permeability values was expected.

### Biphasic Theory

In 1976, Torzilli and Mow proposed a new model for determining the mechanical properties of AC. This model describes the response behavior of cartilage in terms of two phases. The solid phase is "flow independent" and is controlled by the material properties of the solid matrix components. The fluid phase is controlled by the movement of fluid through the solid matrix and gives rise to the viscoelastic properties of the cartilage. The combination of these two phases describes the *biphasic* model. The previous methods described, Hayes, et al., 1972, and Tobolsky (1960), are limited to

describing only those portions of the cartilage response which resembled the behavior of their phenomenological models. Unlike these models, biphasic theory is based upon the microstructure of the cartilage itself. The material properties determined by this theory are derived from the overall load response and reflect the physical contributions made by solid and fluid components.

The solid matrix, which determines the response of the solid phase, consist of collagen fibrils and proteoglycan aggregates which account for approximately 20% of the wet weight of human cartilage (Muir, 1979). As an assumption of the biphasic theory this porous, solid matrix is treated as an isotropic, linear elastic solid. As previously noted, the fluid phase accounts for the period of cartilage relaxation. At equilibrium the cartilage resistance force is generated by the closely packed PGs and simple bulk compression of the solid matrix. The stresses generated in the solid during loading are described by

$$\sigma^s = \alpha p \mathbf{I} + \lambda_s \mathbf{e} \mathbf{I} + 2\mu_s \mathbf{e} \quad (10)$$

where;  $\sigma^s$  is the stress tensor of solid phase,  $\mathbf{e}$  and  $e$  are the strain tensor and dilatation of the solid matrix, respectively,  $p$  is the pressure,  $\alpha$  is the ratio of solid volume to fluid volume,  $\mu_s$  and  $\lambda_s$  are the Lamé constants for the solid matrix, and  $\mathbf{I}$  is the identity matrix.

The fluid phase is controlled by the viscoelastic response and is governed by

$$\sigma^f = -p \mathbf{I} \quad (11)$$

Under quasi-static conditions the mixture of the two phases is given by

$$\text{div } \sigma^{s,f} + \pi^{s,f} = 0 \quad (12)$$

where  $\pi^{s,f}$  are the diffusive forces arising from the frictional drag. Under these

conditions body forces are given by

$$\pi^f = -\pi^s = K(v^s - v^f). \quad (13)$$

where  $K$  is the constant drag coefficient and  $v^{s,f}$  are the velocities of the solid and fluid phases, respectively. The permeability,  $k$ , describes the ease with which the fluid passes through the solid matrix. The permeability is related to the drag coefficient by

$$k = 1/(1+\alpha)^2 K \quad (14)$$

(Lai and Mow, 1980). The continuity equation governing the mixture of the incompressible solid and liquid is

$$\text{div } v^f + \alpha \text{ div } v^s = 0. \quad (15)$$

(Mow, et al., 1980).

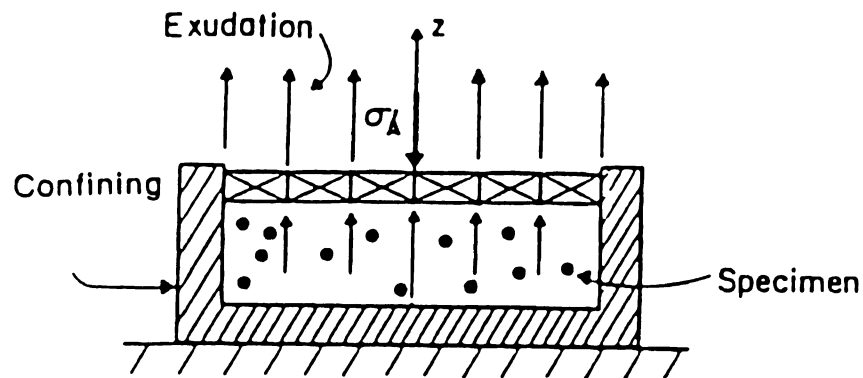
Biphasic solutions have been derived for both confined and unconfined compression-creep tests (Mow, et al., 1980; Armstrong, et al., 1984). Under confined compression a constant load is applied to a laterally confined cartilage specimen by a rigid, porous, platen, Figure 33. In an unconfined compression test the cartilage is compressed between two impermeable platens, Figure 34.

The results of these tests have shown that cartilage creep-relaxation is dependent on the characteristic gel diffusion time ( $t_g$ ), for a biphasic material this diffusion time is given by

$$t_g = d^2/H_A k \quad (16)$$

where; ( $d$ ) is the fluid flow length and ( $H_A$ ) is the aggregate modulus of the elastic solid ( $\lambda_s + 2\mu_s$ ). For confined compression  $d$  is the radius of the platen. For unconfined compression  $d$  is equal to the thickness of the cartilage ( $h$ ).

## CONFINED COMPRESSION

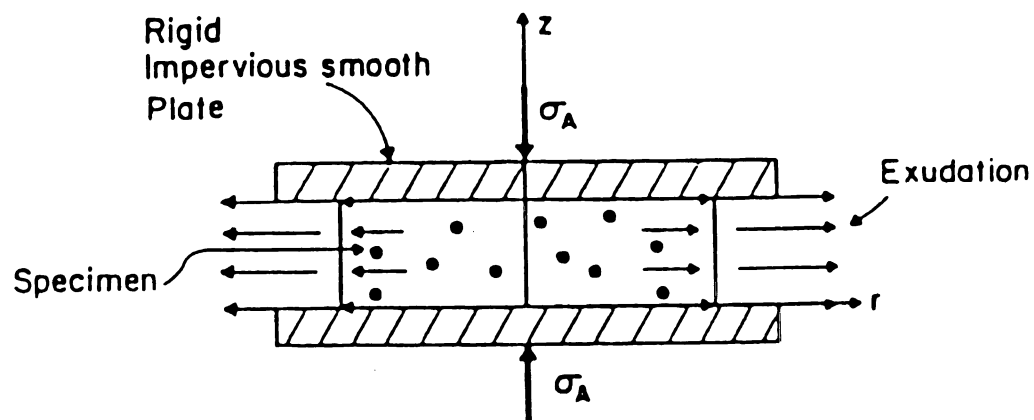


COMPRESSION DIRECTION ↓

FLOW DIRECTION ↑

Figure 33: The confined compression test.

## UNCONFINED COMPRESSION



COMPRESSION DIRECTION ↓

FLOW DIRECTION ↔

Figure 34: The unconfined compression test.

When the strain rates created during loading are fast in comparison to  $t_f$  the cartilage behaves like a single phase, incompressible, elastic material. At strain rates very slow in comparison to  $t_f$  the interstitial fluid pressure does not contribute to the cartilage response and no relaxation is observed.

In 1987, Mak, et al., published load-deformation solutions for cartilage under creep and stress-relaxation indentation conditions. These solutions begin with constitutive equations (10) - (15). To account for the *in situ* geometry of the cartilage under indentation conditions a cylindrical, porous, rigid indenter was used. The free draining interface between the cartilage surface and the porous indenter provides an additional boundary condition required to determine a unique solution. The complex Laplace transforms required for the solution of these indentation tests are inverted via computer computation, see Biphasic Analysis.

From the stress-relaxation indentation solution it has been shown that under conditions of rate controlled loading the relaxation behavior of cartilage is dependent upon the rate of compression parameter ( $R_o$ ) where,

$$R_o = H_A k / V_o h \quad (17)$$

and  $V_o$  is the rate of loading. Under instantaneous load conditions the biphasic stress-relaxation solution is identical to that of Hayes, et al., 1972, assuming  $\nu = \nu_s$ . Agreement between these two solutions occurs again when the cartilage reaches complete equilibrium (for  $\nu = \nu_s$ ). For a porous indentation test complete relaxation requires approximately 10,000 seconds (Mak, et al., 1987).

Current development is in progress on a triphasic theory (Gu, et al., 1993). The fixed charge density (FCD) associated with the PGs and the counter ions create a

swelling pressure within the cartilage (Lai, et al., 1993). Under a mechano-electrochemical, triphasic theory the stresses induced by this swelling pressure are incorporated into the existing biphasic theory.

### Biphasic Analysis

To maintain compatibility with our available testing equipment, and retain the *in situ* geometry of the patella for histology, biphasic indentations stress-relaxation tests were employed. Analysis was carried out using the least square, curve fitting algorithm previously discussed (Mow, et al., 1989). The stress-relaxation response data was collected in our laboratories using a rigid, porous, cylindrical indenter. Test data was then transferred via computer to Dr. Wenbo Zhu at the University of Maryland where the curve fitting analysis was performed. An outline of the curve fitting algorithm is presented below. Although this outline is based upon the creep solution published in 1989 (Mow, et al.), the methodology used is the same for a stress-relaxation test.

The algorithm begins with the Laplace transform solution for creep displacement ( $\bar{u}(s)$ ) (Mak, et al., 1987).

$$\bar{u}(s) = \frac{P\eta_s}{4_s a^2 (s\eta_s - 1) [w]^T [g^*]}$$

(18)

where P is the resistive cartilage load; a is the radius of the porous indenter;  $[w]^T$  are Simpson's weights and  $[g^*]$  is a matrix solution to a Fredholm integral equation.  $\eta_s$  is defined as

$$\eta_s = (1-\nu_s)/(1-2\nu_s) \quad (19)$$

where  $\nu_s$  is the Poisson's ratio of the solid matrix.

Due to the extensive computations required for the biphasic solution, standard curve fitting programs were inefficient. However, all theoretical biphasic solutions are dependent upon the similarity variable  $t' = t/t_s$  (i.e.  $t/(a^2/H_A k)$ ) and the dimensionless parameters; indentation load ( $P/2\mu_s a^2$ ), aspect ratio ( $a/h$ ) and the Poisson's ratio of the solid matrix ( $\nu_s$ ). These variables provided the key to the problem.

Figure 35, demonstrates how changes in  $t_s$  effect the creep solution. For any given set of dimensionless parameters there exists a theoretical displacement curve  $u(t')$  which will provide the solution for experimental displacement curve  $u(t)$  when  $t' = t$  (i.e.  $a^2/H_A k = 1$ ). Therefore, master curves can be generated and shifted to other  $t_s$  values along the logarithmic time axis. The amount of shift (S) is given by

$$\log_{10} (t) - \log_{10} (t') = S \quad (20)$$

By the definition of  $t'$  this can be expressed as,

$$S = \log_{10} (a^2/kH_A) \quad (21)$$

This shift is demonstrated graphically by Figure 36.

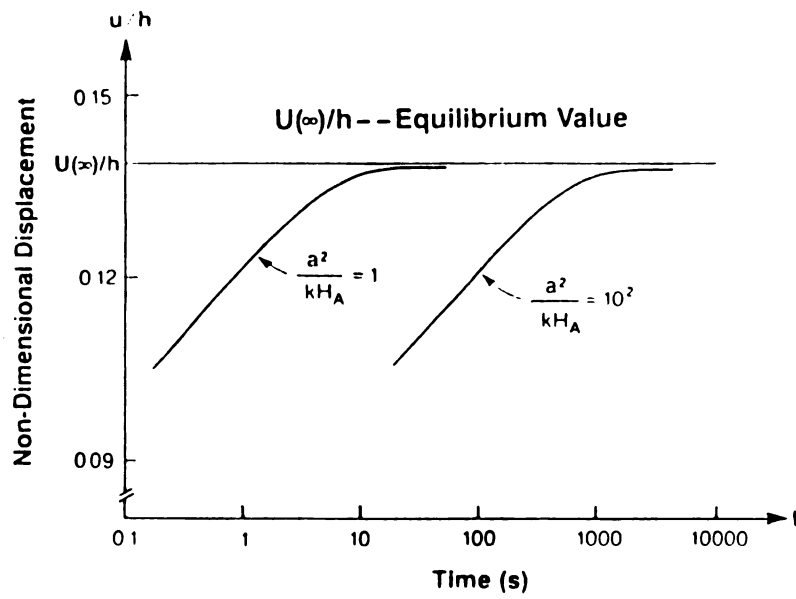


Figure 35: Creep relaxation as a function of  $t_f$ .

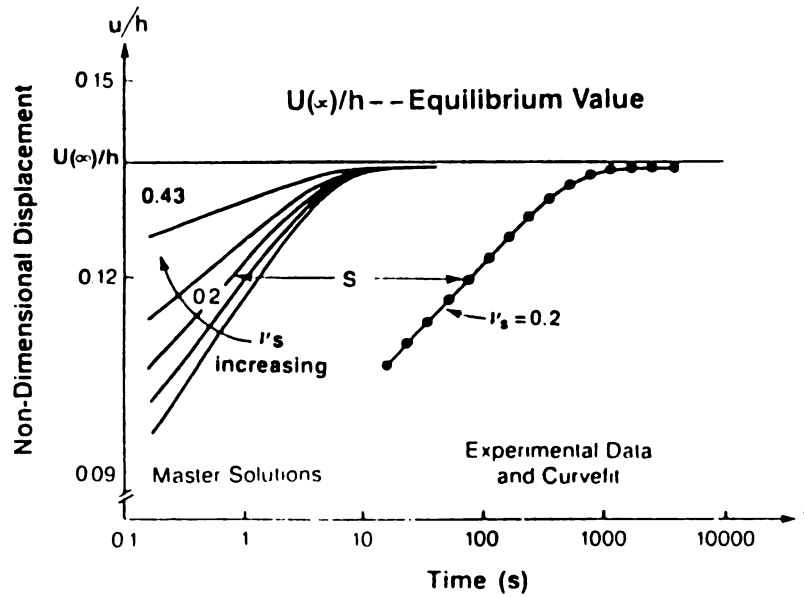


Figure 36: Shifting of theoretical biphasic response curves by  $S = \log_{10}(a^2/kH_A)$ .

From equation (20) it can be seen that  $t'$  can be written as a function of  $t$  and  $S$ . Therefore, for a given set of dimensionless parameters,  $u(t')$  is a function of  $\log(t)$  and  $S$ .

The last constraint of the curve fit requires that at  $t' = \infty$  the curve must fit the dimensionless equilibrium equation,

$$\frac{u(\infty)}{h} = \frac{a}{h} \left[ \frac{Po}{2a^2\mu_s} \right] \left[ \frac{(1-\nu_s)}{2K(a/h, \nu_s)} \right] \quad (22)$$

From equation (22) it can be seen that for a given set of experimental values for  $P$ ,  $h$ , and  $a$  the displacement is only dependent on the relationship between  $\mu_s$  and  $\nu_s$ . Therefore, if a value for  $\mu_s$  could be determined, then the theoretical curve fit would depend on  $\nu_s$  and the amount of shift,  $S$ . By forcing  $S = 0$  this dependence can be reduced to only  $\nu_s$ .

Master solutions are first begun by determining values for  $\mu_s$  from equation (22) based on ten discrete values for  $\nu_s$  (from 0-0.499) and experimental values for  $P$ ,  $u(\infty)$  and  $a/h$ . Each of the paired values of  $\mu_s$  and  $\nu_s$  ( $n=10$ ) creates a unique dimensionless variable group  $(P/2\mu_s a^2, a/h, \nu_s)$ . In turn, each of these dimensionless groups are placed back into the displacement solution,  $u(\log t, s)$ . Master solutions are then calculated at 15 values of  $\log(t)$  for each dimensionless group. This procedure provides master solutions defined with respect to  $\nu_s$  and  $t$ , for a given aspect ratio  $(a/h)$ , leaving  $(P/2\mu_s a^2)$  as the parameter.

Due to the large number of repetitive calculations required, a bicubic spline was chosen for curve fitting because of its simplicity. The curve fitting process is achieved

by minimizing the error between the actual experimental curve and the spline of the creep solution. From Figures 35 and 36 it can be seen that the shape of the master curves are dependent on  $\nu_s$ , and the position of these curves on S. Fitting the experimental data is achieved by minimizing the least square sum of the differences with respect to the  $\nu_s$  and S values.

Once  $\nu_s$ , S and  $\mu_s$  have been determined the *in situ* aggregate modulus ( $H_A$ ) and the permeability (k) can be calculated from

$$H_A = 2\mu_s (1-\nu_s)/(1-2\nu_s) \quad (23)$$

and

$$k = (a^2/H_A) 10^8 \quad (24)$$

A large amount of computer computation time was required to perform the curve fitting routine. For practical purposes the experimental curve data was condensed. Forty representative load-time points were selected via computer from each raw data file. Among these points were the peak resistive load and the final equilibrium load. Experimental values for the cartilage thickness (h) and loading rate were also required by the algorithm and were also included in the information sent to Dr. Zhu.

### Statistical Analysis

Within group comparisons (test vs. control) were carried out on the three parameters (Gu, Gr and  $\eta$ ) for both the acute and synovitis studies using a Student's 't' test for paired samples. Based upon the results of the background studies, and an extensive literature review, the effects of fissuring and synovitis were assumed (a priori) to have a degenerative affect on both the stiffness and flow viscosity of AC. Therefore,

a one tailed hypothesis (test < control) was used for these statistical comparisons. Differences were considered to be statistical when a one tailed P value less than 0.05 was calculated.

Between group comparisons were carried out on results of the acute study groups (e.g. time zero, high impact, test side Gu vs. one day, high impact, test side Gu). These comparisons were performed using the Student's 't' test for random variables, with a Bonferroni's adjustment for multiple comparisons. The null hypothesis assumed equal means between the compared groups. These between group comparisons were used to detect the possibility of an interaction between the cartilage fissures and surgical synovitis. All of the student's 't' tests were carried out on a personal computer using a spreadsheet program (Excel).

Statistical analysis was not performed on the biphasic results of the porous test because of the small number of observations (n=2) from each test group. However visual assessments and comparisons were made with results from previous biphasic studies.

### Histology

Upon the completion of mechanical testing, the patellae were placed in 10% buffered formalin for histology. After examining the results of the rigid indenter tests, patellar pairs which represented the mean results of each group were chosen for histologic examination. Using routine methods, cross sections were cut from these patellae and the cartilage was stained with safranin-O to reveal PG content.

## **ACUTE STUDY RESULTS**

### **Blunt Impact**

As previously noted all impacts were high level. The average peak load for both the time zero and one day, high impact groups was  $631 \pm 102$  N. This is approximately 12 percent higher than the average peak loads recorded in the previous closed joint study and approximately 22 percent greater than those recorded in the open joint study. The average impact parameters and fissure status are provided for the time zero and one day impact groups in Table 24 in the Appendix.

Impact pressure profiles were obtained from the pressure sensitive Fuji film. Figure 37 shows a typical pressure profile from the acute study. Bimodal loading patterns were indicated by two distinct areas of staining. A visual comparison of loading patterns was made between the pressure film results of the acute and open joint studies. This comparison revealed no apparent differences in impact loading between the two studies.

### **Gross Observations**

The time zero joints inspected during removal of the patellae appeared normal. No visible differences were observed in the synovial lining, synovial fluid or AC between the test and control sides. Staining the AC surface with india ink revealed impact fissures in four of the six test patellae. These fissures typically ran proximal to distal

Fi

al

th

de

no

Up

syr

flui

reve

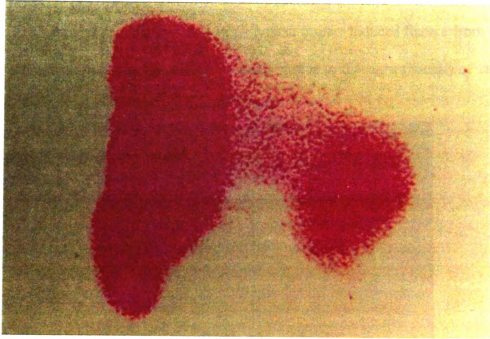


Figure 37: A typical pressure profile from the acute study.

along the lateral side of the patella centerline. This fissure formation is consistent with those reported in the background studies. The occurrence of these fissures are documented in Table 24 in the Appendix.

The tissue surrounding the test joints of the one day, high impact group was noticeably damaged. The tissues adjacent to the sutures were visibly filled with blood. Upon opening the joint capsule a similar appearance could be seen from the inside. The synovial fluid appeared orange in color and traces of blood were observed. The synovial fluid within the control joints appeared normal. An initial comparison of the cartilage revealed no visible differences between the test and control patellae. After staining the

AC with india ink, five out of six of the impacted patellae were found to have fissures, see Table 24 in the Appendix. These fissures were similar in appearance to those in the time zero impact group. Figure 38 shows a typical impact induced fissure from the acute study, the indentation sites are visible as small circles to the right (lateral) of the fissure which were left by the thickness needle probe.



Figure 38: Typical impact fissures created during the acute study. The sites of the indentation tests are visible as small circular defects to the right (lateral) of the fissures.

The solid indenter tests, those farthest to the right in Figure 38, form a vertical line down the lateral facet of the patella. By visual inspection it was determined that the average distance between the site of indentation and the impact fissures was between 2 and 3 indenter radii (i.e. 1-1.5 mm.). (See Appendix Table 24).

The joint tissue and synovial fluid of the one day, sham group had the same appearance as those described in the one day, high impact group. Upon inspection of the AC no differences were detected between the test and control patellae. Staining with india ink failed to reveal any differences in the surface integrity between the test and control cartilage.

#### **Mechanical Test: (Solid Indenter)**

##### **Time Zero, High Impact**

A comparison of instantaneous stiffness ( $G_u$ ) values showed that the test side cartilage was on average 11.5% softer than control. The relaxed stiffness ( $G_r$ ) was an average 6.8% less on the test side, while the flow viscosity ( $\eta$ ) was increased by an average of 54.6%. Within group comparisons revealed that the difference between  $G_u$  values (test vs. control) was significant ( $P = 0.04$ ). The differences in parameters  $G_r$  and  $\eta$ , however, were not statistically significant. A complete list of the solid indenter test results for the time zero, high impact group are presented in Table 25 in the Appendix.

##### **One Day, Shams (No Impact)**

Unlike the time zero, high impact group, the average  $G_u$  value for the one day, sham group was basically unchanged on the test side (1.5% decrease). Test side  $G_r$  values, on the contrary, were decreased by an average of 13.2%. The  $\eta$  values were also decrease by 14.7% on the average. A within groups comparison revealed that  $G_r$  values were significantly lower on the test side,  $P = 0.024$ . The differences in  $G_u$  and  $\eta$  were not found to be significant. A complete list of results for the one day, sham group is

provided in Table 26 in the Appendix.

#### One Day, High Impact

All three mechanical parameters were reduced on the test side.  $G_u$  was decreased an average of 21.9%,  $G_r$  by 14.3%, and  $\eta$  by 23.4%. These decreasing trends are similar to those observed in the open joint study at high impact levels one day post-surgery. Within group comparisons showed that the average test side  $G_r$  and  $\eta$  were significantly lower than their respective control values,  $P = 0.011$  and  $P = 0.042$ .  $G_u$  was borderline with a  $P$  value of 0.050. A complete list of results for the one day, high impact group are compiled in Table 27 in the Appendix.

#### Between Group Comparisons and Interactions

Multiple comparisons revealed no significant differences between the time zero, high impact parameters and those in the one day, high impact group. This result statistically suggests that the 24 hour exposure of the fissured cartilage to the surgically disrupted joint environment had no additive degenerative affect on its mechanical response. Similar comparisons were made between the one day, sham group and one day, high impact group. These comparisons also revealed no significant differences. Statistically this suggests that the fissures and surgical synovitis did not interact to enhance the degeneration of the cartilage beyond that which would have been created by each of them working simultaneously alone.

Further comparisons were also carried out between the time zero, high impact group and the one day, sham group. These comparisons revealed the test side  $G_r$  values to be significantly lower in the sham group with a  $P = 0.008$ . This statistical

significance suggests that the individual softening effects of fissures and surgical synovitis affect the mechanical stiffness differently, specifically the equilibrium stiffness.

#### Mechanical Test: (Porous indenter)

##### Biphasic results

The biphasic analysis provided three material properties; shear modulus of the solid matrix ( $\mu_s$ ), Poisson's ratio ( $\nu_s$ ), and the permeability of the cartilage ( $k$ ). For direct comparison with previous biphasic studies, the aggregate modulus was also calculated ( $H_A$ ) using equation (22), see Biomechanical Properties. The biphasic results of the porous indentation tests are compiled in Tables 28 and 29 in the Appendix. In several cases the biphasic algorithm was unable to simultaneously fit the large peak load and fast rate of relaxation of the stress-relaxation data. For these cases the analysis was aborted. For these aborted cases the biphasic material properties are not available, and are represented by dashed lines in Tables 28 and 29. The material properties calculated for both the 1 and 2 second porous tests were combined for presentation in this results section.

The aggregate modulus values for the control patellae of all three acute study groups ranged from 0.400 to 0.968 MPa. This range of values is comparable to average values for bovine femoral condyle cartilage (0.47-0.90 MPa) (Mow, et al., 1989). The Poisson's ratio ( $\nu_s$ ) for the control patellae were essential 0.00 ( except for rabbit 9326 which was 0.058). This value is 100% smaller than the range of 0.25-0.40 measured for bovine cartilage by Mow, et al., 1989. This value is, however, close to the average Poisson's ratio of 0.08 reported for normal human cartilage (Whipple, et al.,

1985). The permeability values ( $k$ ) for the control patellae ranged from 0.205 to 1.040  $\text{m}^4/\text{Ns}(\times 10^{-14})$ . These control permeability values are 1.4 - 7.2 times larger than the range of average values measured for bovine cartilage (Mow, et al., 1989). However, they do fall within the 0.05-1.95 range measured for human cartilage by Armstrong and Mow (1987).

The test side  $H_A$  values for the time zero group ranged from 0.332-0.864 MPa. The test side ranges for the one day, sham and impact groups were 0.400-0.540 and 0.842-0.968 MPa, respectively. These ranges are all comparable to average values measured for bovine cartilage. Like controls, the test side values for Poisson's ratio were essentially 0.0 (except rabbit 9326 which was 0.019). The test side permeability values for the time zero group ranged from 0.836 to 2.370  $\text{m}^4/\text{Ns}(\times 10^{-14})$ . The test side ranges for the one day, sham and impact groups were 0.203-0.870 and 0.896-3.620  $\text{m}^4/\text{Ns}(\times 10^{-14})$ , respectively. These values are 1.4 to 25.5 times greater than the largest average bovine permeability measured by Mow, et al., in 1989. While the permeability values for the one day, sham group do fall within the range for human AC permeability (0.05-1.95, Armstrong and Mow, 1987), the permeability values for the time zero and one day impact groups are both relatively high in comparison.

Overall, the control and test side values for the aggregate modulus were comparable to previously determined bovine values. For both impact groups (time zero and one day) the test side modulus values were lower than their controls. For the one day, impact group the test side moduli were consistently 50-60% lower than their controls. Under biphasic theory the Poisson's ratio reflects the ability of fluid to move through the cartilage (Mow and Hayes, 1991). A biphasic Poisson's ratio of 0.50 would

suggest no fluid flow through the cartilage and no relaxation. Therefore,  $\nu$ , values near, or at 0.0, indicate a large afflux of fluid through the cartilage. These low  $\nu$ , values reflect the algorithms attempt to match the fast rate of relaxation in the indentation tests. This rapid relaxation is also evident in the large permeability values. The test side permeability values for all of the acute study groups demonstrated a general increase on the test side. In the time zero group this increase suggests that the presence of impact fissures alone can increase cartilage permeability as hypothesized. Interestingly, 3 out of 4 of the test side permeability values from the sham group were also greater than their controls. This suggests that exposing cartilage to a surgically damaged joint environment may also increase permeability. The combined effects of surgery and fissures, may have both played a role in the increased permeability measured in the one day, impact group.

#### Elastic/Viscoelastic Results

The elastic ( $G_u$  and  $G_r$ ) and viscoelastic ( $\eta$ ) results for the porous indentation tests are compiled in Tables 30 and 31 in the Appendix. The material parameters calculated for both the 1 and 2 second porous tests are combined for presentation in this results section.

In general, the test and control  $G_u$  values for all three of the acute study groups were consistently 50-60% lower for the porous indenter tests than those calculated for the solid indenter. This decrease is consistent with the predicted response. The test and control values for  $G_r$  were also visibly decreased by approximately 50% in comparison to those from the solid indenter. According to the biphasic model, if the cartilage were truly at equilibrium no difference in the experimental  $G_r$  values would occur between the

solid and porous indentation tests (for  $\nu = \nu_s = 0.40$ ). These differences may be due to the closer proximity of the porous tests to the site of fissuring and/or their relative relaxation periods (i.e. 1000 sec. for the porous tests vs. 150 sec. for the solid). The large variations between individual flow viscosity values made comparisons between the porous and solid indenter results difficult. No apparent increasing or decreasing trend could be discerned for either the test or control side values.

### Histology

The surface integrity of all 6 control patellae in the acute study appeared histologically smooth and healthy. In both the time zero and one day, impact groups impact fissures were observed. These fissures were oriented at 45 degrees to the articulating surface and extended down into the middle zone of the cartilage (Figure 39). No distinct loss of PGs could be accessed in any of the test side patellae. It had been anticipated that exposure to a surgically damaged synovial environment would result in a loss of PGs. Failure to observe such a loss may be due to the small number of paired observations in each group ( $n = 2$ ) and/or the short period of exposure (24 hours). Some pre-existing pathologies were noted in patellae from each acute group. These pathologies included a loss of PG staining in the deep zone and a loss of tidemark (i.e. the boundary line where the cartilage and subchondral bone meet), see Figure 40. These pathologies were typically bilateral, appearing on both the test and control sides in equal intensity, and therefore are not believed to have played a part in the mechanical differences measured between the test and control sides.

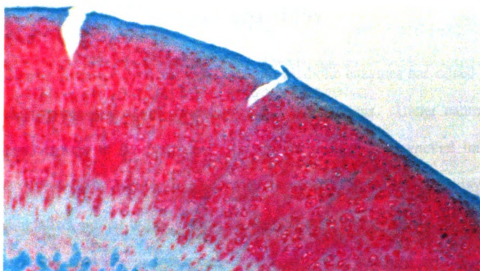


Figure 39: A histological cross section of two impact fissures.

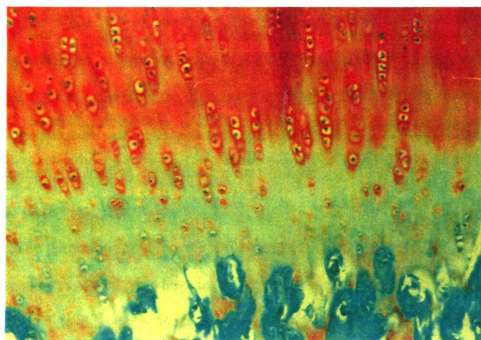


Figure 40: Histological cross section showing the loss of PGs and tidemark observed in some of the patellae in the acute study groups.

## **SYNOVITIS STUDY**

Recent research involving cytokines and catabolic enzymes has raised questions about the possible role of the synovium in OA pathogenesis. Under natural impact conditions, damage to the peripheral joint tissues, such as the synovial lining, may provoke the release of such substances. Such a transient injury response may result in a softening affect similar to that created by surgical arthrotomy. In the open joint study the release of cytokines and enzymes by the surgically damaged synovial lining is believed to have contributed to the decreased stiffness measurements at early post-surgery time points. Under the experimentally controlled conditions of the closed joint study, the test patellae alone suffered trauma. The surrounding soft tissues were unharmed. Without damage to the synovial lining an acute biochemical response may not have been induced. This might explain the differences in stiffness responses between the open and closed joint studies, particularly at early time points (e.g. 6 days post-impact). It is hypothesized that loading the cartilage during this transient softened period may increase the rate of cartilage degeneration.

The purpose of the synovitis study was to address the possibility of inducing an inflammatory synovial response in the rabbit model without the artificial use of arthrotomy. In this study, blunt trauma to the synovial tissue was investigated as a means of producing synovitis by mechanical means. This will help us assess whether or

not a synovitis can be produced during a natural impact scenario which in turn softens the cartilage.

Further investigations were also carried out to determine whether an interaction occurs between the impact fissures and traumatized synovium enhancing the degeneration of AC. In the acute study, such an interaction could not be statistically proven. However, due to the overall decreases measured in the one day impact group of the acute study, we felt that further investigation of a possible interaction was warranted.

#### The Synovitis *In Vivo* Study

The original synovitis study (Part I) included two treatment groups. The first group, the sham group, received blunt trauma to the soft tissue surrounding the right patella. Following the induction of this trauma these rabbits were then returned to their cages. This group was used to determine whether or not trauma to the synovial tissue alone could create a secondary effect on the mechanical response of AC. In the second group, after traumatizing the synovial tissue, the rabbits were placed in the restraining chair and a high level impact was delivered to the patella of the traumatized joint. This group was used to determine whether cartilage fissures interact with the traumatized synovium to produce an additional degradation in the mechanical response of AC. This may help answer the question of whether or not synovitis played a role in the difference between the low and high impact groups of the open joint study.

Both groups, sham and impact, were exercised daily following the induction of synovial trauma and/or impact, until being euthanized for testing. By exercising the animals, we hoped to further stimulate and maintain a synovial response. Six rabbits

were used in each of these two treatment groups.

The open joint study sham results suggested that use of the restraining chair during surgery may have had degenerative affects on the test side cartilage (Ide, 1992). To address this, two additional groups were added to the synovitis study (i.e. Part II). Both groups received blunt trauma to the synovial tissue surrounding the test joint while restrained in the chair. The rabbits in the first group (shams) were returned to their cages following the synovial trauma. The second group received a high level impact to the test patella following the synovial trauma. Like the two groups in Part I, these test groups also received daily exercise following the induction of trauma to stimulate and maintain the synovial response.

All of the rabbits in the synovitis study were housed individually and allowed cage activity. The rabbits were exercised for 15 minutes daily on an enclosed treadmill beginning the day after trauma induction. Six days after trauma induction the rabbits were euthanized and their patellae removed for mechanical testing. At this time tissue samples were removed from the synovial tissue medial and lateral to the patellae. This tissue was placed in 10% buffered formalin and prepared for histological examination.

#### Soft Tissue Trauma/Blunt Impact

The rabbits were placed under anesthesia using the ketamine, xyaline and were maintained by isoflurine during trauma induction. In the original study, Part I, the rabbits received synovial trauma without the use of the restraining chair. The right hind limb of these rabbits was held in a flexed position (approximately 45° of flexion) by an assisting veterinary technician. Blunt trauma was then induced in the synovial tissue

adjacent to the patella by repeated tapping with a common household hammer. The area targeted for damage was the synovial lining directly lateral and medial to the patella. In these areas the synovium is unprotected by superior ligament and muscle cover. The trauma was continued until cutaneous hemorrhaging was observed in the tissue around the patella (approximately 50 taps). Care was taken to not strike the patella during this procedure. Five minutes after the induction of synovial trauma the sham rabbits were returned to their cages. For the impact group, five minutes after the induction of synovial trauma the rabbits were placed in the restraining chair where they received a high level patellar impact.

In Part II, induction of the synovial trauma was carried out while the rabbits' hind limb was held hyperflexed in the restraining chair. The sham rabbits remained in the restraining chair for five minutes following the induction of the synovial trauma, and were then returned to their cages. The impact rabbits remained in the restraining chair for five minutes following the synovial trauma, and then they received a high level patellar impact.

All of the patellar impacts in the synovitis study were carried out using the gravity impactor and data collection system previously described (see Open Joint Study Materials and Methods).

### Testing Procedure

Indentation tests were carried out using both solid and porous indenters. The test sites and procedures were identical to those used in the Acute Study. After being mechanically tested, the patellae were prepared for routine histology.

### Biomechanical Properties

The biomechanical analysis methods used were the same as those described in the Acute Study, Materials and Methods. A 2x2 ANOVA was performed on the paired results of the solid indenter tests of all four synovitis study groups. This ANOVA was performed to detect the effects of impact fissures, and/or the use of the restraining chair on the mechanical response of the AC.

Within group comparisons were performed on the results of the solid indenter tests to detect differences between the mechanical response characteristics of the test and control side cartilage. These within group comparisons were performed using a Student's 't' test for paired samples. It was anticipated, a priori, that both synovitis and impact fissures would cause a decrease in the shear moduli and flow viscosity of the cartilage. Based on this assumption, a one tailed hypothesis (test < control) was used for the within group comparisons.

Due to the small number of rabbits analyzed by the biphasic theory, n=2 per study group, statistical analysis was not performed on the results of the porous tests. However, comparisons were drawn between the results of these tests and the results of previous biphasic studies.

## **SYNOVITIS STUDY RESULTS**

### **Blunt Impact**

As previously noted, all patellar impacts were of high level. The average peak impact load for the synovitis impact groups was  $549 \pm 124$ . This is approximately equal to the average high level impact value reported for the closed joint study and is approximately 12% higher than that reported in the open joint study. Impact fissures were observed in 6 of the 9 rabbits impacted. The impact parameters and fissure status of these rabbits are tabulated in Table 32 in the Appendix.

The following results are presented in two parts. In part one, the results of the original two synovitis groups (Part I) will be presented. In these groups the synovial trauma was induced without the use of the restraining chair. In Part II, the results of the second study groups will be presented. In these two groups the synovial trauma was induced while the rabbits were restrained in the chair.

### **PART I: (Synovitis created without the use of the restraining chair)**

---

#### **Part I: Gross Observations**

##### **Sham Group**

On the day of testing, six days after traumatizing the synovial tissues, the test joints appeared normal when compared with their control. Upon opening the joints, the

synovial tissue and fluid of the test and control legs appeared normal. No abnormalities were noted in the test or control patellar cartilage prior to staining their articular surfaces with india ink. Upon staining the cartilage baseline pathology was detected in the AC of five sham rabbits. This pathology included surface roughness and some fissuring. Typically the patterns of pathology were bilateral, that is to say that they were present on both the test and control patellae in equal intensity.

### Impact Group

Six days after trauma, the external joint tissues appeared normal on the test side when compared to controls. Upon opening the joints no abnormalities were noted in the synovial lining or fluid of either the test or control joints. An initial examination of the cartilage revealed no signs of fissuring on the test side. After staining with india ink, fissures were detected in five of the six test patellae, Table 32 in the Appendix. These fissures were present on the lateral facet running proximal to distal along the centerline of the patella.

## Part I: Mechanical Tests (Solid indenter)

### Sham group

The results of the solid indenter test are presented in Table 33 in the Appendix. A visual comparison of the average values revealed that in all cases the test side parameters were larger than their controls. Gu test values were an average of 18.3% greater, Gr values 10.9%, and  $\eta$  was up by 20.3%. Based on the a priori one tailed hypothesis (test < control) it was obvious that none of the test values were statistically different than their respective controls.

### Impact group

All test side mechanical parameters were visibly decreased in comparison to their controls, Table 34 in the Appendix. Test side  $G_u$  values were down by 29.1%.  $G_r$  was decreased an average of 17.0% and  $\eta$  an average of 25.3%. All three test side parameters;  $G_u$ ,  $G_r$ , and  $\eta$ , were found to be significantly less than their controls with P values of 0.027, 0.013, and 0.011, respectively.

### Part I: Mechanical Tests (porous indenter)

The biphasic material properties for the sham and impact groups are presented in Tables 35 and 36 in the Appendix. The material properties for the porous tests performed at the 1 and 2 second loading rates have been combined in this results section.

The control side, aggregate modulus ( $H_A$ ) values for both the sham and impact groups ranged from 0.571-1.243 and 0.549-0.792 MPa, respectively. These values are comparable to the range of average bovine modulus values, 0.47-0.90 MPa, measured by Mow, et al., 1989. The Poisson's ratios for the sham and impact groups ranged from 0.0-0.288 and 0.0-0.298, respectively. These ranges are low compared to the average range of 0.25-0.40 measured for bovine cartilage (Mow, et al., 1989), but are comparable to the average values 0.08 and 0.14 determine for normal human and porcine cartilage (Spilker, et al., 1992; Whipple, et al., 1989). The control side permeability values for the sham and impact groups ranged from 0.138-3.52 and 0.300-1.818  $m^4/Ns(x10^{-14})$ . These ranges are 3 to 25 times larger than the average range 0.043-0.142 measured for bovine cartilage (Mow, et al., 1989). Although these permeability values are high, they do fall within the 0.05-1.95 range measured for human AC by Armstrong

and Mow (1987).

The test side aggregate modulus values ranged from 0.521-0.828 MPa for the sham group, and from 0.348-0.728 MPa for the impact group. These ranges, like their respective controls, are comparable to the range of average bovine values (Mow, et al., 1989). The test side Poisson's ratios ranged from 0.0-0.288 for the sham group. In the impact group all Poisson's ratios were 0.00. Like controls, these test side values are low compared to the range of bovine values, and are closer in comparison to those values calculated for human and porcine cartilage. The test side permeability values for the sham and impact groups ranged from 0.103-1.101 and 0.279-0.792  $\text{m}^4/\text{Ns}(\times 10^{-14})$ , respectively. These ranges, like controls, are higher than the average range of bovine values but fall within the range of values measured for human cartilage.

Overall, aggregate modulus values were comparable to previously determined bovine values. Control and test side Poisson's ratios, in general, were low in comparison to previously determined values. In fact in ten of the sixteen porous tests a Poisson's ratio of 0.00 was measured. This reflects the algorithms attempt to fit the fast rate of relaxation occurring during the indentation tests. This high rate of relaxation was also reflected in the large permeability values measured in both the test and control patellae. No definitive increase in permeability was noted in the test side cartilage of the impact group as anticipated. This lack of change in the surface permeability of the test side cartilage may be due to the small number of observations ( $n = 2$ ).

#### Part I: Elastic/Viscoelastic Results

The mechanical parameters ( $G_u$ ,  $G_r$  and  $\eta$ ) calculated for the porous indenter test

are presented in Table 37 and 38 in the Appendix. For discussion purposes the results of the 1 and 2 second porous tests were combined.

Overall, the test and control values of Gu for both the sham and impact groups were decreased by 50% or more compared with the average solid indenter values. This is consistent with a priori predictions. Test and control values for Gr in general were also below the average values of the solid indenter results. This decrease is contrary to the equivalence between the porous and solid indented values which had been predicted. As noted in the acute study, this may be due to the closer proximity of the porous test sites to the area of fissuring, and/or the longer relaxation period available in the porous tests. The small number of observations and large variations in flow viscosity values made comparisons between the porous and solid indenter results difficult. No discrete increasing or decreasing trends were noted.

#### **Part I: Histology (Articular cartilage)**

Two animals were selected from each synovitis study group for histological analysis. These subjects were chosen based on the results of their solid indenter tests. The rabbits with results which most closely represented the overall mean values of the group were chosen for analysis.

One of the four control patellae ( $n = 2$  each from the sham and impact groups) contained pre-existing surface fissures. In the remaining three, the surface integrity was smooth and healthy. The sham test patella, which corresponded to the fissured control patella, also possessed pre-existing pathological fissures. No impact fissures were visible in either of the two test patellae from the impact groups. A discernable loss of PGs

could not be determined in any of the test side patellae as an effect of their treatment. A pre-existing loss of PGs was, however, observed in 3 of the 4 sham patellae. These patellae also showed a loss of tidemark definition. Interestingly, in these 3 patellae the pathology appeared to be limited to the medial facet. These pathologies were similar in appearance to those shown in Figure 40.

### Part I. Histology (Synovial lining)

Isolating synovial samples for examination proved not to be a simple task. The tissues collected in the first 2/3 of the specimens contained little or no trace of synovial lining. These specimens were taken from the tissue attached to the femoral head after removal of the patella. The specimens collected in the last third of the experiments were removed from tissue attached to the lateral and medial edges of the recovered patella. This method seemed to work better, but some specimens still contained no synovial lining. The findings from these histologic sections are presented below.

#### Sham group

Synovial samples were examined from two sham rabbits. Only small sections of synovial lining were visible in the first rabbit examined. The medial and lateral control joint specimens were similar in appearance. The synovial lining on both sides consisted of a single layer of cells. No signs of inflammation such as hypertrophy or lymphocyte invasion were noted. The lateral and medial test samples were identical to those of their contralateral control.

The control sections from the second animal contained no synovial lining. However, large areas of synovial lining were visible on the lateral and medial specimens

of the test joint. In comparison to the control sections from the first animal, segments of the lining appeared to be thickened. These hypertrophic sections lay between stretches of normal appearing synovial lining. These thickened areas were at times three or more cells deep. No lymphocytes were noted in these hypertrophic areas.

#### Impact group

Again two animals were histologically analyzed. The first rabbit contained no synovial membrane in the medial control specimen. The small section of synovial lining which was present on the lateral side appeared to be normal.

Both lateral and medial test specimens from the first rabbit contained synovial membrane. One area on the medial side appeared to be thickened. On the lateral side two villi which appeared to be detached from the main body of tissue appeared hypertrophic. No leukocytes were observed.

The control specimens from the second animal contained no synovial membrane. In the corresponding test specimens, only the medial side contained a small section of synovium. This small section appeared normal.

### **PART II: (Synovitis created while restrained in the chair)**

---

---

#### Part II: Gross Observations

##### Sham group

Six days after trauma induction the test limbs appeared normal. Upon opening the test joints the synovial lining and fluid appeared normal compared with controls.

Prior to staining the cartilage with india ink, both test and control patellae appeared healthy. Staining revealed surface anomalies in only two of the six animals. Again, the pathology was typically present in both paired patellae.

#### Impact Group

Like shams, no external differences were detected in the test side limb when compared with their controls. Upon opening the joints the synovial lining and fluid appeared normal in all the control and test legs. No observable fissures were initially detected in the test side cartilage. Upon staining with india ink, fissures were detected in two of the three test patellae. These fissures were similar in appearance to those described in the Part I impact group.

#### Part II: Mechanical Tests (Rigid indenter)

##### Sham group

From Table 39, it can be easily seen that only small differences exist between test and control parameters. The  $G_u$  and  $G_r$  values were a mere 5.1% and 1.2% lower than their controls, and  $\eta$  is essentially unchanged with an increase of only 0.6%. None of these small differences were found to be significant.

##### Impact group

Similar to the shams, the impact group also showed little change in the test side parameters, Table 40. All three were only slightly decreased on the test side.  $G_u$  was down 1.6%,  $G_r$  3.0%, and  $\eta$  12.3%. None of these differences were found to be statistically significant.

## Part II: Mechanical Tests (Porous indenter)

The biphasic material results for the sham and impact groups are presented in Tables 41 and 42. As in Part I, the results of the 1 and 2 second porous tests are combined for discussion in this results section.

The control side aggregate modulus ( $H_A$ ) values for the sham and impact groups ranged from 0.394-0.672 and 0.534-0.669 MPa, respectively. These values are comparable to the range of average bovine values, 0.47-0.90 MPa, measured by Mow, et al., 1989. The Poisson's ratios for the sham and impact groups ranged from 0.0-0.015 and 0.0-0.116, respectively. These ranges are low compared to the average range of 0.25-0.40 measured for bovine cartilage (Mow, et al., 1989), but are comparable to the average values 0.08 and 0.14 determine for normal human and porcine cartilage (Spilker, et al., 1992; Whipple, et al., 1989). The control side permeability values for the sham and impact groups ranged from 0.150-1.003 and 0.223-1.410  $\text{m}^4/\text{Ns}(\times 10^{-14})$ . These ranges are 1.1 to 10 times larger than the average range of 0.043-0.142 found for bovine cartilage by Mow, et al., 1989. Although, these permeability values are high, they do fall within the 0.05-1.95 range measured by for human AC by Armstrong and Mow (1987).

The test side aggregate modulus values ranged from 0.626-0.917 MPa for the sham group, and 0.494-1.171 MPa for the impact group. These test side ranges, like their respective controls, are comparable to the range of average bovine values (Mow, et al., 1989). The test side Poisson's ratios range from 0.0-0.101 for the sham group and 0.0-0.166 for the impact group. Like the control side values, these test side ratios

are low compared to the range of bovine values, but are comparable to the values calculated for human and porcine cartilage. The test side permeability values for the sham and impact values ranged from 0.262-0.688 and 0.603-0.1.05  $\text{m}^4/\text{Ns}(\times 10^{-14})$ , respectively. These tests ranges, like controls, are higher than the average range of bovine values but fall within the range of values measured for human cartilage.

Overall, aggregate modulus values were comparable to previously determined bovine values. Control and test side Poisson's ratios, in general, were low in comparison to previously determined values. In fact in 8 of the 14 porous tests (which had values) a Poisson's ratio of 0.00 was measured. This reflects the algorithms attempt to fit the fast rate of relaxation occurring during the indentation tests. This high rate of relaxation is also reflected in the large values of permeability measured on both the test and control sides. No definitive increase in permeability was noted on the test side of the impact group. This lack of change in permeability on the test side may be due to the small number of observations.

## Part II: Elastic/Viscoelastic Results

The mechanical parameters ( $G_u$ ,  $G_r$  and  $\eta$ ) calculated for the porous indenter test are presented in Table 43 and 44 in the Appendix. For discussion purposes the results of the 1 and 2 second porous tests are combined.

Overall, the test and control  $G_u$  values for both the sham and impact groups were decreased by 50% or more compared to the average solid indenter values. This is consistent with the a priori prediction. Test and control values for  $G_r$ , in general, were also below the average values reported for the solid indenter. This decrease is contrary

to the equivalence between the porous and solid indenter results which had been predicted. As in Part I, this decrease may be due to the closer proximity of the porous test sites to the area of fissuring, and/or the longer relaxation period available to the porous tests. The small number of observations and large variations made comparisons between the porous and solid indenters flow viscosity values difficult. No discrete increasing or decreasing trend were noted.

## Part II: Histology (Articular cartilage)

Two animals were selected from each synovitis study group for histological analysis. These subjects were chosen based on the results of their solid indenter tests. The rabbits with results which most closely represented the overall mean values of the group were chosen for analysis.

The surface integrity of 3 out of 4 of the control patellae (n=2 each from the sham and impact groups) were smooth and healthy. The fourth control patella contained 3 pathological fissures. The surfaces of the sham group test patellae were all smooth and healthy. Impact fissures were, however, noted in one of the two test side patellae of the impact group. These fissures began at a 45° angle to the articular surface and extended down into the middle zone of the cartilage. No discernable loss of PG content was detected in the test side cartilage as an effect of treatment in any of the sham or impact patellae. However, a pathological loss of PGs was noted in three of the four sham patellae, as well as a loss of tidemark definition. These pre-existing pathologies appeared to be limited to the medial facet of these three patellae.

**Part II: Histology (Synovial lining)**

As in Part I, the specimens collected in the first 2/3 of the synovitis study contained little or no trace of synovial lining. These specimens were taken from the tissue attached to the femoral head after removal of the patella. The specimens collected in the last third of the experiments were removed from tissue attached to the lateral and medial edges of the recovered patella. This method seemed to work better, but some specimens still contained no synovial lining. The findings from these histologic sections are presented below.

**Sham group**

The synovial lining of two rabbits were examined. The medial and lateral specimens from the control joint of the first rabbit appeared normal. The synovial lining consisted of a single layer of cells. No signs of inflammation (hypertrophy or leukocytes) were noted.

Of the specimens taken from the test joint of the first rabbit, only the medial side contained synovial lining. Several large villi were observed which contained hypertrophic areas three or more cells thick. These villi were not observed in the medial specimen of the control joint. No leukocytes were visible in these thickened synovial villi.

The lateral and medial specimens from the control joint of the second rabbit contained only small sections of synovial membrane. In these sections the lining appeared to be normal. On the test side both the lateral and medial specimens showed thickened areas. No signs of leukocyte invasion were noted.

### Impact group

Of the three animals in this group two were histologically examined. The control specimens from the first rabbit contained small sections of synovium on both the lateral and medial sides which appeared normal. The corresponding test specimens, however, did contain areas on both the lateral and medial side which appeared to be thickened. No leukocytes were observed. The control specimens from the second rabbit examined contained synovial lining only in the medial specimen. This small section of synovial lining appeared normal. The corresponding test specimen from this rabbit also contained synovial membrane only in the medial specimen. This section did display a thickened cellular layer. No leukocytes were noted in the vicinity of this hypertrophy.

### Chair and Impact Interactions

The ANOVA detected an effect of placing the rabbits in the restraining chair while inducing synovial trauma. This difference was detected in both the test and control Gr values,  $P = 0.006$  and  $P = 0.018$  respectively. That is to say that a significant difference was detected between the combined Gr values from the Part I sham and impact groups and those of the combined sham and impact groups from Part II. Overall the combined Gr values from Part II were on average 17.4% greater than those from Part I. The contrast tests performed following the ANOVA revealed that the effect of the restraining chair was significant only between the Part I and II sham groups control values ( $P = 0.041$ ) and the impact groups test values ( $P = 0.007$ ).

The ANOVA also detected an effect of impact trauma on Gr values. Contrast tests performed following the ANOVA revealed that this difference was statistical only

between the sham and impact groups in Part I ( $P=0.024$ ). The impact Gr values were lower by 26.9%. This difference is similar to that seen between the low and high level impact groups in the open joint study.

## DISCUSSION

Both the acute and synovitis studies arose out of questions raised by the results of the open and closed joint studies. These questions were based on differences in the mechanical response of cartilage as of function of both impact trauma (fissured vs. unfissured) and model type (open vs. closed joint). Differences in mechanical response were measured between the low and high level impact groups at early time points in the open joint study. At low impact levels a gradual decrease in stiffness was observed over a period of two weeks, this was followed by a gradual recovery back to control levels by one year. At high impact levels an acute drop in stiffness was noted one day following induction trauma. By one year, although stiffness values had returned to normal, a gradual decreasing trend was observed that suggested a path of long term degeneration. The differences in stiffness response between the low and high level groups were attributed to impact fissures present in the cartilage of the high level groups (Ide, 1992).

Upon completion of the open joint study, a second year long impact study was carried out. During this study patellar trauma was performed under closed joint conditions. Results similar to those observed in the open joint study were anticipated. However, although cartilage fissures were again present in the high impact specimens, differences in stiffness responses between the two impact levels were not observed. In fact, prior to one year post-impact none of the low or high level impact groups in the

closed joint study showed any substantial decrease in cartilage stiffness. It was hypothesized that differences between the open and closed joint results were either caused by the small sample size of the open joint study, or by a surgical synovitis induced by arthrotomy. While the effects of surgical synovitis are believed to account for some of the differences between the open and closed joint results, it does not explain differences in stiffness response between the low and high level impact groups within the open joint study. Upon completion of the open and closed joint studies the following questions remained: (1) can impact fissures alter the mechanical response of cartilage, (2) are the degenerative effects of fissures further enhanced in the presence of a surgical synovitis, and (3) if synovitis does enhance the degeneration of cartilage, can it be created under closed joint impact conditions without the use of invasive arthrotomy? To answer these question the acute and synovitis studies were developed.

### Acute Study

The acute study had two main objectives. The first was to measure the isolated effects of fissuring on the mechanical response of the cartilage. It was hypothesized that disruption of the collagen network created by impact fissures would result in a decrease in cartilage stiffness. It has been previously reported that the integrity of the cartilage surface layer plays a key role in creating resistive forces during the loading phase of indentation by maintaining fluid pressure in the tissue (Setton, et al., 1993). It was hypothesized that damage to the surface layer, created by the presence of impact fissures, would result in an increase in permeability. To quantify the effects of fissuring on cartilage permeability, biphasic theory was added to the analysis procedure.

To isolate the effects of fissuring on the mechanical response of cartilage a time zero, high impact group was used. The patellae were impacted following arthrotomy and insertion of pressure film to simulate the open joint study. By removing the patellae immediately following the impact procedure transient post-surgical softening was avoided. Although the average peak impact loads for the acute study were 12 and 22% higher than those reported in the background studies, the impact pressure profiles and fissure sites suggest that the impact conditions within the joints were similar to those seen in the background studies. Histologic analysis of the time zero group detected no discernable loss of PGs in the test side cartilage as an effect of the impact procedure. However, the mechanical tests performed on the time zero, impact group did detect a significant decrease (11.5%) in the unrelaxed shear modulus (i.e. instantaneous stiffness) of the test side cartilage. The instantaneous stiffness of cartilage has been shown to depend on the integrity of the collagen network (Mizrahi, et al., 1986; Parsons and Black, 1987; Jurvelin, et al., 1988). This suggests that a disruption in the collagen network, created by the impact fissures, caused the measured decrease in instantaneous stiffness.

The exact affect of fissuring on the permeability of the cartilage was not completely obvious. The small number of biphasic observations in each acute group (n=4) were further reduced in the time zero group by the inability of the biphasic algorithm to fit the experimental data. This made it impossible to draw a decisive conclusion about the effects of fissuring on the permeability of cartilage. In the two (test vs. control) comparisons that were available, however, the test side permeability values were higher. This suggests that impact fissures may increase the permeability of

cartilage.

The second goal of the acute study was to determine whether an interaction exist between the cartilage fissures and surgically damaged synovium which might enhance their individual degradation affects. It has been suggested that this type of interaction may occur (Walker, et al., 1991). Of particularly interest were the effects of such an interaction one day post-surgery, since large differences in stiffness were noted at this time point between the high and low impact groups of the open joint study. To determine the interactive effects of fissuring and surgical synovitis it was necessary to first define their individual effects. The effects of fissuring were determined in the time zero impact group. However, the effects of surgical synovitis alone on the mechanical response of cartilage were yet unknown. To determine these effects the one day, sham group was devised. This group exposed the test cartilage to a surgically damaged synovium for 24 hours before mechanical tests were performed. This group was analogous to the 1 day, low impact group of the open joint study. That is to say that both these groups exposed unfissured patellar cartilage to surgical synovitis for 24 hours before testing. The results of the mechanical tests performed on the sham specimens revealed that the test side relaxed modulus (Gr) had been significantly reduced by (13.2%) due to the 24 hour exposure to the damage joint environment. This reduction was shown to be significantly larger than the decrease in Gr values measured in the time zero group. As previously mentioned the equilibrium stiffness of cartilage has been shown to be directly related to the PG content of cartilage (Parsons and Black, 1987; Jurvelin, et al., 1988). The histological analysis of the one day, sham group was unable to detect any loss of PGs as an effect of the surgical exposure. This may have been due

to the small number of histologic comparisons from each of the acute study groups (n=2). Another possibility may be that surface PGs were not removed but were altered by exposure to blood or enzymes from the damaged synovium (Ghadailly, et al., 1983; Walker, et al., 1991). It has been suggested that not only the quantity, but also the quality, of PGs can affect the load carrying capabilities of cartilage (Jurvelin, et al., 1988). Changes in the functional structure of PGs caused by surgical damage may account for the drop in Gr values measured in the one day, sham group. Interestingly a decrease in Gr was not observed in the one day, low impact group of the open joint study. This may have been due to the small number of observations made at this time point (n=3).

The biphasic results for the one day, sham group, although based on a small number of observations, showed that in 3 out of 4 cases the test side permeability was increased. It has been suggested that a partial cleavage of PGs may decrease the viscosity of the cartilage matrix allowing it to flow under stress (Parsons and Black, 1987). This may explain the increased permeability trend, as well as the decreased flow viscosity values measured on the test side.

With the individual effects of fissuring and surgical synovitis determined these two factors were next combined for analysis in the one day, high impact group. This group was identical in procedure to the 1 day, high impact group of the open joint study. The mechanical test results of this group showed a significant decrease in the modulus values (Gu by 21.9% and Gr by 14.3%) as well as the flow viscosity (23.4%). Although the decrease in Gr was not as substantial as those measured at one day in the open joint study, the overall decreasing trends were similar. A visual examination of the results

from all three acute study groups suggests that the mechanical response of the one day, high impact group was a combination of the individual effects of fissuring and synovitis. However, the reductions in  $G_u$  and  $\eta$  were larger than those measured in the time zero, impact and one day, sham groups. This suggests that an interaction between the fissures and damaged synovium may have taken place. It has been suggested that fissured cartilage may be more permeable to cytokines and enzymes present in synovial fluid (Walker, et al., 1991). Although, histology was unable to detect a loss of PGs on the test side (even adjacent to fissured areas), it is possible that an alteration in PG structure, as mentioned previously, may have occurred. The number of PGs altered by cytokine and enzyme exposure may have been increased by an increase in permeability created by the presence of impact fissures. Although this interaction could not be statistically proven, such a phenomena may have contributed to the larger decreases in  $G_u$  and  $\eta$  measured in the one day, impact group.

The biphasic results from the one day, impact group demonstrated an increase in test side permeability in all 3 available comparisons. These increases in permeability also seem to support the decrease measured in flow viscosity. However, due to the small number of observations, it was not apparent whether these increases in permeability were greater than those observed in the time zero impact and one day sham groups.

### Synovitis Study

The primary objective of the synovitis study was to determine whether a synovial inflammation, similar to that produced by arthrotomy, could be created by mechanical trauma to the synovial tissue lining the joint. The results of the acute study suggest that

the presence of synovitis can have a degrading affect on the mechanical response of AC. The acute study also suggests, although not statistically, that if cartilage fissures are present simultaneously with a synovitis that their degenerative affects may be enhanced. If a synovitis can be induced experimentally through blunt impact, then its possible that such inflammation may also occur following a natural impact situation. Loading of the cartilage during this softened state may act to further degrade mechanical properties and accelerate the degenerative processes.

The original synovitis sham group was developed to investigate the possibility of inducing a synovitis through the use of blunt trauma. This trauma was carried out on the synovial tissue directly medial and lateral to the patella. This synovial trauma was performed without the use of the restraining chair (Part I). For six days following synovial trauma the rabbits were exercised to aggravate the injured tissue in order to elicit and/or maintain a synovial response. Histologic analysis of the cartilage revealed no change in the PG content of the test side patellae. However, examination of the synovial lining revealed areas that appeared to be thickened (i.e. hypercellular) in the test side joints. This suggests that a traumatic synovitis was produced as a result of blunt impact. The results of the mechanical test showed that none of the test side parameters ( $G_u$ ,  $G_r$  and  $\eta$ ) had been decreased as anticipated. In fact they had all increased ( $G_u=18.3\%$ ,  $G_r=10.9\%$  and  $\eta=25.3\%$ ). These results are similar to those reported by Altman, et al., 1984, and Myers, et al., 1986, in canine cartilage following ACL transection prior to any signs of surface fissuring. Altman, et al., measured increases in the shear moduli ( $G_u$ ,  $G_r$ ) and retardation spectrums (creep equivalent of  $H(\tau)$ ) in the cartilage during this time period. These increases in stiffness were measured

concurrently with a decrease in the depth of creep indentation and an increase in cartilage swelling. Altman, et al., attributed these increases to tissue edema. A similar swelling may have occurred in the synovitis sham group. This edema may have resulted from enzymatic exposure. Collagenolytic activity in cartilage has been shown to be directly related to the degree of synovial inflammation (Pelletier, et al., 1985). It is possible that in response to the blunt trauma cytokines and/or enzymes may have been released from the damaged synovium. Typically the large negative charge associated with the PGs prevents the penetration of these degradative substances into the cartilage (Okada, et al., 1992). However, these substances may be able to penetrate the surface layer of the cartilage, where collagen content is high, but PG content is low. This may have allowed enzymatic weakening of the superficial layer without compromising the overall tensile strength of the collagen network. Under the strain of daily exercise this weakened superficial layer may have been loosened. This disruption of the surface collagen may have allowed underlying PGs to imbibe more water (Donahue, et al., 1983). This swelling in turn would create increased tension in the collagen network and hydrostatic pressure in the interstitial water (Maroudas, et al., 1979; Mizrahi, et al., 1986). These increases in collagen tension and fluid pressure would account for the increases measured in stiffness and flow viscosity measured in the sham group.

No definitive increase or decrease in test side permeability was apparent from the biphasic results for the sham group. These biphasic results are similar to findings by Myers, et al., 1986. As previously mentioned, like Altman, et al., 1984; Myers, et al., also measured an increase in canine cartilage stiffness following ACL transection prior to the development of surface disruptions. However, the results of their confined creep

tests were unable to detect any changes in permeability of the intact cartilage.

In the second group from the original synovitis study (Part I) synovial trauma was again induced without the use of the restraining chair. Five minutes after synovial trauma, however, the rabbits underwent a high level patellar impact. This group was used to determine whether or not the presents of fissures would altered the mechanical responses seen in the sham group. A histological examination of the test side synovial lining revealed thickened areas (hyperplasia) in one of the two animals analyzed. Histological examination of the AC, however, did not reveal a loss of PGs as a result of the synovial trauma and/or patellar impact. The solid indenter test results revealed that all three mechanical parameters had been significantly reduced ( $Gu=29.1\%$ ,  $Gr=17.0\%$  and  $\eta=25.3\%$ ). These decreasing trends were similar to those reported in the one day impact group of the acute study. These decreases, although less in intensity, were also similar to those seen in the six day, high impact group of the open joint study. The similarity between these groups suggests that the affects of synovial trauma on the AC were similar to, although less severe than, those created by arthrotomy. The differences between the impact and sham groups in Part I suggests that synovial trauma may have an increased degenerative effect on cartilage when fissures are present. Upon comparison with the results of the time zero, impact group from the acute study, it would appear that the decrease in instantaneous stiffness measured in the synovitis impact group is probably an effect of the cartilage fissures. These fissures may have increased the permeability of the cartilage allowing synovial enzymes and cytokines to penetrate deeper into matrix of the cartilage. This increased penetration by enzymes and cytokines may have allowed further degradation of the cartilage matrix, especially in the fissured regions

(Walker, et al., 1991). A scenario such as this may account for the secondary decreases measured in Gr and  $\eta$ .

The biphasic results of the synovitis impact group (Part I) revealed no changes in the permeability of the test cartilage. The reasons for this lack of change are not quite clear. These results appear to be contradictory to the increased cartilage permeability measured in the fissured specimens of the acute study. The inability to measure a decrease may be due to the small number of observations ( $n=2$  rabbits). Interestingly, however, Myers, et al., 1986, was also unable to detect any changes in the permeability of canine cartilage following ACL transection at later time points when cartilage fibrillation was noted in conjunction with decreases in stiffness. Myers, et al., provided no explanation for these results.

The same two groups, sham and impact, were used in Part II of the synovitis study. Unlike Part I, however, synovial trauma was induced while the rabbit's test leg was held in hyperflexion by the restraining chair. The solid indenter results of both the sham and impact groups in Part II demonstrated no significant decrease in Gu, Gr or  $\eta$  in the test cartilage. The increases which had been measured in the sham group during Part I were also not detected in Part II. From these results it would appear that the synovial response was somehow altered by placing the rabbit in the restraining chair during trauma induction. The exact cause of this altered response is not clear. Although some areas of hyperplasia were noted in the synovial lining of the test joints, the extent of synovial damage is unknown. Spatial constraints imposed by the sides of the restraining chair made the delivery of the synovial trauma more difficult. The inability to make a normal swing with the hammer may have reduced the amount of damage

imparted by each tap. Another possibility is that a damage shielding effect may be created by hyperflexion of the knee. In Part I the synovial trauma was carried out while the leg was manually held at 45 degrees of flexion. During impact, the synovial tissue was relatively free to deform. It is likely that under these conditions the synovial lining was not only damaged by compressive forces, but may have suffered damage due to stretch deformation. When hyperflexed, as in Part II, the synovial tissues surrounding the knee are stretched tightly over the underlying bone. Striking the synovial tissue under this scenario may have allowed the impact force to be more directly absorbed by the underlying bone, decreasing synovial damage due to excessive stretch. This may have resulted in a decreased level of synovial trauma which was not strong enough to alter the mechanical properties of the cartilage. This reduction in synovial damage may explain the lack of change measured in the sham group, however, it does not explain the lack of stiffness change in the impact group. This is probably due to the small number of observations in this group ( $n = 3$  rabbits) and the fact that only one of the three test patellae was fissured.

As in Part I, the biphasic results of Part II also did not demonstrate any definitive increase or decrease in the test side permeability in either the sham or impact group. This maybe due to the small number of observations in each group. Especially the impact group where the small sample size was further reduced by the inability of the algorithm to fit the experimental data from two of the porous tests.

The elastic and viscoelastic results of the porous tests were purposely excluded from the discussion of the acute and synovitis study due to their lack of additive

information. Overall porous  $G_u$  values were reduced approximately 50% compared to the average values calculated for the solid indenter tests. This reduction was anticipated. The relatively slow indentation rates (1 and 2 seconds) used for the porous tests allowed cartilage relaxation during loading resulting in low peak forces ( $P$ ). From equation (1) it is apparent that a decrease in peak load would directly results in a decrease in  $G_u$ . The porous  $G_r$  values were also decreased below solid indenter values. This change was not initially expected. It was anticipated that at equilibrium the solid and porous results would agree, just as the elastic solution of Hayes, et al., 1972, and the biphasic stress-relaxation solution of Mak, et al., 1987, agree at equilibrium for  $\nu = \nu_s$ . Two possible reasons have been proposed to explain these differences. The first being that both the solid and porous indenter  $G_r$  values were determined at different relaxation times, 150 and 1000 seconds, respectively. According to Mow, et al., 1989, both of these times are less than the average time required for complete cartilage relaxation. Therefore, the longer relaxation time associated with the porous test should allow a larger amount of relaxation resulting in smaller relaxation loads. Based on previous comparison tests carried out in our lab, this may account for approximately 10% of the decrease in the porous  $G_r$  values. However, the porous  $G_r$  values were typically more than 10% lower than the solid indenter values. A second contributing factor may be due to the permeable boundary conditions created by using the porous indenter. Spilker, et al., 1992, performed a finite element comparison between the stress-relaxation behavior of cartilage indented by both a porous and solid indenter. Under similar loading conditions the reaction forces generated in cartilage by the solid indenter were greater than those of the porous indenter at all time points along the response curves, except equilibrium. This

difference was due to larger fluid pressure within the cartilage created by the impermeable surface condition of the solid indenter. Therefore, at time points short of true equilibrium the calculation of Gr for the solid indenter would be greater than that for the porous indenter due to larger resistive loads. The small number of observations and variations in the flow viscosity values made comparisons with the permeability values difficult. It could not be determined whether or not increases in permeability corresponded with decreases in flow viscosity as hypothesized.

## SUMMARY

The current investigations rose out of questions generated by the differing results of the previous open and closed joint studies. The acute study was devised to address two main objectives. The first objective was to define the effects of impact induced fissures on the mechanical behavior of AC. The second goal was to determine whether the degenerative affects of these fissure were enhanced by the presence of a surgical synovitis. Otherwise stated, to determine whether or not an interaction exist between the fissures and synovitis. The results of the acute study revealed that the presence of impact fissures can significantly reduced the unrelaxed shear modulus of AC. This reduction in stiffness is probably due to a disruption of the collagen network created by the fissures. The results also revealed that by exposing the cartilage to a surgical damaged joint environment for 24 hours a significant reduction in the relaxed shear modulus can be created. Although histological analysis revealed no loss of PGs, this decrease in equilibrium stiffness may be the result of a partial breakdown of the cartilage matrix invoked by exposure to enzymes and/or blood from the surgically damaged synovium. Statistically an interaction between the two factors, fissures and surgical synovitis, could not be proven. However, exposure of fissured cartilage to a surgical synovitis did result in an overall significant decreases in shear moduli and flow viscosity. The presence of fissures may have enhanced the affects of the cytokines and enzymes by allowing deeper

penetration into the cartilage.

It was hypothesized that by loading the cartilage (e.g. exercise) during the softened state created by synovitis, the rate of cartilage degeneration could be accelerated. The synovitis study was developed to investigate the possibility of inducing a synovitis by mechanical means under closed joint conditions. The synovitis was induced by blunt trauma to the synovial tissue surrounding the patella. In Part I, synovial trauma was induced while the rabbits hind limb was hand held at 45 degrees of flexion. Following synovial trauma, half of these rabbits received a high level patellar impact to induce cartilage fissures. The rabbits were exercised to maintain and provoke a synovial response. Histological examination of the traumatized synovial lining revealed areas of hyperplasia. Although histological analysis was unable to detect any loss of cartilage proteoglycans in the traumatized joints, the results of the indentation tests did reveal mechanical changes in the test cartilage. In the sham group, which received only synovial trauma, the intact test cartilage showed an increase in shear moduli ( $G_u$  and  $G_r$ ) and flow viscosity ( $\eta$ ). These increases were believed to be an effect of edema created by the exposure of the intact cartilage to a trauma induced synovitis. Five of the six rabbits which received patellar impact in addition to synovial trauma had observable cartilage fissures. The indentation results of this group revealed significant decreases in all three mechanical parameters ( $G_u$ ,  $G_r$  and  $\eta$ ). These reductions in stiffness and viscosity were attributed to both the disruption of the collagen network created by the fissures, and exposure of the cartilage to the damage synovial environment. These fissures are believed to have increased the permeability of the cartilage surface layer. This increased permeability may have allowed deeper penetration by enzymes and

cytokines released from the damage synovium, thereby enhancing their degradative affects on the cartilage.

Two study groups were also used in Part II of the synovitis study. In both groups the rabbits received synovial trauma while their hind limb was held in hyperflexion by the surgical restraining chair. In addition to synovial trauma, one of the two groups also received patellar impact to induce cartilage fissures. Histological analysis revealed areas of hyperplasia in the traumatized synovial linings. The mechanical results of both the impact and sham groups revealed no significant changes in the stiffness or viscosity of the test cartilage. This lack of change may be the result of a reduction in the extent of synovial trauma created by hyperflexion of the test limb. Hyperflexion stretches the synovial membrane tightly over the underlying bone. In this stretched state the brunt of impacts may have been directly transmitted to the bone diminishing the extent of synovial damage. The spacial constraints created by the use of the restraining chair prevented full length hammer strokes further reducing the ability to induce synovial trauma. In the impact group a lack of cartilage fissuring (1 out of 3) was also believed to be responsible for failure to measure a reduction in the unrelaxed modulus.

## **RECOMMENDATIONS**

The results of both the acute and synovitis study suggests that the load carrying capabilities of impact fissured cartilage can be significantly reduced by exposure to a synovitis. The synovitis study further suggested that a traumatic synovitis can be created by mechanical means under closed joint conditions. Extraneous loading of the cartilage in this softened condition may enhance its degeneration. Future long term, closed joint studies should include further investigation into the use of synovitis as a means of accelerating cartilage degeneration. To more closely simulate a natural impact scenario a trauma method should be developed to induce both cartilage fissuring and synovial damage simultaneously. This may require re-design of the restraining chair in order to prevent possible damage shielding effects created by hyperflexion of the test limb. In addition to the histological analysis used in the synovitis study, future studies should also include biochemical determination of synovial enzyme and cytokine levels, and cartilage water content. This will provide a means of verifying the existence, degree and effects of synovial inflammation.

## APPENDIX

**Table 3: Six Day Low Impact Force Parameters from the Blunt Impact Procedure**

<u>Rabbit</u>	<u>Peak Load</u>	<u>Impact Rise Time</u>	<u>Impact Duration</u>	<u>Trauma Status</u> {+ = fissure(s)} {- = no fissure(s)}
A36	191	2.7	8.5	-
S3M	155	1.8	6.7	-
G5	--	--	--	-
CKGO	--	--	--	-
DS36	169	2.2	6.5	-
BUTCH	195	2.9	6.9	-
A42	169	2.5	9.1	-
B4	142	2.6	10.6	-
<b>Average</b>	<b>168 ± 23.1 (N)</b>	<b>2.5 ± 0.4 (ms)</b>	<b>8.1 ± 1.6 (ms)</b>	<b>no impact fissures</b>

Table 4: Six Day High Impact Force Parameters from the Blunt Impact Procedure

<u>Rabbit</u>	<u>Peak Load</u>	<u>Impact Rise Time</u>	<u>Impact Duration</u>	<u>Trauma Status</u> {+ = fissure(s)} {- = no fissure(s)}
B36	534	3.4	14.1	+
S3	431	2.4	6.9	+
CKBAR	578	3.5	14.5	-
B44	418	1.9	19.6	+
KCATF	489	4.0	9.5	+
BUSTER	387	2.4	8.9	-
B1	623	6.1	15.3	-
B5	489	2.6	6.2	+
Average	493 ± 81.4 (N)	3.3 ± 1.3 (ms)	11.9 ± 4.7 (ms)	5 of 8 fissured

Table 5: Three Month Low Impact Force Parameters from the Blunt Impact Procedure

<u>Rabbit</u>	<u>Peak Load</u>	<u>Impact Rise Time</u>	<u>Impact Duration</u>	<u>Trauma Status</u> {+ = fissure(s)}
I23	169	1.5	6.2	-
I20	164	2.0	7.8	-
I21	164	1.7	7.6	-
I29	155	1.6	12.2	-
I26	151	1.6	8.3	-
I24	178	1.5	9.9	-
I27	137	1.6	11.2	-
<b>Average</b>	<b>160 ± 13 (N)</b>	<b>1.6 ± 0.2 (ms)</b>	<b>9.0 ± 2.1 (ms)</b>	<b>no impact fissures</b>

Table 6: Three Month High Impact Force Parameters from the Blunt Impact Procedure

<u>Rabbit</u>	<u>Peak Load</u>	<u>Impact Rise Time</u>	<u>Impact Duration</u>	<u>Trauma Status</u> {+ = fissure(s)} {- = no fissure(s)}
CKROY	489	3.1	8.0	+
I19	667	4.0	9.0	+
I7	489	2.6	7.9	-
I17	534	3.6	9.1	+
I28	623	4.5	10.6	-
I30	623	3.4	8.8	+
I25	578	3.7	9.5	+
<b>Average</b>	<b>572 ± 69.8 (N)</b>	<b>3.6 ± 0.6 (ms)</b>	<b>8.9 ± 0.9 (ms)</b>	<b>5 of 7 fissured</b>

Table 7: Six Month, Low Impact Closed Joint Force Parameters from the Blunt Impact Procedure

<u>Rabbit</u>	<u>Peak Load</u>	<u>Impact Rise Time</u>	<u>Impact Duration</u>	<u>Trauma Status</u> {+ = fissure(s)} {- = no fissure(s)}
CKOH10	160	0.16	1.0	-
I34	169	0.16	0.4	-
I31	111	0.32	1.4	-
I58	160	0.14	1.1	-
I63	169	0.22	0.9	-
I65	160	0.18	1.0	+
I70	187	0.34	0.9	-
I69	125	0.34	1.4	-
Mean ± SD	155 ± 25 (N)	0.23 ± 0.09 (ms)	1.0 ± 0.3 (ms)	1 of 8 fissured

**Table 8: Six Month, High Impact Closed Joint Force Parameters from the Blunt Impact Procedure**

<b><u>Rabbit</u></b>	<b><u>Peak Load</u></b>	<b><u>Impact Rise Time</u></b>	<b><u>Impact Duration</u></b>	<b><u>Trauma Status</u></b> {+ = fissure(s)} {- = no fissure(s)}
321	623	0.48	1.1	+
I37	579	0.48	1.1	+
I59	490	0.26	0.9	+
I62	757	0.50	1.3	-
I68	490	0.38	1.8	+
BB2	579	0.42	1.4	+
I67	427	0.38	1.1	+
I39	534	0.28	0.8	+
<b>Average</b>	<b>560 ± 101 (N)</b>	<b>0.40 ± 0.09 (ms)</b>	<b>1.2 ± 0.3 (ms)</b>	<b>7 of 8 fissured</b>

**Table 9: One Year, Low Impact Closed Joint Force Parameters from the Blunt Impact Procedure**

<b><u>Rabbit</u></b>	<b><u>Peak Load</u></b>	<b><u>Impact Rise Time</u></b>	<b><u>Impact Duration</u></b>	<b><u>Trauma Status</u></b> {+ = fissure(s)} {- = no fissure(s)}
BN3	156	0.14	0.9	-
I6	169	0.22	0.8	-
I4	125	0.15	0.8	+
I15	134	0.24	1.1	+
I3	151	0.19	1.1	-
<b>Mean <math>\pm</math> SD</b>	<b>147 <math>\pm</math> 18 (N)</b>	<b>0.19 <math>\pm</math> 0.04 (ms)</b>	<b>0.9 <math>\pm</math> 0.2 (ms)</b>	<b>2 of 5 fissured</b>

Table 10: One Year, High Impact Closed Joint Force Parameters from the Blunt Impact Procedure

<u>Rabbit</u>	<u>Peak Load</u>	<u>Impact Rise Time</u>	<u>Impact Duration</u>	<u>Trauma Status</u> {+ = fissure(s)} {- = no fissure(s)}
GAG	757	0.48	1.1	+
I1G	668	0.36	0.9	+
I2	490	0.44	1.1	+
BC5	579	0.50	1.2	+
I8	579	0.50	1.1	+
I12	712	0.50	1.2	+
BAA	579	0.36	0.8	
<b>Average</b>	<b>623 ± 93 (N)</b>	<b>0.45 ± 0.06 (ms)</b>	<b>1.1 ± 0.2 (ms)</b>	<b>6 of 6 fissured</b>

**Table 11: Results of Mechanical Tests on the 6 Day, Low Level Impact Closed Joint Group**  
**6 DAY, LOW IMPACT, CLOSED JOINT (Lateral Facet)**

<u>Rabbit</u>	<u>TEST SIDE</u>				<u>CONTROL SIDE</u>				<u>RATIO OF TEST TO CONTROL</u>			
	<u>Gu (MPa)</u>	<u>Gr (MPa)</u>	<u><math>\eta</math></u>	<u>Gu (MPa)</u>	<u>Gr (MPa)</u>	<u><math>\eta</math></u>	<u>Gu(t/c)</u>	<u>Gr(t/c)</u>	<u><math>\eta(t/c)</math></u>	<u>Gu(t/c)</u>	<u>Gr(t/c)</u>	<u><math>\eta(t/c)</math></u>
DS36	0.797	0.187	12.662	1.121	0.169	15.544	0.711	1.107	0.815	0.711	1.107	0.815
	0.367	0.167	4.574	0.387	0.167	5.841	0.948	1.000	0.783	0.948	1.000	0.783
B4	0.865	0.278	12.317	1.263	0.321	16.496	0.685	0.866	0.747	0.685	0.866	0.747
	1.029	0.336	13.151	1.367	0.271	9.599	0.753	1.240	1.370	0.753	1.240	1.370
A42	0.778	0.179	11.116	0.395	0.174	5.224	1.970	1.029	2.128	1.970	1.029	2.128
	0.634	0.223	6.845	0.679	0.187	12.141	0.934	1.193	0.564	0.934	1.193	0.564
BUTCH	0.885	0.200	18.460	0.386	0.168	4.803	2.293	1.190	3.843	2.293	1.190	3.843
	1.114	0.289	16.907	0.607	0.216	7.662	1.835	1.338	2.207	1.835	1.338	2.207
G5	0.760	0.218	11.759	0.957	0.271	12.951	0.794	0.804	0.908	0.794	0.804	0.908
	0.471	0.198	5.762	0.827	0.312	11.226	0.570	0.635	0.513	0.570	0.635	0.513
S3M	1.703	0.173	20.609	0.473	0.108	6.319	3.600	1.602	3.261	3.600	1.602	3.261
	1.056	0.164	12.933	0.717	0.144	5.286	1.473	1.139	2.447	1.473	1.139	2.447
CKGO	0.283	0.214	4.289	0.386	0.167	7.258	0.733	1.281	0.591	0.733	1.281	0.591
	0.362	0.139	4.259	0.418	0.161	6.511	0.866	0.863	0.654	0.866	0.863	0.654
A36	0.401	0.105	6.461	0.657	0.148	10.665	0.610	0.709	0.606	0.610	0.709	0.606
	0.58	0.163	6.613	0.716	0.174	8.519	0.810	0.937	0.776	0.810	0.937	0.776
Mean	0.755	0.202	10.545	0.710	0.197	9.128	1.224	1.058	1.388	1.224	1.058	1.388
±SD	0.365	0.058	5.224	0.322	0.063	3.709	0.827	0.253	1.059	0.827	0.253	1.059

**Table 12: Results of the Mechanical Tests on the 6 Day, High Level Impact, Closed Joint Group**  
**6 DAY, HIGH IMPACT, CLOSED JOINT (Lateral Facet)**

	<u>TEST SIDE</u>			<u>CONTROL SIDE</u>			<u>RATIO OF TEST TO CONTROL</u>		
	<u>Gu (MPa)</u>	<u>Gr (MPa)</u>	<u><math>\eta</math></u>	<u>Gu (MPa)</u>	<u>Gr (MPa)</u>	<u><math>\eta</math></u>	<u>Gu(t/c)</u>	<u>Gr(t/c)</u>	<u><math>\eta(t/c)</math></u>
<b>Rabbit</b>									
KCATF	0.837	0.129	13.362	0.316	0.106	3.872	2.649	1.217	3.451
	0.470	0.130	10.023	0.229	0.093	2.052	2.052	1.398	4.885
B5	0.342	0.169	3.012	0.690	0.272	9.578	0.496	0.621	0.314
	0.510	0.243	5.223	0.773	0.312	8.005	0.660	0.779	0.652
B1	0.901	0.275	14.715	0.621	0.294	6.428	1.451	0.935	2.289
	0.716	0.251	9.804	0.636	0.271	7.280	1.126	0.926	1.347
CKBAR	2.431	0.321	27.376	1.202	0.289	16.589	2.022	1.111	1.650
	0.498	0.183	8.971	0.998	0.278	17.415	0.499	0.658	0.515
B36	1.127	0.146	11.895	0.512	0.139	6.921	2.201	1.050	1.719
	0.565	0.140	5.999	0.749	0.193	12.028	0.754	0.725	0.499
S3	0.792	0.149	9.908	0.823	0.111	9.776	0.962	1.342	1.014
	0.746	0.157	10.072	0.643	0.136	8.725	1.160	1.154	1.154
BUSTR	0.707	0.132	10.042	0.664	0.142	7.047	1.065	0.930	1.425
	0.927	0.163	8.796	0.888	0.135	10.642	1.044	1.207	0.827
B44	1.048	0.342	15.783	1.007	0.245	16.104	1.041	1.396	0.980
	0.759	0.269	7.211	0.613	0.177	8.267	1.238	1.520	0.872
<b>Mean</b>	<b>0.836</b>	<b>0.200</b>	<b>10.762</b>	<b>0.710</b>	<b>0.200</b>	<b>9.421</b>	<b>1.276</b>	<b>1.061</b>	<b>1.475</b>
<b>±SD</b>	<b>0.476</b>	<b>0.072</b>	<b>5.545</b>	<b>0.247</b>	<b>0.078</b>	<b>4.341</b>	<b>0.637</b>	<b>0.279</b>	<b>1.198</b>

**Table 13: Results of the Mechanical Tests on the 3 Month, Low Level Impact, Closed Joint Group**  
**3 MONTH, LOW LEVEL, CLOSED JOINT (lateral facet)**

	<u>TEST SIDE</u>			<u>CONTROL SIDE</u>			<u>RATIO OF TEST TO CONTROL</u>		
	<u>Gu (MPa)</u>	<u>Gr (MPa)</u>	<u><math>\eta</math></u>	<u>Gu (MPa)</u>	<u>Gr (MPa)</u>	<u><math>\eta</math></u>	<u>Gu(t/c)</u>	<u>Gr(t/c)</u>	<u><math>\eta(t/c)</math></u>
<u>Rabbit</u>									
I20	0.515	0.209	6.641	0.267	0.153	2.786	1.929	1.366	2.384
	0.419	0.157	5.280	0.467	0.206	6.502	0.897	0.762	0.812
	0.661	0.247	7.732	0.839	0.275	11.072	0.788	0.898	0.698
I21	0.530	0.203	7.126	0.388	0.160	2.535	1.366	1.269	2.811
	0.397	0.186	3.706	0.347	0.184	3.340	1.144	1.011	1.110
	0.424	0.199	8.211	1.035	0.251	19.336	0.410	0.793	0.425
I23	0.838	0.289	10.542	1.229	0.297	17.324	0.682	0.973	0.609
	0.513	0.239	6.506	0.888	0.319	10.221	0.578	0.749	0.637
	1.156	0.412	12.988	1.113	0.373	15.517	1.039	1.105	0.837
I24	1.003	0.309	19.753	0.519	0.205	8.283	1.933	1.507	2.385
	0.645	0.273	6.655	0.877	0.258	11.415	0.735	1.058	0.583
	0.563	0.229	12.317	0.494	0.236	7.531	1.140	0.970	1.636
I27	1.081	0.235	20.001	0.639	0.201	17.348	1.692	1.169	1.153
	0.315	0.166	5.071	0.240	0.173	2.667	1.313	0.960	1.901
	1.503	0.223	31.114	1.812	0.244	28.609	0.829	0.914	1.088
I26	0.286	0.110	3.145	0.295	0.108	3.640	0.969	1.019	0.864
	0.178	0.108	1.464	0.084	0.082	2.530	2.119	1.317	0.579
	0.234	0.194	5.321	0.165	0.146	12.562	1.418	1.329	0.424
I29	1.447	0.330	24.465	0.691	0.271	13.478	2.094	1.218	1.815
	0.619	0.251	11.263	0.600	0.252	9.051	1.032	0.996	1.244
	1.172	0.270	18.297	0.927	0.272	17.702	1.264	0.993	1.034
Mean	0.690	0.230	10.838	0.663	0.222	10.640	1.208	1.065	1.192
±SD	0.392	0.071	7.745	0.418	0.071	6.959	0.503	0.207	0.700

**Table 14: Results of the Mechanical Tests on the 3 Month, High Level Impact, Closed Joint Group**  
**3 MONTH, HIGH LEVEL, CLOSED JOINT**

	<u>TEST SIDE</u>			<u>CONTROL SIDE</u>			<u>RATIO OF TEST TO CONTROL</u>			
	<u>Gu (MPa)</u>	<u>Gr (MPa)</u>	<u>n</u>	<u>Gu (MPa)</u>	<u>Gr (MPa)</u>	<u>n</u>	<u>Gu(t/c)</u>	<u>Gr(t/c)</u>	<u>n(t/c)</u>	
<u>Rabbit</u> 17	0.817	0.338	20.458	0.877	0.314	9.972	0.932	1.076	2.052	
	0.445	0.241	10.146	0.710	0.315	3.708	0.627	0.765	2.736	
	0.561	0.221	11.739	0.661	0.346	8.034	0.849	0.639	1.461	
I19	0.463	0.153	6.905	0.864	0.236	13.761	0.536	0.648	0.502	
	0.489	0.197	4.465	0.470	0.204	5.979	1.040	0.966	0.747	
	0.766	0.257	8.186	0.508	0.200	5.699	1.508	1.285	1.436	
CKRO	0.755	0.258	6.440	1.041	0.183	9.160	0.725	1.410	0.703	
	0.831	0.252	7.182	0.873	0.307	8.988	0.952	0.821	0.799	
	0.885	0.264	13.734	0.883	0.325	10.453	1.002	0.812	1.314	
I17	1.176	0.279	20.458	0.541	0.228	9.972	2.174	1.224	2.052	
	0.614	0.248	10.146	0.492	0.203	3.708	1.248	1.222	2.736	
	0.959	0.255	11.739	0.628	0.235	8.034	1.527	1.085	1.461	
I25	0.828	0.329	12.301	1.194	0.298	26.965	0.693	1.104	0.456	
	0.595	0.262	13.147	0.548	0.259	5.895	1.086	1.012	2.230	
	0.752	0.288	6.382	1.145	0.312	20.063	0.657	0.923	0.318	
I28	0.318	0.118	13.393	0.295	0.128	11.204	1.078	0.922	1.195	
	0.178	0.113	4.599	0.084	0.078	2.098	2.119	1.449	2.192	
	0.234	0.120	4.291	0.165	0.181	4.868	1.418	1.538	0.881	
I30	0.731	0.143	18.172	0.724	0.211	19.059	1.010	0.790	0.953	
	0.798	0.236	19.762	0.515	0.211	9.136	1.550	1.118	2.163	
	0.748	0.182	9.652	1.067	0.232	22.738	0.701	0.784	0.424	
Mean	0.664	0.226	11.109	0.680	0.232	10.452	1.116	1.028	1.372	
±SD	0.246	0.066	5.200	0.305	0.077	6.613	0.458	0.259	0.772	

**Table 15: Results of the Mechanical Tests on the 6 Month, Low Level Impact, Closed Joint Group**  
**6 MONTH, LOW IMPACT, CLOSED JOINT**

	<u>TEST SIDE</u>			<u>CONTROL SIDE</u>			<u>RATIO OF TEST TO CONTROL</u>			
	<u>Gu (MPa)</u>	<u>Gr (MPa)</u>	<u><math>\eta</math></u>	<u>Gu (MPa)</u>	<u>Gr (MPa)</u>	<u><math>\eta</math></u>	<u>Gu(t/c)</u>	<u>Gr(t/c)</u>	<u><math>\eta(t/c)</math></u>	
<u>Rabbit</u> <u>ckoh</u>	0.808	0.260	24.153	0.545	0.197	5.538	1.483	1.320	4.361	
	0.838	0.330	15.284	0.644	0.233	10.603	1.301	1.416	1.441	
	0.638	0.281	7.697	0.575	0.220	5.695	1.110	1.277	1.352	
	3.804	0.316	54.031	2.629	0.257	36.479	1.447	1.230	1.481	
I34	2.185	0.294	27.526	2.335	0.278	26.310	0.936	1.058	1.046	
	1.063	0.186	20.916	2.061	0.269	22.974	0.516	0.691	0.910	
	2.491	0.130	18.100	2.228	0.226	25.296	1.118	0.575	0.716	
	0.280	0.071	1.390	0.691	0.157	7.104	0.405	0.449	0.196	
I58	1.405	0.116	11.574	1.249	0.261	12.997	1.125	0.444	0.891	
	1.058	0.263	22.130	2.215	0.333	33.096	0.478	0.791	0.669	
	0.933	0.277	15.497	1.094	0.313	15.156	0.853	0.885	1.023	
	0.511	0.235	3.936	0.714	0.257	5.697	0.715	0.915	0.691	
I63	0.548	0.133	13.311	0.246	0.070	6.664	2.229	1.907	1.998	
	0.373	0.114	4.576	0.351	0.113	4.867	1.061	1.005	0.940	
	0.331	0.124	2.872	0.516	0.167	6.585	0.641	0.743	0.436	
	1.760	0.163	21.660	0.285	0.110	9.802	6.174	1.479	2.210	
I65	1.054	0.122	15.050	0.213	0.048	12.875	4.946	2.559	1.169	
	1.062	0.073	18.622	0.625	0.181	5.736	1.697	0.404	3.247	
	1.379	0.188	16.283	0.748	0.092	10.818	1.844	2.040	1.505	
	0.486	0.172	7.078	0.364	0.128	5.053	1.335	1.340	1.401	
I70	0.318	0.165	3.146	0.193	0.097	0.923	1.653	1.697	3.408	
	1.460	0.081	14.928	1.485	0.098	13.776	0.983	0.828	1.084	
	0.617	0.121	6.365	0.698	0.129	7.238	1.166	1.073	1.454	
	1.105	0.181	14.860	0.986	0.180	12.374	1.504	1.148	1.448	
Mean ±SD	0.814	0.080	11.127	0.759	0.083	9.538	1.338	0.537	0.985	

**Table 16: Results of the Mechanical Tests on the 6 Month, High Level Impact, Closed Joint Group**  
**6 MONTH, HIGH IMPACT, CLOSED JOINT**

<u>Rabbit</u>	<u>TEST SIDE</u>			<u>CONTROL SIDE</u>			<u>RATIO OF TEST TO CONTROL</u>			
	<u>Gu (MPa)</u>	<u>Gr (MPa)</u>	<u>n</u>	<u>Gu (MPa)</u>	<u>Gr (MPa)</u>	<u>n</u>	<u>Gu(t/c)</u>	<u>Gr(t/c)</u>	<u>m(t/c)</u>	
S321	0.923	0.301	21.652	1.210	0.277	32.167	0.763	1.086	0.673	
	0.636	0.314	10.417	0.943	0.275	16.818	0.674	1.143	0.619	
	0.442	0.306	5.152	0.371	0.182	5.225	1.192	1.676	0.986	
I37	2.448	0.302	38.080	2.396	0.244	33.534	1.022	1.238	1.136	
	0.916	0.279	9.327	2.101	0.344	25.325	0.436	0.811	0.368	
	0.639	0.234	4.895	0.921	0.277	9.215	0.694	0.845	0.531	
I59	2.538	0.395	39.191	1.829	0.330	36.293	1.388	1.195	1.080	
	1.252	0.303	13.606	2.195	0.423	24.630	0.570	0.715	0.552	
	0.696	0.216	5.920	1.767	0.365	17.914	0.394	0.591	0.330	
I62	1.997	0.211	22.573	1.559	0.170	24.364	1.280	1.242	0.926	
	1.461	0.305	22.290	0.897	0.240	15.386	1.628	1.271	1.449	
	1.284	0.314	16.885	1.066	0.266	14.354	1.205	1.183	1.176	
I68	0.656	0.240	9.077	0.994	0.310	18.433	0.660	0.774	0.492	
	0.830	0.346	8.890	0.968	0.361	11.174	0.857	0.960	0.796	
	0.839	0.346	10.851	0.636	0.247	5.383	1.319	1.262	2.016	
BB2	0.366	0.167	6.081	0.438	0.125	7.791	0.835	1.328	0.781	
	0.524	0.260	5.775	0.451	0.180	4.529	1.164	1.446	1.275	
	0.362	0.189	5.831	0.533	0.219	7.271	0.679	0.860	0.802	
I70	0.487	0.190	7.174	0.920	0.220	15.615	0.530	0.863	0.459	
	0.916	0.289	18.018	0.342	0.166	3.523	2.675	1.743	5.115	
	0.742	0.280	18.165	0.487	0.190	3.523	1.523	1.473	5.156	
I39	2.144	0.311	42.608	1.623	0.275	22.883	1.321	1.131	1.862	
	1.357	0.347	14.574	1.684	0.379	17.826	0.806	0.914	0.818	
	0.976	0.262	14.133	1.305	0.317	16.610	0.748	0.827	0.851	
Mean	1.060	0.278	15.465	1.152	0.266	16.241	1.015	1.107	1.260	
±SD	0.639	0.056	11.013	0.615	0.077	9.691	0.499	0.300	1.267	

Table 17: Results of Mechanical Testing on the 1 Year, Low Level Impact, Closed Joint Group

1 YEAR, LOW IMPACT, CLOSED JOINT											
Rabbit	TEST SIDE			CONTROL SIDE			RATIO OF TEST TO CONTROL				
	Gu (MPa)	Gr (MPa)	$\eta$	Gu (MPa)	Gr (MPa)	$\eta$	Gu(t/c)	Gr(t/c)	$\eta(t/c)$		
BN3	1.030	0.280	19.894	0.421	0.177	11.510	2.447	1.582	1.728		
	0.482	0.218	4.415	3.523	0.529	124.425*	0.137	0.412	0.035		
	0.145	0.126	0.486	0.607	0.286	6.231	0.239	0.441	0.078		
I6	2.345	0.206	27.565	3.833	0.112	22.019	0.612	1.839	1.252		
	1.934	0.219	17.969	0.351	0.110	4.329	5.510	1.991	4.151		
	0.588	0.201	0.762	0.327	0.121	2.000	1.798	1.661	0.381		
I3	1.236	0.129	14.387	1.247	0.150	18.728	0.991	0.860	0.768		
	0.465	0.133	8.173	0.755	0.139	9.392	0.616	0.957	0.870		
	0.954	0.180	16.468	1.717	0.203	22.589	0.556	0.887	0.729		
I4	0.996	0.237	14.630	1.241	0.269	16.450	0.803	0.881	0.889		
	0.777	0.237	9.322	1.061	0.269	13.006	0.732	0.881	0.717		
	0.475	0.139	9.132	1.023	0.202	18.457	0.464	0.692	0.495		
I15	0.28	0.143	2.609	1.37	0.249	19.814	0.204	0.574	0.132		
	0.242	0.131	1.591	0.479	0.183	4.581	0.505	0.715	0.347		
Mean	0.854	0.184	10.529	1.283	0.214	13.008	1.115	1.027	0.898		
±SD	0.639	0.051	8.253	1.100	0.109	7.200	1.414	0.521	1.046		

\* = outlier

**Table 18: Results of Mechanical Testing on the 1 Year, High Level Impact, Closed Joint Group**  
**1 YEAR, HIGH IMPACT, CLOSED JOINT**

Rabbit	<u>TEST SIDE</u>			<u>CONTROL SIDE</u>			<u>RATIO OF TEST TO CONTROL</u>		
	<u>Gu (MPa)</u>	<u>Gr (MPa)</u>	<u><math>\eta</math></u>	<u>Gu (MPa)</u>	<u>Gr (MPa)</u>	<u><math>\eta</math></u>	<u>Gu(t/c)</u>	<u>Gr(t/c)</u>	<u><math>\eta(t/c)</math></u>
I1G	0.414	0.196	3.682	0.890	0.161	15.854	0.465	1.217	0.232
	0.478	0.205	5.573	0.457	0.174	6.093	1.046	1.178	0.915
	0.339	0.195	2.217	0.429	0.223	3.969	0.790	0.874	0.559
GAG	0.409	0.177	13.873	0.667	0.177	13.401	0.613	1.000	1.035
	0.631	0.289	10.913	0.905	0.270	14.167	0.697	1.070	0.770
	0.187	0.133	1.970	1.245	0.280	17.705	0.150	0.475	0.111
I8	1.311	0.212	22.506	0.619	0.127	9.104	2.118	1.669	2.472
	0.847	0.252	11.747	0.883	0.218	11.816	0.959	1.156	0.994
	0.359	0.196	3.332	0.487	0.219	4.055	0.737	0.895	0.822
I12	0.649	0.188	15.697	0.918	0.231	18.716	0.707	0.814	0.839
	0.470	0.191	7.149	1.268	0.362	19.642	0.371	0.528	0.364
	0.524	0.234	4.106	0.589	0.238	5.770	0.890	0.983	0.712
I2	0.787	0.229	17.171	0.726	0.205	14.901	1.084	1.117	1.152
	0.494	0.237	7.557	0.336	0.172	4.844	1.470	1.378	1.560
	1.531	0.144	20.742	1.578	0.255	29.349	0.970	0.565	0.707
BC5	1.300	0.284	16.166	1.636	0.351	21.335	0.795	0.809	0.758
	1.099	0.346	13.701	0.912	0.331	11.121	1.205	1.045	1.232
Mean	0.696	0.218	10.477	0.856	0.235	13.050	0.886	0.987	0.896
±SD	0.393	0.053	6.616	0.387	0.067	7.058	0.447	0.306	0.542

**Table 19: Results of Mechanical Tests on the 6 Day Sham, Closed Joint Group**

<b>6 DAY SHAM, CLOSED JOINT</b>									
<u>Rabbit</u>	<u>TEST SIDE</u>			<u>CONTROL SIDE</u>			<u>RATIO OF TEST TO CONTROL</u>		
	<u>Gu (MPa)</u>	<u>Gr (MPa)</u>	<u><math>\eta</math></u>	<u>Gu (MPa)</u>	<u>Gr (MPa)</u>	<u><math>\eta</math></u>	<u>Gu(t/c)</u>	<u>Gr(t/c)</u>	<u><math>\eta(t/c)</math></u>
59	1.39	0.325	5.54	1.116	0.311	4.92	1.246	1.045	1.126
DS	2.376	0.617	7.423	1.325	0.455	5.58	1.793	1.356	1.330
CA75	0.708	0.363	6.055	0.834	0.31	6.7	0.849	1.171	0.904
RU12	1.107	0.35	19.666	1.036	0.328	19.298	1.069	1.067	1.019
CK	1.177	0.369	20.536	1.145	0.333	18.796	1.028	1.108	1.093
	1.248	0.271	13.037	1.076	0.242	12.141	1.160	1.119	1.074
	0.631	0.227	6.424	0.922	0.354	9.108	0.687	0.641	0.705
CWMAX	0.506	0.185	8.955	0.916	0.262	6.341	0.552	0.706	1.412
	0.359	0.179	3.207	0.672	0.231	16.615	0.531	0.775	0.193
Mean	1.056	0.321	10.093	1.004	0.314	11.055	0.991	0.999	0.984
$\pm$ SD	0.612	0.133	6.282	0.192	0.068	5.837	0.397	0.238	0.363

Table 20: Three Month, Low Impact, Supplemental Group, Force Parameters from the Blunt Impact Procedure

<u>Rabbit</u>	<u>Peak Load</u>	<u>Impact Rise Time</u>	<u>Impact Duration</u>	<u>Trauma Status</u> {+ = fissure(s)} {- = no fissure(s)}
JOR4	174	0.18	1.0	-
JR25	191	0.16	1.0	-
I78	187	0.16	0.9	-
I79	169	0.20	0.8	-
B102	200	0.22	0.6	-
B03	209	0.22	0.8	-
I81	236	0.20	0.6	+
B8515	214	0.12	0.9	-
Average	174 ± 73 (N)	0.18 ± 0.03 (ms)	0.83 ± 0.16 (ms)	1 of 8 fissured

Table 21: Three Month, High Impact, Supplemental Group, Force Parameters from the Blunt Impact Procedure

<u>Rabbit</u>	<u>Peak Load</u>	<u>Impact Rise Time</u>	<u>Impact Duration</u>	<u>Trauma Status</u> {+ = fissure(s)} {- = no fissure(s)}
B07	801	0.42	1.0	+
B012	579	0.42	0.9	-
BA102	712	0.32	0.9	+
B06	579	0.24	0.5	*
JR21	579	0.36	0.8	+
JR03	534	0.36	0.8	+
I76	623	0.44	1.0	+
I75	441	0.38	0.9	+
Average	605 ± 111 (N)	0.37 ± 0.06 (ms)	0.85 ± 0.16 (ms)	6 of 8 fissured

\* Luxated

Table 22: Results of the Mechanical Tests on the 3 Month, Low Impact, Supplemental Group

## THREE MONTH, LOW IMPACT, OPEN JOINT

TEST SIDE				CONTROL SIDE			RATIO OF TEST TO CONTROL			
	<u>Gu (MPa)</u>	<u>Gr (MPa)</u>	<u>η</u>	<u>Gu (MPa)</u>	<u>Gr (MPa)</u>	<u>η</u>	<u>Gu(t/c)</u>	<u>Gr(t/c)</u>	<u>η(t/c)</u>	
Rabbit JRO4	1.257	0.264	19.658	0.919	0.188	20.633	1.368	1.404	0.953	
	1.218	0.330	18.062	0.729	0.198	10.801	1.671	1.667	1.672	
	1.002	0.303	16.142	0.972	0.242	14.772	1.031	1.252	1.093	
JR25	0.848	0.168	20.935	1.074	0.282	23.158	0.790	0.596	0.904	
	0.925	0.257	13.944	0.983	0.337	9.682	0.941	0.763	1.440	
	0.895	0.295	12.896	0.734	0.302	6.671	1.219	0.977	1.933	
I78	1.398	0.263	22.821	1.632	0.251	26.761	0.857	1.048	0.853	
	1.083	0.274	15.039	1.017	0.317	11.406	1.065	0.864	1.319	
	1.052	0.387	12.751	0.986	0.305	8.231	1.067	0.864	1.319	
I79	0.600	0.236	5.860	0.722	0.193	13.589	0.831	1.223	0.431	
	0.903	0.350	8.888	0.920	0.274	15.020	0.982	1.277	0.592	
	1.196	0.359	16.833	0.882	0.344	9.504	1.356	1.044	1.771	
B102	0.463	0.111	5.974	0.482	0.168	4.163	0.961	0.661	1.435	
	0.668	0.204	6.032	0.310	0.136	2.801	2.155	1.500	2.154	
	1.066	0.377	10.391	0.515	0.221	3.537	2.070	1.706	2.938	
B8515	0.957	0.268	21.849	0.519	0.193	10.124	1.844	1.389	2.158	
	0.414	0.215	5.322	0.608	0.260	3.537	0.681	0.827	0.714	
	0.874	0.175	12.989	0.911	0.192	10.534	0.959	1.911	1.233	
B03	1.260	0.299	14.744	0.837	0.244	11.341	1.505	1.225	1.300	
	0.648	0.235	5.805	0.799	0.284	8.300	0.811	0.827	0.699	
	0.757	0.083	9.421	1.459	0.213	16.039	0.519	0.390	0.587	
I81	1.085	0.162	11.094	1.095	0.176	8.987	0.991	0.920	1.234	
	1.218	0.154	6.651	0.44	0.075	3.786	2.768	2.053	1.757	
Mean	0.947	0.251	12.787	0.850	0.235	1.187	1.237	1.121	1.336	
±SD	0.264	0.083	5.557	0.310	0.067	6.135	0.545	0.393	0.610	

## HIGH IMPACT, 3 MONTH, OPEN JOINT

	TEST SIDE			CONTROL SIDE			RATIO OF TEST TO CONTROL		
	Gu (MPa)	Gr (MPa)	$\eta$	Gu (MPa)	Gr (MPa)	$\eta$	Gu(t/c)	Gr(t/c)	$\eta(t/c)$
Rabbit									
B07	1.515	0.206	15.932	1.050	0.201	16.201	1.443	1.025	0.983
	0.713	0.195	5.909	0.844	0.247	8.775	0.845	0.789	0.673
	0.526	0.211	4.487	0.288	0.137	2.187	1.826	1.540	2.052
B012	2.331	0.291	34.132	0.937	0.249	16.511	2.488	1.169	2.067
	1.717	0.324	13.046	0.798	0.241	7.827	2.152	1.344	1.667
	0.621	0.218	3.706	0.684	0.262	6.219	0.908	0.832	0.596
BA102	0.262	0.092	2.343	0.778	0.225	12.736	0.337	0.409	0.184
	0.335	0.135	2.179	0.768	0.297	7.051	0.436	0.455	0.309
	0.411	0.192	2.820	0.759	0.322	6.682	0.542	0.596	0.422
B06	0.780	0.057	5.835	0.889	0.208	14.808	0.877	0.274	0.394
	1.397	0.125	10.853	0.752	0.218	7.871	1.858	0.573	1.379
	0.884	0.250	4.696	0.185	0.099	0.975	4.778	2.525	4.816
JR03	0.883	0.145	14.062	1.683	0.247	28.362	0.525	0.587	0.496
	2.140	0.348	26.005	0.838	0.229	11.269	2.554	1.520	2.308
	2.015	0.386	28.896	0.564	0.172	6.707	3.573	2.244	4.308
JR21	1.660	0.218	21.993	1.090	0.204	13.932	1.523	1.069	1.579
	0.414	0.126	5.957	0.607	0.203	5.666	0.682	0.621	1.051
I76	1.327	0.165	12.344	0.957	0.189	14.679	1.387	0.873	0.841
	0.769	0.207	9.962	0.319	0.156	3.001	2.411	1.327	3.320
	1.070	0.265	10.761	3.512	0.274	20.248	0.305	0.967	0.531
I75	0.915	0.178	14.17	1.127	0.243	24.175	0.812	0.733	0.586
	1.326	0.255	17.729	1.063	0.262	15.404	1.247	0.973	1.151
	0.937	0.249	11.424	0.956	0.295	13.932	0.980	0.844	0.820
Mean	1.085	0.210	12.141	0.933	0.225	11.531	1.499	1.013	1.414
±SD	0.595	0.081	8.793	0.644	0.053	6.909	1.109	0.552	1.255

**Table 24: Results of the High Level, Blunt Impacts for the Acute Study Impact**

<i>Test Condition</i>	<i>Rabbit</i>	<i>Peak Load</i>	<i>Time to Peak</i>	<i>Impact Duration</i>	<i>Trauma Status</i>
-----------------------	---------------	------------------	---------------------	------------------------	----------------------

Table 24: Results of the High Level, Blunt Impacts for the Acute Study Impact

<u>Test Condition</u>	<u>Rabbit</u>	<u>Peak Load</u>	<u>Time to Peak</u>	<u>Impact Duration</u>	<u>Trauma Status</u> {+ = fissure(s)} {- = no fissure(s)}
Time Zero, High Impact, Open Joint	9326	623	27	135	+
	HT02	668	26	141	+
	45KG	668	34	99	+
	P3	579	36	103	+
	P4	534	35	103	-
	KV3	757	36	122	-
One Day, High Impact, Open Joint	9308	712	48	135	+
	9324	410	26	139	+
	9309	757	34	131	+
	9325	534	33	105	+
	OC521	668	36	108	-
	I43	668	38	137	+
Mean ± SD		631 ± 102 (N)	24 ± 6 (ms)	122 ± 17 (ms)	9 of 12 fissured

Table 25: Results of the Solid Indenter Mechanical Tests on the Time Zero, High Impact, Acute Rabbit Group

TIME ZERO, HIGH IMPACT, OPEN JOINT											
Rabbit	TEST SIDE			CONTROL SIDE			RATIO OF TEST TO CONTROL				
	Gu (MPa)	Gr (MPa)	$\eta$	Gu (MPa)	Gr (MPa)	$\eta$	Gu(t/c)	Gr(t/c)	$\eta(t/c)$		
9326	0.451	0.152	5.761	0.500	0.154	9.886	0.902	0.987	0.583		
	0.420	0.173	3.468	0.474	0.233	4.709	0.886	0.742	0.736		
	0.384	0.178	3.904	0.473	0.198	6.701	0.812	0.899	0.583		
HT02	0.944	0.189	14.109	1.058	0.320	15.234	0.892	0.591	0.926		
	0.802	0.259	9.495	0.870	0.288	9.885	0.922	0.899	0.961		
	0.768	0.264	10.926	0.581	0.234	9.136	1.322	1.128	1.196		
45KG	0.626	0.137	19.814	0.945	0.175	19.633	0.662	0.783	1.009		
	0.885	0.278	53.536	1.345	0.287	18.604	0.658	0.969	2.878		
	0.972	0.280	87.897	0.887	0.217	15.309	1.096	1.290	5.742		
P3	0.722	0.330	55.823	0.722	0.277	7.344	1.000	1.191	7.601		
	1.470	0.138	13.127	1.637	0.123	13.517	0.898	1.122	0.971		
	1.711	0.190	16.358	1.202	0.169	8.907	1.423	0.824	1.837		
P4	0.883	0.131	8.624	1.083	0.159	10.938	0.815	0.867	0.788		
	0.629	0.117	12.151	0.912	0.135	23.450	0.690	0.867	0.518		
	0.674	0.178	12.413	1.275	0.199	17.198	0.529	0.894	0.722		
KV3	0.765	0.196	12.914	0.608	0.168	9.911	1.258	1.167	1.303		
	0.683	0.181	12.623	0.981	0.249	19.243	0.696	0.727	0.656		
	0.548	0.255	5.477	0.625	0.284	7.738	0.877	0.898	0.708		
	0.549	0.258	5.205	0.636	0.292	7.795	0.863	0.884	0.668		
Mean	0.783*	0.204	19.138	0.885	0.219	12.376	0.905	0.947	1.599		
±SD	0.333	0.061	22.123	0.327	0.060	5.294	0.234	0.183	1.896		

\* = Significantly lower than control values, based on a one tailed hypothesis for  $P < 0.05$ .

**Table 26: Results of the Solid Indenter Mechanical Tests on the One Day, Sham Operated (No Impact), Acute Rabbit Group**  
**ONE DAY, NO IMPACT, OPEN JOINT**

Rabbit	TEST SIDE			CONTROL SIDE			RATIO OF TEST TO CONTROL		
	Gu (MPa)	Gr (MPa)	$\eta$	Gu (MPa)	Gr (MPa)	$\eta$	Gu(t/c)	Gr(t/c)	$\eta(t/c)$
P6	1.725	0.155	15.843	1.731	0.173	16.761	0.997	0.896	0.945
	0.906	0.143	8.011	0.353	0.137	2.429	2.567	1.044	3.298
	0.747	0.143	6.531	0.341	0.128	4.342	2.191	1.117	1.504
P7	0.589	0.108	8.850	0.820	0.122	11.094	0.718	0.885	0.798
	0.601	0.130	4.371	0.861	0.165	7.408	0.698	0.788	0.590
	0.206	0.085	1.254	0.445	0.160	3.735	0.463	0.518	0.336
P1	0.724	0.178	31.219	0.688	0.163	14.136	1.052	1.092	0.935
	0.639	0.236	7.037	0.634	0.194	11.590	1.008	1.216	0.607
	0.795	0.261	9.153	0.715	0.206	9.326	1.112	1.267	1.309
P2	1.459	0.161	16.264	0.771	0.128	12.429	1.892	1.258	1.309
	0.766	0.145	6.793	0.945	0.199	8.381	0.811	0.729	0.811
	0.347	0.116	3.483	1.327	0.253	11.986	0.261	0.458	0.291
CKTOM	0.861	0.102	11.964	1.060	0.146	18.942	0.812	0.699	0.632
	0.517	0.156	4.671	0.652	0.176	7.728	0.793	0.886	0.604
	0.295	0.108	2.475	0.555	0.126	8.689	0.532	0.857	0.285
K6	1.592	0.188	22.375	1.016	0.236	20.606	1.567	0.797	1.086
	0.593	0.176	6.489	0.827	0.276	7.727	0.717	0.638	0.840
	0.895	0.246	10.457	0.729	0.293	9.278	1.228	0.840	1.127
Mean	0.792	0.158*	8.847	0.804	0.182	10.366	1.079	0.889	0.943
±SD	0.420	0.050	5.435	0.339	0.053	4.955	0.612	0.238	0.676

\* = Significantly lower than control values, based on a one tailed hypothesis for  $P < 0.05$ .

**Table 27: Results of the Solid Indenter Mechanical Tests on the One Day, High Impact, Acute Rabbit Group**

**ONE DAY, HIGH IMPACT, OPEN JOINT**

Rabbit	TEST SIDE			CONTROL SIDE			RATIO OF TEST TO CONTROL		
	Gu (MPa)	Gr (MPa)	$\eta$	Gu (MPa)	Gr (MPa)	$\eta$	Gu(t/c)	Gr(t/c)	$\eta(t/c)$
143	0.899	0.234	14.488	0.791	0.228	12.070	1.137	1.026	1.200
	0.461	0.226	3.908	0.599	0.277	6.181	0.770	0.816	0.632
	0.828	0.206	11.813	1.003	0.249	18.771	0.826	0.827	0.629
OC521	0.270	0.146	4.693	0.743	0.223	15.849	0.363	0.655	0.296
	0.276	0.173	2.166	0.364	0.187	4.159	0.758	0.925	0.521
	0.683	0.211	12.777	0.463	0.207	7.862	1.475	1.019	1.625
9308	0.750	0.137	9.871	0.482	0.168	7.722	1.556	0.815	1.278
	1.359	0.249	19.391	1.442	0.274	17.907	0.942	0.909	1.083
	0.892	0.292	10.830	0.512	0.219	6.576	1.742	1.333	1.647
9324	0.464	0.188	4.974	0.351	0.152	5.504	1.322	1.237	0.904
	0.375	0.162	3.417	0.378	0.144	2.877	0.992	1.125	1.188
	0.224	0.105	1.582	0.271	0.141	2.165	0.827	0.745	0.731
9309	0.820	0.144	13.100	2.142	0.203	21.964	0.383	0.709	0.596
	0.630	0.190	5.442	1.405	0.234	19.263	0.448	0.812	0.283
	0.692	0.270	6.905	0.955	0.256	14.772	0.725	1.055	0.467
9325	0.326	0.099	3.884	0.787	0.216	8.372	0.414	0.458	0.464
	0.328	0.086	4.751	0.622	0.216	8.044	0.527	0.398	0.591
	0.355	0.113	5.489	0.315	0.194	2.037	1.127	0.582	2.695
Mean	0.591 <sup>+</sup>	0.180 <sup>*</sup>	7.749 <sup>*</sup>	0.757	0.210	10.116	0.907	0.858	0.935
±SD	0.301	0.061	4.972	0.489	0.041	6.425	0.419	0.251	0.607

<sup>+</sup> = Borderline significantly lower than control values, based on a one tailed hypothesis, P = 0.05.

<sup>\*</sup> = Significantly lower than control values, based on a one tailed hypothesis, P > 0.05.

**Table 28: Biphasic Material Properties for the Acute Study Porous Tests, Rate = 1.0 Sec.**

<u>Test Condition</u>	<u>Rabbit</u>	<u>Shear Modulus (<math>\mu_s</math>)</u>		<u>Poissons Ratio (<math>\nu_s</math>)</u>		<u>Aggregate Modulus (<math>H_A</math>)</u>		<u>Permeability (<math>\times 10^{-4}</math>)</u>	
		<u>Test</u>	<u>Control</u>	<u>Test</u>	<u>Control</u>	<u>Test</u>	<u>Control</u>	<u>Test</u>	<u>Control</u>
Time Zero High Impact	HT02 9326	---	0.322	---	0.000	---	0.644	---	0.612
		0.432	---	0.000	---	0.864	---	0.836	---
Sham No Impact	P2 CKTOM	0.329	0.227	0.000	0.000	0.658	0.454	0.870	0.599
		0.225	0.270	0.000	0.000	0.450	0.540	1.063	0.527
Day One High Impact	9309 9308	0.204	0.484	0.000	0.000	0.408	0.968	1.067	0.391
		0.217	0.429	0.000	0.000	0.434	0.858	3.620	0.461

**Table 29: Biphasic Material Properties for the Acute Study Porous Tests, Rate = 2.0 Sec.**

<u>Test Condition</u>	<u>Rabbit</u>	<u>Shear Modulus (<math>\mu_s</math>)</u>		<u>Poissons Ratio (<math>\nu_s</math>)</u>		<u>Aggregate Modulus (<math>H_A</math>)</u>		<u>Permeability (<math>\times 10^{-4}</math>)</u>	
		<u>Test</u>	<u>Control</u>	<u>Test</u>	<u>Control</u>	<u>Test</u>	<u>Control</u>	<u>Test</u>	<u>Control</u>
Time Zero High Impact	HT02 9326	0.326	0.422	0.000	0.000	0.652	0.844	0.779	0.733
		0.163	0.355	0.019	0.058	0.332	0.757	2.370	1.040
Sham No Impact	P2 CKTOM	0.175	0.250	0.000	0.000	0.350	0.500	0.795	0.158
		0.200	0.200	0.000	0.000	0.400	0.400	0.203	0.205
Day One High Impact	9309 9308	0.243	---	0.000	---	0.486	---	1.012	---
		0.162	0.421	0.000	0.000	0.324	0.842	0.896	0.469

**Table 30: Elastic and Viscoelastic Parameters for the Acute Study, Porous Tests, Rate = 1.0 sec.**

<u>Test Condition</u>	<u>Rabbit</u>	<u>Test Side</u>			<u>Control Side</u>		
		<u>(Gu MPa)</u>	<u>Gr (MPa)</u>	<u><math>\eta</math></u>	<u>Gu (MPa)</u>	<u>Gr (MPa)</u>	<u><math>\eta</math></u>
Time Zero High Impact	HT02	0.253	0.138	0.375	0.310	0.139	0.818
	9326	0.321	0.273	1.462	0.328	0.208	17.124
One Day Sham	P2	0.183	0.091	4.603	0.222	0.094	10.768
	CKTOM	0.145	0.067	5.347	0.149	0.057	10.900
One Day High Impact	9309	0.156	0.062	3.483	0.134	0.070	4.849
	9308	0.138	0.011	16.611	0.411	0.187	16.429

**Table 31: Elastic and Viscoelastic Parameters for the Acute Study, Porous Tests, Rate = 2.0 sec.**

<u>Test Condition</u>	<u>Rabbit</u>	<u>Test Side</u>			<u>Control Side</u>		
		<u>(Gu MPa)</u>	<u>Gr (MPa)</u>	<u><math>\eta</math></u>	<u>Gu (MPa)</u>	<u>Gr (MPa)</u>	<u><math>\eta</math></u>
Time Zero High Impact	HT02	0.536	0.134	1.380	0.303	0.120	0.935
	9326	0.189	0.193	----	0.270	0.209	95.499
One Day Sham	P2	0.237	0.105	0.522	0.224	0.12	7.492
	CKTOM	0.166	0.055	19.194	0.184	0.090	7.612
One Day High Impact	9309	1.39	0.071	3.593	0.309	0.180	5.277
	9308	0.136	0.057	16.450	0.272	0.183	10.878

**Table 32: Results of the High Level, Blunt Impacts for the Synovitis Study Impact Groups**

<u>Test Condition</u>	<u>Rabbit</u>	<u>Peak Load (lbs)</u>	<u>Time to Peak (ms)</u>	<u>Impact Duration (ms)</u>	<u>Trauma Status</u> {+ = fissure(s)} {- = no fissure(s)}
Six Day Synovitis, In Chair, High Impact	JKLOT	130	35	106	+
	K16	120	31	82	-
	K5	120	35	101	-
Six Day Synovitis, No Chair, High Impact	K3	170	36	114	+
	K13	90	17	42	-
	K1	150	35	108	+
	K4	84	26	129	+
	K35	105	37	68	+
	K38	140	35	76	+
<b>Mean ± SD</b>		<b>123 ± 26.3</b>	<b>32 ± 7</b>	<b>92 ± 27</b>	<b>6 of 9 fissured</b>

**Table 33: Results of the Solid Indenter Mechanical Tests on the 6 Day Synovitis Study, Sham Group**  
(Synovitis created without the use of the restraining chair)

<u>Rabbit</u>	<u>TEST SIDE</u>			<u>CONTROL SIDE</u>			<u>RATIO OF TEST TO CONTROL</u>			
	<u>Gu (MPa)</u>	<u>Gr (MPa)</u>	<u><math>\eta</math></u>	<u>Gu (MPa)</u>	<u>Gr (MPa)</u>	<u><math>\eta</math></u>	<u>Gu(t/c)</u>	<u>Gr(t/c)</u>	<u><math>\eta(t/c)</math></u>	
P1	0.790	0.164	11.919	0.467	0.085	8.174	1.692	1.929	1.458	
	0.370	0.133	4.060	0.212	0.068	2.521	1.745	1.956	1.610	
	0.584	0.127	12.397	0.649	0.098	8.943	0.900	1.337	1.386	
173	0.570	0.120	8.230	1.013	0.135	8.681	0.563	0.889	0.948	
	1.116	0.281	14.658	1.406	0.271	26.954	0.794	1.037	0.544	
	0.873	0.227	13.925	0.913	0.296	7.566	0.956	0.767	1.840	
172	0.567	0.252	5.552	0.635	0.250	15.760	0.893	1.008	0.352	
	1.199	0.252	11.910	0.854	0.120	11.581	1.404	2.100	1.028	
	0.386	0.182	4.476	0.295	0.086	3.268	1.308	2.116	1.370	
JR18	0.808	0.152	8.909	0.983	0.156	8.726	0.822	0.974	1.021	
	2.582	0.276	31.427	1.496	0.204	17.310	1.726	1.353	1.816	
	1.214	0.262	15.088	1.394	0.253	16.941	0.871	1.036	0.891	
171	0.648	0.215	7.157	0.858	0.253	10.095	0.755	0.850	0.709	
	1.545	0.197	29.361	0.708	0.215	4.699	2.182	0.916	6.248	
	1.039	0.225	14.204	1.291	0.329	16.587	0.805	0.684	0.856	
180	1.055	0.310	9.667	0.701	0.243	6.199	1.505	1.276	1.559	
	1.497	0.259	30.379	1.129	0.257	27.731	1.326	1.008	1.095	
	1.019	0.249	20.457	0.733	0.248	12.906	1.390	1.004	1.585	
KEY	0.467	0.188	5.056	0.509	0.185	7.640	0.917	1.016	0.662	
	0.531	0.246	5.649	0.351	0.188	6.326	1.513	1.309	0.893	
	0.817	0.326	10.391	0.555	0.307	6.129	1.472	1.062	1.695	
Mean ±SD	0.451	0.256	5.183	0.278	0.182	1.956	1.622	1.407	2.650	
	0.937	0.223	12.730	0.792	0.201	10.579	1.235	1.229	1.464	
	0.507	0.058	8.319	0.381	0.077	7.019	0.426	0.429	1.191	

\* = Significantly less than control values, based on a one tailed hypothesis,  $P < 0.05$ .

**Table 34: Results of the Solid Indenter Mechanical Tests on the 6 Day Synovitis, Impact Group**  
**of the restraining chair)**

**Table 34: Results of the Solid Indenter Mechanical Tests on the 6 Day Synovitis, Impact Group**  
(Synovitis created without the use of the restraining chair)

	<u>TEST SIDE</u>			<u>CONTROL SIDE</u>			<u>RATIO OF TEST TO CONTROL</u>			
	<u>Gu (MPa)</u>	<u>Gr (MPa)</u>	$\eta$	<u>Gu (MPa)</u>	<u>Gr (MPa)</u>	$\eta$	<u>Gu(t/c)</u>	<u>Gr(t/c)</u>	$\eta(t/c)$	
<b>Rabbit</b> K13	0.473	0.082	12.491	1.315	0.231	23.542	0.359	0.355	0.531	
	0.700	0.162	10.016	1.074	0.247	16.699	0.652	0.656	0.600	
	0.509	0.211	4.563	0.654	0.214	9.978	0.778	0.986	0.457	
<b>K3</b>	0.597	0.172	16.843	0.380	0.111	13.384	1.571	1.550	1.258	
	0.234	0.124	4.306	0.472	0.164	9.445	0.496	0.756	0.456	
	0.312	0.175	4.980	0.222	0.123	1.329	1.405	1.423	3.747	
<b>K1</b>	1.559	0.322	29.597	2.075	0.367	35.121	0.751	0.877	0.843	
	1.602	0.346	22.104	1.264	0.375	15.770	1.267	0.923	1.402	
	0.898	0.297	9.886	1.374	0.333	17.937	0.654	0.892	0.551	
<b>K4</b>	1.283	0.155	14.454	2.631	0.268	24.622	0.488	0.578	0.587	
	0.444	0.172	3.341	1.226	0.237	14.603	0.362	0.726	0.229	
	0.419	0.157	3.265	0.594	0.175	3.493	0.705	0.897	0.935	
<b>K35</b>	0.437	0.158	11.145	0.602	0.170	10.746	0.726	0.929	1.037	
	0.499	0.156	8.658	0.983	0.27	14.214	0.508	0.578	0.609	
	0.303	0.133	4.322	0.702	0.239	18.599	0.432	0.556	0.232	
<b>K38</b>	0.888	0.132	16.107	0.563	0.109	14.599	1.577	1.211	1.103	
	0.519	0.207	5.54	0.428	0.164	4.084	1.213	1.262	1.357	
	0.481	0.177	9.326	0.575	0.218	7.388	0.837	0.812	1.262	
<b>Mean</b>	<b>0.675*</b>	<b>0.185*</b>	<b>10.608*</b>	<b>0.952</b>	<b>0.223</b>	<b>14.197</b>	<b>0.821</b>	<b>0.887</b>	<b>0.955</b>	
<b>±SD</b>	<b>0.414</b>	<b>0.070</b>	<b>7.140</b>	<b>0.625</b>	<b>0.080</b>	<b>8.253</b>	<b>0.406</b>	<b>0.313</b>	<b>0.792</b>	

\*Significantly less than control values, based on a one tailed hypothesis,  $P < 0.05$ .

**Table 35: Biphasic Material Properties for the Synovitis Study Porous Tests, Rate = 1.0 sec. (Synovitis induced without the use of restraining chair).**

<u>Test Condition</u>	<u>Rabbit</u>	<u>Shear Modulus (<math>\mu_s</math>)</u>		<u>Poissons Ratio (<math>\nu_s</math>)</u>		<u>Aggregate Modulus (<math>H_A</math>)</u>		<u>Permeability (<math>\times 10^{14}</math>)</u>	
		<u>Test</u>	<u>Control</u>	<u>Test</u>	<u>Control</u>	<u>Test</u>	<u>Control</u>	<u>Test</u>	<u>Control</u>
Sham Group	I71	0.255	0.609	0.021	0.020	0.521	1.243	1.101	0.514
	JR18	0.414	0.300	0.000	0.000	0.828	0.600	0.477	0.586
Impact Group	K13	0.174	0.326	0.000	0.000	0.348	0.652	1.380	1.818
	K1	0.269	0.223	0.000	0.298	0.538	0.775	0.886	0.231

**Table 36: Biphasic Material Properties for the Synovitis Study Porous Tests, Rate = 2.0 sec. (Synovitis induced without the use of restraining chair).**

<u>Test Condition</u>	<u>Rabbit</u>	<u>Shear Modulus (<math>\mu_s</math>)</u>		<u>Poissons Ratio (<math>\nu_s</math>)</u>		<u>Aggregate Modulus (<math>H_A</math>)</u>		<u>Permeability (<math>\times 10^{14}</math>)</u>	
		<u>Test</u>	<u>Control</u>	<u>Test</u>	<u>Control</u>	<u>Test</u>	<u>Control</u>	<u>Test</u>	<u>Control</u>
Sham Group	I71	0.228	0.192	0.288	0.247	0.766	0.571	0.103	0.138
	JR18	0.318	0.455	0.000	0.000	0.636	0.910	0.380	3.520
Impact Group	K13	0.313	0.396	0.000	0.000	0.626	0.792	0.279	0.300
	K1	0.364	0.271	0.000	0.012	0.728	0.549	0.532	1.250

**Table 37: Elastic and Viscoelastic Parameters for the Synovitis Study, Porous tests, Rate = 1.0 sec. (Synovitis created without the use of the restraining chair).**

<u>Test Condition</u>	<u>Rabbit</u>	<u>Test Side</u>			<u>Control Side</u>		
		<u>(Gu MPa)</u>	<u>Gr (MPa)</u>	<u><math>\eta</math></u>	<u>Gu (MPa)</u>	<u>Gr (MPa)</u>	<u><math>\eta</math></u>
Sham Group	I71	0.224	0.078	28.755	0.194	0.138	5.448
	JR18	0.234	0.112	12.855	0.367	0.162	18.642
Impact Group	K13	0.121	0.060	3.033	0.173	0.115	12.166
	K1	0.178	0.099	6.681	0.150	0.212	0.296

**Table 38: Elastic and Viscoelastic Parameters for the Synovitis Study, Porous tests, Rate = 2.0 sec. (Synovitis created without the use of the restraining chair).**

<u>Test Condition</u>	<u>Rabbit</u>	<u>Test Side</u>			<u>Control Side</u>		
		<u>(Gu MPa)</u>	<u>Gr (MPa)</u>	<u><math>\eta</math></u>	<u>Gu (MPa)</u>	<u>Gr (MPa)</u>	<u><math>\eta</math></u>
Sham Group	I71	0.192	0.079	24.058	0.358	0.230	8.881
	JR18	0.273	0.145	9.292	0.211	0.108	8.067
Impact Group	K13	0.252	0.075	21.969	0.309	0.195	10.048
	K1	0.226	0.138	7.242	0.140	0.122	2.741

**Table 39: Results of the Solid Indenter Mechanical Tests on the 6 Day Synovitis, Sham Group**  
(Synovitis created while restrained in chair)

	<u>TEST SIDE</u>			<u>CONTROL SIDE</u>			<u>RATIO OF TEST TO CONTROL</u>		
	<u>Gu (MPa)</u>	<u>Gr (MPa)</u>	<u><math>\eta</math></u>	<u>Gu (MPa)</u>	<u>Gr (MPa)</u>	<u><math>\eta</math></u>	<u>Gu(t/c)</u>	<u>Gr(t/c)</u>	<u><math>\eta(t/c)</math></u>
Rabbit 9305	0.985	0.236	20.255	0.839	0.240	14.586	1.174	0.983	1.389
	1.362	0.249	18.075	1.071	0.278	13.841	1.272	0.896	1.306
	0.380	0.174	3.363	0.429	0.166	4.371	0.886	1.048	0.769
9306	0.820	0.239	18.881	1.080	0.259	22.420	0.759	0.923	0.842
	0.460	0.172	8.812	0.495	0.179	6.934	0.929	0.961	1.271
	0.600	0.285	10.412	0.938	0.295	18.515	0.640	0.966	0.562
9303	1.870	0.335	29.263	1.247	0.235	22.687	1.500	1.426	1.290
	0.710	0.302	8.389	1.116	0.315	13.533	0.636	0.959	0.620
	1.344	0.418	21.100	0.769	0.257	8.289	1.748	1.626	2.546
9304	1.608	0.197	27.785	1.372	0.161	21.887	1.172	1.224	1.269
	1.125	0.237	15.140	0.871	0.258	11.349	1.292	0.919	1.334
	1.035	0.262	14.007	0.743	0.25	7.650	1.393	0.989	1.831
I57	0.726	0.242	17.233	0.925	0.248	16.308	0.785	0.976	1.057
	0.807	0.327	9.798	0.935	0.352	14.183	0.863	0.929	0.691
	1.227	0.359	15.628	1.223	0.416	17.309	1.003	0.863	0.903
PSA	0.991	0.161	12.868	1.334	0.169	19.511	0.743	0.953	0.660
	1.279	0.196	14.168	2.023	0.266	21.311	0.632	0.737	0.665
	0.759	0.190	10.319	1.650	0.278	19.136	0.460	0.683	0.539
Mean	1.005	0.255	15.305	1.059	0.258	15.212	0.994	1.003	1.086
±SD	0.394	0.071	6.658	0.387	0.065	5.699	0.350	0.224	0.514

\* = Significantly less than control values, based on a one tailed hypothesis,  $P < 0.05$ .

**Table 40: Results of Solid Indenter Mechanical Tests on the 6 Day Synovitis, Impact Group**  
(Synovitis created while restrained in chair)

TEST SIDE				CONTROL SIDE			RATIO OF TEST TO CONTROL			
Rabbit	Gu (MPa)	Gr (MPa)	$\eta$	Gu (MPa)	Gr (MPa)	$\eta$	Gu(t/c)	Gr(t/c)	$\eta(t/c)$	
JKLOT	1.091	0.223	16.535	0.775	0.172	15.324	1.408	1.297	1.079	
	0.661	0.247	6.132	1.450	0.295	14.143	0.456	0.837	0.434	
	0.682	0.203	9.108	0.893	0.303	13.085	0.764	0.670	0.696	
K16	1.085	0.262	16.762	0.793	0.210	15.751	1.368	1.248	1.064	
	0.831	0.338	10.337	0.701	0.300	14.990	1.185	1.127	0.690	
	0.648	0.345	7.731	0.786	0.323	8.424	0.824	1.068	0.918	
K5	0.626	0.199	12.499	0.690	0.269	11.785	0.907	0.740	1.061	
	0.567	0.249	5.160	0.372	0.239	3.136	1.524	1.042	1.645	
	0.578	0.246	7.832	0.417	0.273	8.424	1.386	0.901	0.930	
Mean	0.752	0.257	10.233	0.764	0.265	11.674	1.901	0.992	0.946	
$\pm$ SD	0.205	0.053	4.233	0.311	0.049	4.229	0.367	0.219	0.340	

\* = Significantly less than control values, based on a one tailed hypothesis,  $P < 0.05$ .

**Table 41: Biphasic Material Properties for the Synovitis Study Porous Tests, Rate = 1.0 sec. (Synovitis induced while restrained in chair).**

<u>Test Condition</u>	<u>Rabbit</u>	<u>Shear Modulus (<math>\mu_s</math>)</u>		<u>Poissons Ratio (<math>\nu_s</math>)</u>		<u>Aggregate Modulus (<math>H_A</math>)</u>		<u>Permeability (<math>\times 10^{14}</math>)</u>	
		<u>Test</u>	<u>Control</u>	<u>Test</u>	<u>Control</u>	<u>Test</u>	<u>Control</u>	<u>Test</u>	<u>Control</u>
Sham Group	9304	0.318	0.331	0.000	0.015	0.636	0.672	0.621	0.470
	9305	0.313	0.197	0.000	0.000	0.626	0.394	0.688	1.003
Impact Group	K16	0.513	0.268	0.110	0.166	1.171	0.669	0.767	0.223
	JKLOT	0.327	0.267	0.000	0.000	0.654	0.534	0.603	1.410

**Table 42: Biphasic Material Properties for the Synovitis Study Porous Tests, Rate = 2.0 sec. (Synovitis induced while restrained in chair).**

<u>Test Condition</u>	<u>Rabbit</u>	<u>Shear Modulus (<math>\mu_s</math>)</u>		<u>Poissons Ratio (<math>\nu_s</math>)</u>		<u>Aggregate Modulus (<math>H_A</math>)</u>		<u>Permeability (<math>\times 10^{14}</math>)</u>	
		<u>Test</u>	<u>Control</u>	<u>Test</u>	<u>Control</u>	<u>Test</u>	<u>Control</u>	<u>Test</u>	<u>Control</u>
Sham Group	9304	0.311	0.304	0.101	0.000	0.701	0.608	0.262	0.150
	9305	0.454	0.350	0.010	0.000	0.917	0.700	0.393	0.748
Impact Group	K16	---	0.322	---	0.016	---	0.655	---	0.412
	JKLOT	0.247	---	0.000	---	0.494	---	1.050	---

**Table 43:** Elastic and Viscoelastic Parameters for the Synovitis Study, Porous tests, Rate = 1.0 sec. (Synovitis created while restrained in chair).

<u>Test Condition</u>	<u>Rabbit</u>	<u>Test Side</u>			<u>Control Side</u>		
		<u>(Gu MPa)</u>	<u>Gr (MPa)</u>	<u><math>\eta</math></u>	<u>Gu (MPa)</u>	<u>Gr (MPa)</u>	<u><math>\eta</math></u>
Sham Group	9304	0.231	0.113	14.105	0.213	0.078	19.154
	9305	0.205	0.155	1.949	0.145	0.068	7.444
Impact Group	K16	0.36	0.288	5.256	0.171	0.117	9.297
	JKLOT	0.240	0.112	12.725	0.155	0.180	0.478

165

**Table 44:** Elastic and Viscoelastic Parameters for the Synovitis Study, Porous tests, Rate = 2.0 sec. (Synovitis created while restrained in chair).

<u>Test Condition</u>	<u>Rabbit</u>	<u>Test Side</u>			<u>Control Side</u>		
		<u>(Gu MPa)</u>	<u>Gr (MPa)</u>	<u><math>\eta</math></u>	<u>Gu (MPa)</u>	<u>Gr (MPa)</u>	<u><math>\eta</math></u>
Sham Group	9304	0.212	0.102	15.754	0.217	0.133	8.190
	9305	0.303	0.190	7.186	0.288	0.174	5.270
Impact Group	K16	---	---	---	---	---	---
	JKLOT	0.258	0.136	11.388	0.390	0.261	4.916

## REFERENCES

## REFERENCES

- Akizuki, S.; Mow, V.C.; Muller, F.; Pita, J.C.; Howell, D.S.; and Manicourt, D.H. "Tensile Properties of Human Knee Joint Cartilage: I. Influence of Ionic Conditions, Weight Bearing, and Fibrillation of the Tensile Modulus." Journal of Orthopaedic Research, Vol. 4, pp 379-392, 1986.
- Altman, R.; Asch, E.; Bloch, D.; Bole, G.; Borenstein, D.; Brandt, K.; Christy, W.; Cooke, T.D.; Greenwald, R.; Hochberg, M.; Howell, D.; Kaplan, D.; Koopman, W.; Longley, S. III.; Mankin, H.; McShane, D.J.; Medsger, T. Jr.; Meenan, R.; Mikkelsen, W.; Moskowitz, R.; Murphy, W.; Rothschild, B.; Segal, M.; Sokoloff, L.; and Wolfe, F. "Development of Criteria for the Classification and Reporting of Osteoarthritis." Arthritis and Rheumatism, Vol. 29, No. 8, pp 1039-1049, 1986.
- Altman, R.D.; Fries, J.F.; Bloch, D.A.; Carstens, J.; Cooke, T.D.; Genant, H.; Gofton, P.; Groth, H.; McShane, D.J.; Murphy, W.A.; Sharp, J.T.; Spitz, P.; Williams, C.A.; and Wolfe, F. "Radiographic Assessment of Progression in Osteoarthritis." Arthritis and Rheumatism, Vol. 30, No. 11, pp 1214-1225, 1987.
- Altman, R.D.; Tenenbaum, J.; Latta, L.; Riskin, W.; Blanco, L.N.; and Howell, D.S. "Biomechanical and Biochemical Properties of Dog Cartilage in Experimentally Induced Osteoarthritis." Annals of the Rheumatic Diseases, Vol. 43, pp 83-90, 1984.
- Armstrong, C.G. and Mow, V.C. "Variations in the Intrinsic Mechanical Properties of Human Articular Cartilage with Age, Degeneration, and Water Content." The Journal of Bone and Joint Surgery, Vol.64-A, No. 1, 1982.
- Armstrong, C.G.; Lai, W.M.; and Mow, V.C. "An Analysis of the Unconfined Compression of Articular Cartilage." Journal of Biomechanical Engineering, Vol. 106, pp 165-173, 1984.
- Armstrong, C.G.; Schoonbeck, J.; Moss, G.; Mow, V.C.; and Wirth, C.R. "Characterization of Impact-Induced Microtrauma to Articular Cartilage." Biomedical Sciences Department of General Motors Research Laboratories, Warren, MI, 48090, pp 153-156.

Askew, M.J. and Mow, V.C. "The Biomechanical Function of the Collagen Fibril Ultrastructure of Articular Cartilage." Journal of Biomechanical Engineering, Vol. 100, pp 105-115, 1978.

Bader, D.L.; Kempson, G.E.; Egan, J.; Gilbey, W.; and Barrett, A.J. "The Effects of Selective Matrix Degradation on the Short-Term Compressive Properties of Adult Human Articular Cartilage." Biochimica et Biophysica Acta, Vol. 1116, pp 147-154, 1992.

Beesley, J.E.; Jessup, E.; Pettipher, R.; and Henderson, B. "Microbiochemical Analysis of Changes in Proteoglycan and Collagen in Joint Tissues During the Development of Antigen-Induced Arthritis in the Rabbit." Matrix, Vol. 12, pp 189-196, 1992.

Brandt, K.D.; Braunstein, E.M.; Visco, D.M.; O'Connor, B.; Heck, D.; and Albrecht, M. "Anterior (Cranial) Cruciate Ligament Transection in the Dog: A Bona Fide Model of Osteoarthritis, Not Merely of Cartilage Injury and Repair." The Journal of Rheumatology, Vol. 18, No. 3, pp 436-446.

Brandt, K.D.; Myers, S.L.; Burr, D.; and Albrecht, M. "Osteoarthritic Changes in Canine Articular Cartilage, Subchondral Bone, and Synovium Fifty-Four Months After Transection of the Anterior Cruciate Ligament." Arthritis and Rheumatism, Vol. 34, No. 12, pp 1560-1570, 1991.

Braunstein, E.; Brandt, K.; Albrecht, M. "Magnetic Resonance Imaging of Canine Osteoarthritis. Evidence that Hypertrophic Cartilage Repair May Persist for 3 Years After Transection of the Anterior Cruciate Ligament." 36th Annual Meeting, Orthopaedic Research Society, February 5-8, 1990, New Orleans, Louisiana, pp 570.

Broom, N.D. "Abnormal Softening in Articular Cartilage." Arthritis and Rheumatism, Vol. 25, No. 10, pp 1209-1216, 1982.

Broom, N.D. "An Enzymatically Induced Structural Transformation in Articular Cartilage - Its Significance with Respect to Matrix Breakdown." Arthritis and Rheumatism, Vol. 31, No. 2, pp 210-218, 1988.

Broom, N.D. "Structural Consequences of Traumatizing Articular Cartilage." Annals of the Rheumatic Diseases, Vol. 45, pp 225-234, 1986.

Buckwalter, J.A.; Kuettner, K.E.; and Thonar, E.J.-M. "Age-Related Changes in Articular Cartilage Proteoglycans: Electron Microscopic Studies." Journal of Orthopaedic Research, Vol. 3, pp 251-257, 1985.

Burton-Wurster, N. and Lust, G. "Fibronectin and Water Content of Articular Cartilage Explants After Partial Depletion of Proteoglycans." Journal of Orthopaedic Research, Vol. 4, pp 437-445, 1986.

Chin, M.V.; Donohue, J.M.; Erdman, A.G.; Oegema, T.R.; and Thompson, R.C. "Biomechanical Analysis of an Adult Canine Patella Under an Indirect Blunt Trauma." 32nd Annual Orthopaedic Research Society, New Orleans, Louisiana, pp 232, 1986.

Chu, M.L. and Yazdani-Ardakani, S. "An *In Vitro* Simulation Study of Impulsive Force Transmission Along the Lower Skeletal Extremity." J Biomechanics, Vol. 19, No. 12, pp 979-987, 1986.

Ehrlich, M.G. "Degradative Enzyme Systems in Osteoarthritic Cartilage." Journal of Orthopaedic Research, Vol. 3, pp 170-184, 1985.

Einhorn, T.A.; Gordon, S.L.; Siegel, S.A.; Hummel, C.F.; Avitable, M.J.; and Carty, R.P. "Matrix Vesicle Enzymes in Human Osteoarthritis." Journal of Orthopaedic Research, Vol. 3, pp 160-169, 1985.

Fife, R.S.; Palmoski, M.J.; and Brandt, K.D. "Metabolism of a Cartilage Matrix Glycoprotein in Normal and Osteoarthritic Canine Articular Cartilage." Arthritis and Rheumatism, Vol. 29, No. 10, pp 1256-1262, 1986.

Finlay, J.B.; Repo, R.U.; and Hardie, R. "Effect of Papain on the Relationship Between Proteoglycans-Content and Impact-Characteristics of Human Articular Cartilage." This work was supported by a grant, number MA-5214, from the Medical Research Council of Canada. April, 1986.

Frost, L. and Ghosh, P. "Microinjury to the Synovial Membrane May Cause Disaggregation of Proteoglycans in Rabbit Knee Joint Articular Cartilage." Journal of Orthopaedic Research, Vol. 2, pp 207-220, 1984.

Gershuni, D.H. and Kuei, S.C. "Articular Cartilage Deformation Following Experimental Synovitis in the Rabbit Hip." Journal of Orthopaedic Research, Vol. 1, No. 3, pp 313-318, 1984.

Ghadially, F.N. Fine Structure of Synovial Joints. Butterworth & Co. Publishers Ltd. pp 151-179, 1983.

Ghadially, F.N.; Ailsby, R.L.; and Oryschak, A.F. "Scanning Electron Microscopy of Superficial Defects in Articular Cartilage." Annals of the Rheumatic Diseases, Vol. 33, pp 327-332, 1974.

Ghadially, F.N. and Roy, S. "Ultrastructure of Rabbit Synovial Membrane." Ann. Rheum. Dis., Vol. 25, pp 318-325, 1966.

Glazer, P.A.; Rosenwasser, M.P.; and Ratcliffe, A. "The Effect of Naproxen and Interleukin-1 on Proteoglycan Catabolism and on Neutral Metalloproteinase Activity in Normal Articular Cartilage *In Vitro*." The Journal of Clinical Pharmacology, Vol. 33, No. 2, pp 109-114, 1993.

Glynn, L.E. "Primary Lesion in Osteoarthritis." The Lancet, pp 574-575, 1977.

Goldenberg, D.L.; Egan, M.S.; and Cohen, A.S. "Inflammatory Synovitis in Degenerative Joint Disease." The Journal of Rheumatology, Vol. 9, no. 2, pp 204-209, 1982.

Gray, H. Gray's Anatomy. Anatomy of the Human Body. 27th Edition, edited by Charles Mayo Goss. Lea & Febiger, Philadelphia, pp323-326, 1963.

Gu, W.Y.; Lai, W.M.; and Mow, V.C. "Transport of Fluid and Ions Through a Porous-Permeable Charged-Hydrated Tissue, and Streaming Potential Data on Normal Bovine Articular Cartilage." J Biomechanics, Vol. 26, No. 6, pp 709-723, pp 1993.

Haut, R.C. "Contact Pressures on Articular Cartilage of the Human Knee During Impact Loading." Research Report. General Motors Research Laboratories, Warren, MI 48090, 1986.

Haut, R.C.; Ide, T.; and DeCamp, C.E. "Mechanical Response of the Rabbit Patello-Femoral Joint to Blunt Impact." Biomechanics Symposium ASME, 1991.

Hayes, W.C.; and Bodine, A.J. "Flow-Independent Viscoelastic Properties of Articular Cartilage Matrix." J Biomechanics, Vol. 11, pp 407-419, 1978.

Hayes, W.C.; Herrmann, L.M.K.; and Mockros, L.F. "A Mathematical Analysis for Indentation Tests of Articular Cartilage." J Biomechanics, Vol. 5, pp 541-551, 1972.

Hlavacek, M. "The Role of Synovial Fluid Filtration by Cartilage in Lubrication of Synovial Joints - I. Mixture Model of Synovial Fluid." J Biomechanics, Vol. 26, No. 10, pp 1145-1150, 1993.

Howell, D.S.; Sapsky, A.I.; Pita, J.C.; and Woessner, J.F. "The Pathogenesis of Osteoarthritis." Seminars in Arthritis and Rheumatism, Vol. 5, No. 4, pp 365-383, 1976.

Hulth, A.; Lindberg, L.; and Telhag, H. "Experimental Osteoarthritis in Rabbits." Acta Orthop. Scand., Vol. 41, pp 522-530, 1970.

Ide, T. "An Analysis of Impact-Induced Trauma to Articular Cartilage." A Thesis, Michigan State University, 1992.

Ide, T.; Haut, R.; and DeCamp, C. "An Evaluation of Impact Induced Trauma to Articular Cartilage Using a Rabbit Model." *Biomechanics Symposium, American Society of Mechanical Engineering*, pp 149-151, 1991.

Johnson-Nurse, C. and Dandy, D.J. "Fracture-Separation of Articular Cartilage in the Adult Knee." *The Journal of Bone and Joint Surgery*, Vol. 67-B, No. 1, pp 42-43, 1985.

Jurvelin, J.; Kiviranta, I.; Säämänen, A.-M.; Tammi, M.; and Helminen, H.J. "Indentation Stiffness of Young Canine Knee Articular Cartilage - Influence of Strenuous Joint Loading." *Journal of Biomechanics*, Vol. 23, No. 12, pp 1239-1246, 1990.

Jurvelin, J.; Kiviranta, I.; Säämänen, A.-M.; Tammi, M.; and Helminen, H.J. "Partial Restoration of Immobilization-Induced Softening of Canine Articular Cartilage After Remobilization of the Knee (Stifle) Joint." *Journal of Orthopaedic Research*, Vol. 7, pp 352-358, 1989.

Jurvelin, J.; Säämänen, A.-M.; Arokoski, J.; Helminen, H.J.; and Kiviranta, I. "Biomechanical Properties of the Canine Knee Articular Cartilage as Related to Matrix Proteoglycans and Collagen." *Engineering in Medicine*, Vol. 17, No. 4, pp 157-162, 1988.

Kempson, L.E.: *Mechanical Properties of Articular Cartilage*. In: *Adult Articular Cartilage*. 2nd ed., ed. by MAR Freeman, Kent, England, Pitman Medical Publishers, pp 333-414, 1979.

Kramer, J.S.; Yelin, E.H.; and Epstein, W.V. "Social and Economic Impacts of Four Musculoskeletal Conditions." *Arthritis and Rheumatism*, Vol. 26, No. 7, pp 901-907, 1983.

Lai, W.M.; Mow, V.C.; and Zhu, W. "Constitutive Modeling of Articular Cartilage and Biomacromolecular Solutions." *Transactions of the ASME*, Vol. 115, pp 474-480, 1993.

Lohmander, L.S.; Dahlberg, L.; Ryd, L.; and Heinegard, D. "Increased Levels of Proteoglycan Fragments in Knee Joint Fluid After Injury." *Arthritis and Rheumatism*, Vol. 32, No. 11, pp 1434-1442, 1989.

Lohmander, L.S.; Lark, M.W.; Dahlberg, L.; Walakovits, L.A.; and Roos, H. "Cartilage Matrix Metabolism in Osteoarthritis: Markers in Synovial Fluid, Serum, and Urine." *Clin Biochem*, Vol. 25, pp 167-174, 1992.

Lukoschek, M.; Boyd, R.D.; Schaffler, M.B.; Burr, D.B.; Radin, E.L. "Comparison of Joint Degeneration Models." *Acta Orthop. Scand.*, Vol. 57, pp 349-353, 1986.

Mak, A.F.; Lai, W.M.; and Mow, V.C. "Biphasic Indentation of Articular Cartilage - I. Theoretical Analysis." J Biomechanics, Vol. 20, No. 7, pp 703-714, 1987.

Mankin, H.J. "The Reaction of Articular Cartilage to Injury and Osteoarthritis." The New England Journal of Medicine, Vol. 291, No. 25, pp 1335-1340, 1974.

Maroudas, A.; Wachtel, E.; Grushko, G.; Katz, E.P.; and Weinberg, P. "The Effect of Osmotic and Mechanical Pressures on Water Partitioning in Articular Cartilage." Biochimica et Biophysica Acta, Vol. 1073, pp 285-294, 1991.

Maroudas, A.; Ziv, I.; Weisman, N.; and Venn, M. "Studies of Hydration and Swelling Pressure in Normal and Osteoarthritic Cartilage." Fifth International Congress on Biorheology Symposium: Some Biorheological Aspects of Joint Diseases. Biorheology, Vol. 22, pp 159-169, 1985.

McDevitt, C.A. and Muir, H. "Biochemical Changes in the Cartilage of the Knee in Experimental and Natural Osteoarthritis in the Dog." The Journal of Bone and Joint Surgery, Vol. 58-B, No. 1, pp 94-101, 1976.

Meachim, G. "Light Microscopy of Indian Ink Preparations of Fibrillated Cartilage." Ann. Rheum. Dis., Vol. 31, pp 457-464, 1972.

Messner, K.; Lohmander, L.S.; and Gillquist, J. "Cartilage Mechanics and Morphology, Synovitis and Proteoglycan Fragments in Rabbit Joint Fluid After Prosthetic Meniscal Substitution." Biomaterials, Vol. 14, No. 3, pp 163-168, 1993.

Michael-Donohue, J.; Buss, D.; Oegema, T.R.; and Thompson, R.C. "The Effects of Indirect Blunt Trauma on Adult Canine Articular Cartilage." The Journal of Bone and Joint Surgery, Vol. 65-A, No. 7, pp 948-957, 1983.

Mizrahi, J.; Maroudas, A.; Lanir, Y.; Ziv, I.; and Webber, T.J. "The 'Instantaneous' Deformation of Cartilage: Effects of Collagen Fiber Orientation and Osmotic Stress." Biorheology, Vol. 23, pp 311-330, 1986.

Mow, V.C.; Gibbs, M.C.; Lai, W.M.; Zhu, W.B.; and Athanasiou, K.A. "Biphasic Indentation of Articular Cartilage - II. A Numerical Algorithm and an Experimental Study." J Biomechanics, Vol. 22, No. 8/9, pp 853-861, 1989.

Mow, V.C.; and Hayes, W.C. Basic Orthopaedic Biomechanics. Raven Press, New York, pp 174-187, 1991.

Mow, V.C.; Lai, W.M.; and Takei, T. "A Geometric Model of Collagen-Proteoglycan Interaction for Kinetic Swelling Experiments." 30th Annual Orthopaedic Research Society, Atlanta, Georgia, pp 36, 1984.

Myers, E.R.; Hardingham, T.E.; Billingham, M.E.J.; and Muir, H. "Changes in the Tensile and Compressive Properties of Articular Cartilage in a Canine Model of Osteoarthritis." 32nd Annual Orthopaedic Research Society, New Orleans, Louisiana, Feb. 17-20, 1986, pp 231.

Nahum, A.M.; Siegel, A.W.; Hight, P.; and Brooks, S.H. "Safer Instrument Pallet Designs are Producing Fewer Leg Injuries in Vehicle Accidents." The SAE Journal, Vol. 77, pp 32-36, 1969.

Nomura, S.; Hiltner, A.; Lando, J.B.; and Baer, E. "Interaction of Water with Native Collagen." Biopolymers, Vol. 16, pp 231-246, 1977.

Noyes, F.R.; Schipplein, O.W.; Andriacchi, T.P.; Saddemi, S.R.; and Weise, M. "The Anterior Cruciate Ligament-Deficient Knee with Varus Alignment." The American Journal of Sports Medicine, Vol. 20, No. 6, pp 707-716, 1992.

Ogata, K.; Whiteside, L.A.; Lesker, P.A.; and Reynolds, F.C. "Acute Effect of Open Joint Wounds on Articular Cartilage and Synovium in Rabbits." The Journal of Trauma, Vol. 19, No. 12, pp 953-956, 1979.

Okada, Y.; Shinmei, M.; Tanaka, O.; Naka, K.; Kimura, A.; Nakanishi, I.; Bayliss, M.T.; Iwata, K.; and Nagase, H. "Localization of Matrix Metalloproteinase 3 (Stromelysin) in Osteoarthritic Cartilage and Synovium." Laboratory Investigation, Vol. 66, No. 6, pp 680-690, 1992.

Parsons, J.R.; and Black, J. "Mechanical Behavior of Articular Cartilage Quantitative Changes with Enzymatic Alteration of the Proteoglycan Fraction." Bulletin of the Hospital for Joint Diseases Orthopaedic Institute, Vol. 47, No. 1, pp 13-30, 1987.

Parsons, J.R.; and Black, J. "The Viscoelastic Shear Behavior of Normal Rabbit Articular Cartilage." J Biomechanics, Vol. 10, pp 21-29, 1977.

Pelletier, J.-P.; Faure, M.-P.; DiBattista, J.A.; Wilhelm, S.; Visco, D.; and Martel-Pelletier, J. "Coordinate Synthesis of Stromelysin, Interleukin-1, and Oncogene Proteins in Experimental Osteoarthritis." American Journal of Pathology, Vol. 142, No. 1 pp 95-105, 1993.

Pelletier, J.-P.; Martel-Pelletier, J.; Ghandur-Mnaymneh, L.; Howell, D.S.; and Woessner, F. Jr. "Role of Synovial Membrane Inflammation in Cartilage Matrix Breakdown in the Pond-Nuki Dog Model of Osteoarthritis." Arthritis and Rheumatism, Vol. 28, No. 5, pp 554-561, 1985.

Pelletier, J.-P.; Martel-Pelletier, J.; Howell, D.S.; Ghandur-Mnaymneh, L.; Enis, J.E.; and Woessner, J.F. Jr. "Collagenase and Collagenolytic Activity in Human Osteoarthritic Cartilage." Arthritis and Rheumatism, Vol. 26, No. 1, pp 63-68, 1983.

Peyron, J. "Inflammation in Osteoarthritis (OA): Review of its Role in Clinical Picture, Disease Progress, Subsets, and Pathophysiology." Osteoarthritis Symposium, pp 115-116, 1981.

Pickvance, E.A.; Oegema, T.R. Jr.; and Thompson, R.C. Jr. "Immunolocalization of Selected Cytokines and Proteases in Canine Articular After Transarticular Loading." Journal of Orthopaedic Research, Vol. 11, No. 3, pp 313-323, 1993.

Radin, E.L.; Ehrlich, M.G.; Chernack, R.; Abernethy, P.; Paul, I.L.; and Rose, R.M. "Effect of Repetitive Impulsive Loading on the Knee Joints of Rabbits." Clinical Orthopaedics and Related Research, No. 131, pp 288-291, 1978.

Radin, E.L.; Parker, H.G.; Pugh, J.W.; Steinberg, R.S.; Paul, I.G.; and Rose, R.M. "Response of Joints to Impact Loading-III." J Biomechanics, Vol. 6, pp 51-57, 1973.

Radin, E.L. and Paul, I.L. "Does Cartilage Compliance Reduce Skeletal Impact Loads?" Arthritis and Rheumatism, Vol. 13, No. 2, pp 139-144, 1970.

Radin, E.L.; Paul, I.L.; and Rose, R.M. "Role of Mechanical Factors in Pathogenesis of Primary Osteoarthritis." The Lancet, pp 519-522, March 4, 1972.

Repo, R.U. and Finlay, J.B. "Survival of Articular Cartilage After Controlled Impact." The Journal of Bone and Joint Surgery, Vol. 59-A, No. 8, pp 1068-1075, 1977.

Ridge, S.C.; Oronsky, A.L.; and Kerwar, S.S. "Induction of the Synthesis of Latent Collagenase and Latent Neutral Protease in Chondrocytes by a Factor Synthesized by Activated Macrophages." Arthritis and Rheumatism, Vol. 23, No. 4, pp 448-454, 1980.

Roughley, P.J.; Nguyen, Q.; and Mort, J.S. "Mechanisms of Proteoglycan Degradation in Human Articular Cartilage." Journal of Rheumatology, Vol. 18, Suppl. 27, pp 52-54, 1991.

Saxne, T. and Heinegård, D. "Synovial Fluid Analysis of Two Groups of Proteoglycan Epitopes Distinguishes Early and Late Cartilage Lesions." Arthritis and Rheumatism, Vol. 35, No. 4, pp 385-390, 1992.

Schmidt, M.B.; Mow, V.C.; Chun, L.W.; and Eyre, D.R. "Effects of Proteoglycan Extraction on the Tensile Behavior of Articular Cartilage." Journal of Orthopaedic Research, Vol. 8, No. 3, pp 353-363, 1990.

Schumacher, H.R.; Gordon, G.; Paul, H.; Reginato, A.; Villanueva, T.; Cherian, V.; and Gibilisco, P. "Osteoarthritis, Crystal Deposition, and Inflammation." Osteoarthritis Symposium, pp 116-119, 1981.

Setton, L.A.; Zhu, W.; and Mow, V.C. "The Biphasic Poroviscoelastic Behavior of Articular Cartilage: Role of the Surface Zone in Governing the Compressive Behavior." J Biomechanics, Vol. 26, No. 4/5, pp 581-592, 1993.

Shinmei, M.; Masuda, K.; Kikuchi, T.; and Shimomura, Y. "The Role of Cytokines in Chondrocyte Mediated Cartilage Degradation." Journal of Rheumatology, Vol. 16, (sup 18), pp 32-34, 1989.

Silyn-Roberts, H. and Broom, N.D. "Fracture Behaviour of Cartilage-on-Bone in Response to Repeated Impact Loading." Connective Tissue Research, Vol. 24, pp 143-156, 1990.

Simon, W.H. and Wohl. D.L. "Water Content of Equine Articular Cartilage: Effects of Enzymatic Degradation and 'Artificial Fibrillation'." Connective Tissue Research, Vol. 9, pp 227-232, 1982.

Spilker, R.L.; Suh, J.-K.; and Mow, V.C. "A Finite Element Analysis of the Indentation Stress-Relaxation Response of Linear Biphasic Articular Cartilage." J of Biomechanical Engineering, Vol. 114, pp 191-201, 1992.

States, J.D. "Traumatic Arthritis--A Medical and Legal Dilemma." Proceedings of the 14th Annual Conference of the American Association for Automotive Medicine, pp 21-28, 1970.

Svalastoga, E. and Reimann, I. "Experimental Osteoarthritis in the Rabbit - I. Histological Changes of the Synovial Membrane." Acta Vet. Scand., Vol. 26, pp 313-325, 1985.

Thompson, R.C. Jr. "An Experimental Study of Surface Injury to Articular Cartilage and Enzyme Responses Within the Joint." Clinical Orthopaedics and Related Research, No. 107, pp 239-248, 1975.

Thompson, R.C. Jr.; Oegema, T.R. Jr.; Lewis, J.L.; and Wallace, L. "Osteoarthritic Changes After Acute Transarticular Load: An Animal Model." The Journal of Bone and Joint Surgery, Vol. 73-A, No.7, pp 990-1001, 1991.

Thompson, R.C. Jr.; Vener, M.J.; Griffiths, H.J.; Lewis, J.L.; Oegema, T.R. Jr.; and Wallace, L. "Scanning Electron-Microscopic and Magnetic Resonance-Imaging Studies of Injuries to the Patellofemoral Joint after Acute Transarticular Loading." The Journal of Bone and Joint Surgery, Vol. 75-A, No. 5, pp 704-713, 1993.

Thonar, E.J.-M.A.; Lenz, M.E.; Klintworth, G.K.; Caterson, B.; Pachman, L.M.; Glickman, P.; Katz, R.; Huff, J.; and Kuettner, K.E. "Quantification of Keratan Sulfate in Blood as a Marker of Cartilage Catabolism." Arthritis and Rheumatism, Vol. 28, No. 12, pp 1367-1376, 1985.

Tobolsky. Properties and Structures of Polymers. Chapter III: Mathematical Treatment of Linear Viscoelasticity. pp 98-129, 1960.

Tomatsu, T.; Imai, N.; Takeuchi, N.; Takahashi, K.; and Kimura, N. "Experimentally Produced Fractures of Articular Cartilage and Bone." The Journal of Bone and Joint Surgery, Vol. 74-B, No. 3, pp 457-462, 1992.

Vener, M.J.; Thompson, R.C. Jr.; Lewis, J.L.; and Oegema, R.T. Jr. "Subchondral Damage After Acute Transarticular Loading: An *In Vitro* Model of Joint Injury." Journal of Orthopaedic Research, Vol. 10, pp 759-765, 1992.

Walker, E.R.; Boyd, R.D.; Wu, D.; Lukoschek, M.; Burr, D.B.; and Radin, E.L. "Morphologic and Morphometric Changes in Synovial Membrane Associated with Mechanically Induced Osteoarthritis." Arthritis and Rheumatism, Vol. 34, No. 5, pp 515-524, 1991.

Whipple, R.R.; Gibbs, M.C.; Lai, W.M.; Mow, V.C.; Mak, A.F.; and Wirth, C.R. "Biphasic Properties of Repair Cartilage at the Articular Surface." Trans. Orthop. Res. Soc., Vol. 10, pp 340-, 1985.

Yang, K.G.; Boyd, R.D.; Kish, V.L.; Burr, D.B.; Caterson, B.; and Radin, E.L. "Differential Effect of Load Magnitude and rate on the Initiation and Progression of Osteoarthritis." 35th Annual Meeting, Orthopaedic Research Society, Las Vegas, Nevada, pp 148, 1989.

MICHIGAN STATE UNIV. LIBRARIES



31293010330391